1-9057

APPLICATION OF PHOTOMETRIC TECHNIQUES TO THE STUDY OF THREE-PHASE FLUIDIZED BED REACTORS USED IN THE HYDROCRACKING OF HEAVY OILS

CONTRACT REPORT NO. 1SU81-00368

TITLE: **APPLICATION OF PHOTOMETRIC TECHNIQUES TO THE STUDY OF THREE-PHASE FLUIDIZED BED REACTORS USED IN THE HYDROCRACKING OF HEAVY OILS**

Final Report

by

Principal Investigator:		Dr. Hugo de Lasa
Consultant	:	Dr. Maurice A. Bergougnou
Research Assistant	:	Mr. S.L.P. Lee
Address	:	Faculty of Engineering Science University of Western Ontario

Work on this project was conducted under the auspices of the Canada Centre for Mineral and Energy Technology, Energy, Mines and Resources, Canada

DSS FILE NUMBER : 20SU.23440-1-9057

DSS CONTRACT SERIAL NUMBER : 1SU81-00368

CANMET PROJECT NUMBER : 421051-06

CANMET SCIENTIFIC AUTHORITY: Dr. D.D.S. Liu

November, 1983

This report should be cited as Contract Report No.: 1SU81-00368

151 NP

OCT 11 1985

MICROMEDIA

ABSTRACT

A photometric technique was developed at the University of Western Ontario to study bubble behaviour in three-phase fluidized beds constituted by fines particles. Both equipment and sensors evolved considerably through the different phases of the present program. Particularly, the capability of a novel custom made U-shaped single core silica fiber (400μm diameter) to be used as a bubble sensor was fully demonstrated employing a bidimensional column (244 cm x 66 cm x 2.54 cm) and a cylindrical column (diameter: 20.3 cm, height: 330 cm). A helium--neon laser beam was introduced at one end of the U probe and the variation of the light intensity, occurring when a gas bubble contacted the sensor, was detected at the other end of the fiber.

Several of these probes and an advanced data acquisition system were employed during the systematic runs to measure bubble velocities, bubble frequency and axial bubble cords. At the same time simultaneous recording of the pressure profiles in the bed allowed the estimation of the hold-ups of the different phases (gas, liquid and solid). This fluid dynamic data was obtained for a three-phase fluidized bed constituted by water, air and 335μm glass beads.

We believe that the novel U-shaped bubble sensor could be applied to study the bubble behaviour and to provide experimental data for optimizing and estimating the performance of real reactors with severe operating conditions of high temperature and pressure, such as the CANMET catalytic hydrocracking process.

TABLE OF CONTENTS

LIST OF TABLES III

LIST OF FIGURES IV

1.0 Introduction 1

2.0 Project Objectives 2

3.0 Equipment Design

3.1 Development of the Data Acquisition System 3

3.2 Development of the Absorption Photometric System 6

3.3 Development of the Fiberoptic Photometric System 8

3.4 Design and Modifications of the Bidimensional Fluidized Bed Column and the Liquid Circuit. 11

3.5 Design of a Mini-fluidized Bed for Calibration of the Laser Beam Absorption. 14

3.6 Development of a Pressure Measurement System 15

3.7 Design of a Cylindrical Fluidized Bed Column 17

4.0 Experimental Results

4.1 Bubble Measurements in Three-Phase Fluidized Beds Using the Absorption Photometric Technique. Bidimensional Column 20

4.2 Bubble Measurements in Three-Phase Fluidized Beds Using the U-Shaped Fiber Optic Probe. Bidimensional Column. 23

4.3 Hold-up Estimation for the Different Phases in Three-Phase Fluidized Beds Using the Pressure Profiles Obtained with the Data Acquisition System. Bidimensional Column. 27

4.4 Bubble Measurements in Three-Phase Fluidized Beds Using the U-Shaped Probe. Cylindrical Column. 29

4.5 Bubble Frequency in Three-Phase Fluidized Bed. Cylindrical Column. 31

4.6 Correlations of Bubble Velocity with Respect to the Characteristic Bubble Length in Three-Phase Fluidized Bed. Cylindrical Column 33

5.0 Actions Indicated in the Original Work Statement not Completed 34

6.0 Report of the Results of the Program

6.1 Presentation of the Results of the Program in the Canadian Society Chemical Engineering Conference, Toronto (1983). 36

6.2 Publication of the Results of the Program in the Canadian Journal of Chemical Engineering. (1984) 36

7.0 Further Research Planned in Three Phase Fluidized Bed

7.1 Proposition of Presentation, American Institute of Chemical Engineering Meeting San Francisco (1984). 36

7.2 Proposition of Presentation, 15th Annual Meeting Fine Particle Society, Florida (1984). 36

8.0 Conclusions 37

9.0 Acknowledgements 38

10.0 Notation 39

11.0 Bibliographic References 42

12.0 Appendices

12.1 Bubble Detection Using a Single Data Acquisition Channel. 44

12.2 Data Acquisition Program for Bubble Measurement in a Bi-dimensional Three-Phase Fluidized Bed Using Four U-Shaped Optical Fiber Probes. 50

12.3 Data Processing Program for Bubble Measurement Using the Data Acquisition Program 4 PROB-ACQ1 53

12.4 Data Acquisition and Data Processing Program for the Determination the Pressure Profile in a Bidimensional Three-Phase Fluidized Bed. 65

12.5 Derivation of the Equations (6),(7) and (8) that Allow the Estimation of the Hold-Up of the Different Phases in Three-Phase Fluidization. 73

LIST OF TABLES

1. Correlations for V_b and ℓ. Bidimensional Column. 77

2. Bubble Classification. Bidimensional Column. 78

3. Bubble Frequencies in a Cylindrical Three Phase Fluidized Bed with a Single Bubble Injector. 79

4. Bubble Frequencies in Cylindrical Three Phase Fluidized Bed with Four Bubble Injectors. 80

5. Correlations for V_b and ℓ. Cylindrical Column. 81

LIST OF FIGURES

1. Three-Phase Fluidized Bed Cold and Atmospheric Bidimensional Column. 82

2. Oscillation of the Laser when a Bubble is Crossing the Beam. Detection System: Direct Laser Crossing the Column. 83

3. Oscillation of the Laser when a Bubble is Crossing the Beam (Data Acquisition System: 1 channel, Column: Bidimensional, Detection System: Direct Laser Crossing the Column). 83

4. Fiber Optic Configuration. The Shaded Area Represents the Section of the Probe where the Cladding was Removed. 84

5. Schematic Representation of the Plexiglass Window Holding the Fibers in the Bidimensional Column. 85

6. Schematic Representtion of the Bi-dimensional Three-Phase Fluidized Bed and Accessories. 86

7. Minifluidized Bed (Liquid-Solid) for Laser Beam Absorption Calibration 87

8. View of the Grid of the Minifluidized Bed. 88

9. Calibration of the Pressure Transducer Manufactured by Data Instruments. 89

10. Microprocessor Report Showing the Pressure Profile in the Fluidized Bed and the Different Hold-Ups. 90

11. Schematic Representation of the Cylindrical Bed Wind-Box. 91

12. Schematic Representation of the "test section", holding the "measuring windows", of the Cylindrical Fluidized Bed. Front view. 92

13. Schematic Representation of the "test section", holding the "measuring windows", of the Cylindrical Fluidized Bed. Lateral view. 93

14. Schematic Representation of the "measuring windows" showing the Horizontal and Vertical Positioning of the Probes. 94

15. Schematic Representation of one of the Plexiglass Sections (with no windows) used in the Cylindrical Fluidized Bed. 95

16. Response of Photodetectors and of the Dual Channel Data Acquisition System Using a 180 ms scale of time (V_ℓ = 1.28 cm/s, Vg = 2.10 cm/s). 96

17. Response of Photodetectors and of the Dual Channel Data Acquisition System Using a 35 ms scale of time (V_ℓ = 1.28 cm/s, Vg = 2.10 cm/s). 97

18. Response of Photodetectors and of the Dual Channel Data Acquisition System Using a 150 ms. scale of time (V_ℓ = 1.51 cm/s, Vg = 3.50 cm/s). 98

19. Response of Photodetectors and the Dual Channel Data Acquisition System Using a 35 ms scale of time (V_ℓ = 1.51 cm/s, Vg = 350 cm/s). 99

20. Relationship of the Bubble Velocity to the Measured Axial Bubble Length estimated with the Absorption Photometric Technique (Liquid: water, Gas: air, Solid: sand of 210μm average size). 100

21. Typical square wave signals recorded by the U-shaped fiber optic sensor. Probes 1 and 2. Bidimensional column. 101

22. Typical square wave signals recorded by the U-shaped fiber optic sensor. Probes 3 and 4. Bidimensional column. 102

23. Cap of spherical shape showing the bubble characteristic dimensions. 103

24. Relationship of the bubble velocity to the measured axial bubble length estimated with the U-shaped optical fiber probes. Bidimensional column. Liquid: water, Gas: Air, Solid:Glass beads of 335μm, Vg=1.19 cm/s. 104

25. Variation of ε_ℓ, εg and (ε_ℓ+ εg) fractions with the velocity of the liquid in a three-phase fluidized bed. Liquid: water, Gas: air, Solid: glass beads of 335 μm, Vg = 1.519 cm/s. 105

26. Variation of the total height of the bed H_b with the Re_ℓ in a three-phase fluidized bed. Liquid: water, Gas: air, Solid: glass beads of 335μm, Vg = 1.519 cm/s. 106

27. Variation of ε_ℓ, εg and (ε_ℓ + εg) fractions with the velocity of the liquid in a three-phase fluidized bed. Liquid: water, Gas: air, Solid: glass beads of 335μm, Vg = 1.898 cm/s. 107

28. Variation of the total height of the bed, H_b with the Re_ℓ in a three-phase fluidized bed. Liquid: water, Gas: air, Solid: glass beads of 335μm, Vg = 1.898 cm/s. 108

29. Variation of ε_ℓ, εg, (ε_ℓ + εg) fractions with the velocity of the liquid in a three-phase fluidized bed. Liquid: water, Gas: air, Solid: glass beads of 335 μm, Vg = 2.278 cm/s. 109

30. Variation of the total height of the bed, H_b with the Re_ℓ in a three-phase fluidized bed. Liquid: water, Gas: air, Solid: glass beads of 335 μm, Vg = 2.278 cm/s. 110

31. Typical square wave signals recorded by the U-shaped fiber optic sensors. Probes 1 and 2. Cylindrical Column. 111

32. Variation of the bubble frequency with the radial position in the cylindrical column. Single injector located at r/R_c = 0, Liquid: water, Gas: air, Solid: glass beads of 335μm, Vg = 1.769 cm/s, V_ℓ = 0.778 cm/s. 112

33. Bubbles in the cylindrical three phase fluidized bed column as viewed by Probes 1 and 2 located at $r/R_c = 0$, Liquid: water, Gas: air, Solid: glass beads of 335μm, Vg = 1.769 cm/s, $V_\ell = 0.7878$ cm/s, 113

34. Bubbles in the cylindrical three phase fluidized bed column as viewed by Probes 1 and 2 located at $r/R_c = 0.25$. Liquid: water, Gas: air, Solid: glass beads of 335μm, Vg = 1.769 cm/s, $V_\ell = 0.778$ cm/s Gas, Injector:one positioned at $r/R_c = 0$. 114

35. Bubbles in the cylindrical three phase fluidized bed column as viewed by Probes 1 and 2 located at $r/R_c = 0.50$. Liquid:water, Gas: air, Solid: glass beads of 335μm, Vg = 1.769 cm/s, V_ℓ = 0.778 cm/s Gas Injector: One positioned at $r/R_c = 0$. 115

36. Bubbles in the cylindrical three phase fluidized bed column as viewed by probes 1 and 2 located at $r/R_c = 0.75$. Liquid:water, Gas: air, Solid: glass beads of 335μm, Vg = 1.769 cm/s, $V_\ell = 0.778$ cm/s, Gas Injector: one positioned at $r/R_c = 0$. 116

37. Variation of the bubble frequency with the radial position in the cylindrical column. Four injectors located as it is described in Figure 11. Liquid: water, Gas:air, Solid: glass beads of 335μm, Vg = 1.630 m/s. 117

38. Bubbles in the cylidrical three phase fluidized bed column as viewed by Probes 1 and 2 located at $r/R_c = 0$. Liquid: water, Gas: air, Solid: glass beads of 335μm, Vg = 1.630 cm/s, V_ℓ = 0.389 cm/s, Gas Injectors: four positioned as it is described Figure 11. 118

39. Bubbles in the cylindrical three phase fluidized bed column as viewed by probes 1 and 2 located at $r/R_c = 0$. Liquid:water, Gas: air, Solid:glass beads of 335μm, Vg = 1.630 cm/s, V_ℓ= 0.778 cm/s Gas Injectors: four positioned as it is described Figure 11. 119

40. Bubbles in the cylindrical three phase fluidized bed column as viewed by probes 1 and 2 located at $r/R_c = 0.25$. Liquid:water, Gas:air, Solid:glass beads of 335μm, Vg = 1.630 cm/s, V_ℓ = 0.778 cm/s, Gas Injectors: four positioned as it is described in Figure 11. 120

41. Bubbles in the cylindrical three phase fluidized bed column as viewed by probes 1 and 2 located at $r/R_c = 0.5$. Liquid: water, Gas: air, Solid: glass beads of 335μm, Vg = 1.630 cm/s, V_ℓ = 0.778 cm/s, Gas Injectors: four positioned as it is described in Figure 11. 121

42. Bubbles in the cylindrical three phase fluidized bed column as viewed by probes 1 and 2 located at $r/R_c = 0.75$. Liquid: water, Gas: air, Solid: glass beads of 335μm, Vg = 1.630 cm/s, V_ℓ = 0.778 cm/s, Gas Injectors: four positioned as it is described in Figure 11. 122

43. Bubbles in the cylindrical three phase fluidized bed column as viewed by probes 1 and 2 located at $r/R_c = 0$. Liquid: water, Gas: air, Solid: glass beads of 335μm, Vg = 1.630 cm/s, V_ℓ = 1.167 cm/s, Gas Injectors: four positioned as it is described in Figure 11. 123

44. Bubbles in the cylindrical three phase fluidized bed column as viewed by probes 1 and 2 located at r/R_c = 0.25. Liquid: water, Gas: air, Solid: glass beads of 335μm, Vg = 1.630 cm/s, V_ℓ = 1.167 cm/s, Gas Injectors: Four positioned as it is described in Figure 11. 124

45. Bubbles in the cylindrical three phase fluidized bed column as viewed by probes 1 and 2 located at r/R_c = 0.5. Liquid: water, Gas: air, Solid: glass beads of 335μm, Vg = 1.630 cm/s, V_ℓ = 1.167 cm/s, Gas Injectors: four positioned as it is described in Figure 11. 125

46. Bubbles in the cylindrical three phase fluidized bed column as viewed by probes 1 and 2 located at r/R_c = 0.75. Liquid: water, Gas: air, Solid: glass beads of 335μ, Vg = 1.630 cm/s, V_ℓ = 1.167 cm/s, Gas Injectors: four positioned as it is described in Figure 11. 126

47. Bubbles in the cylindrical three phase fluidized bed column as viewed by probes 1 and 2 located at r/R_c = 0. Liquid: water, Gas: air, Solid: glass beads of 335μm, Vg = 1.630 cm/s, V_ℓ = 1.556 cm/s, Gas Injectors: four positioned as it is described in Figure 11. 127

48. Bubbles in the cylindrical three phase fluidized bed column as viewed by probes 1 and 2 located at r/R_c = 0.25. Liquid: water, Gas: air, Solid: glass beads of 335μm, Vg = 1.630 cm/s, V_ℓ = 1.556 cm/s, Gas Injectors: four positioned as it is described in Figure 11. 128

49. Bubbles in the cylindrical three phase fluidized bed column as viewed by probes 1 and 2 located at r/R_c = 0.5. Liquid: water, Gas: air, Solid: glass beads of 335μm, Vg = 1.630 cm/s, V_ℓ = 1.556 cm/s, Gas Injectors: four positioned as it is described in Figure 11. 129

50. Bubbles in the cylindrical three phase fluidized bed column as viewed by probes 1 and 2 located at r/R_c = 0.75. Liquid: water, Gas: air, Solid: glass beads of 335 μm, Vg = 1.630 cm/s, V_ℓ = 1.556 cm/s, Gas Injectors: four positioned as it is described in Figure 11. 130

51. Relationship of the bubble velocity to the measured axial bubble length estimated with the U-shaped optical fiber probes. Cylindrical column. Gas Injector: one positioned at r/R_c = 0. Liquid: water, Gas: air, Solid: glass beads of 335μm, Vg = 1.769 cm/s, V_ℓ = 0.778 cm/s. 131

52. Relationship of the bubble velocity to the measured axial bubble length estimated with the U-shaped optical fiber probes. Cylindrical column. Gas Injectors: four. Liquid: water, Gas: air, Solid: glass beads of 335μm, Vg = 1.630 cm/s, V_ℓ = 0.389 cm/s. 132

53. Relationship of the bubble velocity to the measured axial bubble length estimated with U-shaped optical fiber probes. Cylindrical column. Gas Injectors: Four, Liquid: water, Gas: air, Solid: glass beads of 335μm, Vg = 1.630 cm/s, V_ℓ = 0.778 cm/s. 133

54. Relationship of the bubble velocity to the measured axial bubble length estimated with U-shaped optical fiber probes. Cylindrical Column. Gas Injectors: Four. Liquid: water, Gas: air, Solid: glass beads of 335μm Vg = 1.630 cm/s, V_ℓ = 1.167 cm/s. 134

55. Relationship of the bubble velocity to the measured axial bubble length estimated with the U-shaped optical fiber probes. Cylindrical column. Gas Injectors: Four. Liquid: water, Gas: air, Solid: glass beads of 335μm, Vg = 1.630 cm/s, V_ℓ = 1.556 cm/s. 135

56. Relationship of the bubble velocity to the measured axial bubble length estimated with the U-shaped optical fiber probes. Cylindrical column. Gas injectors: four. Liquid: water, Gas: air, Solid: glass beads of 335μm. The data of Figures 53, 54 and 55 are plotted together. 136

57. Relationship of the bubble velocity to the measured axial bubble length estimated with the U-shaped optical fiber probes. Cylindrical column. Gas injectors: four. Liquid: water, Gas: air, Solid: glass beads of 335μm. The data of Figures 51, 53, 54 and 55 are plotted together. 137

1.0 INTRODUCTION

Bubble velocity and bubble size are very important parameters for understanding the behaviour of three phase fluidized beds. Bubbles affect segregation between reacting phases, bed mixing, particle entrainment from the dense bed, gas hold-up and bed expansion. In order to measure bubble parameters in three-phase fluidized beds two approaches have been reported in the literature: (a) the use of bidimensional beds where the bubbles are followed from the walls of the column by means of cinecamera films (Henriksen and Ostergaard, 1974, Kim et al. 1977, Stewart and Davidson, 1964), (b) the in-situ methods (Park et al. 1969, Rigby et al. 1970) where sensors are located inside a three-dimensional bed. Two--dimensional beds unduly constrain the bubbles and affect their behaviour. In-situ probes, specially designed to minimize flow disturbances, are preferable.

Since few references concerning bubble sensors designed to operate at the high temperatures and pressure characteristics of heavy oil hydrocracking processes and H-coal units exist, the development of a probe, based on a single U-shaped fiber, was started by us in 1981 under the auspices of Energy Mines and Resources, Canada. Optical fibers in the form of a bundle or of two opposed fibers were recently proposed by Ishida et al. (1980) and Ishida and Hatano (1983), for two phase (gas-solid) fluidized beds. The novel type of probe for fluidized bed systems presented here, the U-shaped fiber sensor, has the inherent advantage of appropriate control of the light projected and received. This interesting effect is achieved through the adequate selection of fiber materials and probe geometry. Strong light absorbing media, for instance in the heavy oil reactors, require an optimization of the amounts of light brought and collected by the probe. They, thus offer a most interesting field of future application for this bubble sensor.

In summary, the present final report describes our research efforts during the period October 1981 - October 1983 developed under the DSS Contract No. 1SU81-00368, and the significant technical results obtained with the U-shaped fiber optic probe used to measure bubble phenomena in three-phase fluidized beds.

2.0 Project Objectives

The primary objective of the "Application of Photometric Techniques to the Study of Three-Phase Fluidized Bed Reactors" project, proposed in June, 1981, was to engineer and develop a novel photometric probe based on the use of a fiber optic. In effect a successful demonstration of this probe, suitable for high temperatures (600°C), would require an extensive testing of the novel device in a cold bidimensional and a cold cylindrical column that would mimic the operation of catalytic hydrocracking reactors. This task would also include the implementation of a sophisticated data acquisition system (microprocessor, photodetectors, optics, computer programs, computer interfaces) needed to show both the potential and the applicability of the fiber optic sensor.

A secondary objective of the program proposed in 1981 considered the use of the same data acquisition system to measure the pressure profiles in the bed and to estimate the hold-ups of the different phases (gas-liquid-solid).

Then it was visualized already in 1981 that all the generated fluid dynamic data, in addition to providing information of potential direct use for CANMET hydrocracking units, would prove as well that bubble velocity, bubble frequency bubble central cord, fractions of gas, liquid and solids were key operating

parameters that could be directly and easily acquired through a novel fiber optic probe-pressure transducer-interface-microprocessor facility.

We believe, however, that the final implementation of this new development to the high pressure and high pressure hydrocracking CANMET reactor will require further actions which were recently described in a Research Agreement Program Proposal (de Lasa and Bergougnou, 1983).

3.0 EQUIPMENT DESIGN

3.1 Development of the Data-Acquisition System

The development of the data acquisition system was initiated at the end of 1981 with the purchase of an HP-85 microprocessor unit. However, design limitations of the HP-85 microprocessor showed us in March, 1982 that the original data acquisition system could not meet the high speed sampling required by our project (bigger than 1000 samples/sec). After some intense discussions with the system design engineers from Hewlett-Packard, a decision was reached in May, 1982, that the core instrument of the system, the HP-85 microprocessor, would be replaced by a much more powerful high speed digital processor HP-9826 to fulfill our sampling rate demands. The complete listing of the microprocessor items with the accessories purchased in June, 1982 is as follows:

- Digital Processor HP-9826 with 42 bytes of user R/W memory, with one 5-1/4 mini floppy 260 K bytes, integral ASCII keyboard with Option 711 Basic.

- Interface HP98622A

- Interface HP98626A

- Thermal Graphic Printer HP2671G with HPIB Interface.

A basic check-up of the newly arrived microprocessor HP9826A was performed on August, 1982. Some problems were found with the A/D sampling rate. These problems were solved after intense debugging and after consulting Mr. Dickins from Hewlett-Packard in Toronto. Finally a computer program, detailed in Appendix 1, was implemented and operated successfully on the HP9826 microprocessor recording bubbles in a three phase fluidized bed (water-air-sand particles (210μm)) and employing at the same time the laser beam-photodetector arrangement described in Figure 1. We present on Figures 2 and 3 the characteristic responses for two different bubbles, as recorded in the microprocessor, showing the typical duration of the perturbation (70ms), the broad front and the relative sharp bubble tail. At the same time, in September, 1982, we fully tested the double channel acquisition system. The original computer routine was modified to perform an experiment, testing the capabilities described above.

A few problems were encountered then. First, the scanning card did not function properly introducing undesirable noise which strongly perturbated the main signal characterizing the bubble flow. Secondly, the high speed sampling rate required by such experiments, at least 500 samples/second x channel, could not be obtained. Thirdly, the timer card did not generate accurately the required square waves. After extensive phone discussions with Hewlett-Packard (Toronto), Mr. Dickins, the service engineer from Hewlett-Packard, visited our laboratory to solve the scanning card problem. Mr. Dickins did not succeed and the cards were sent back on October 1982 to Hewlett-Packard factory for inspection and testing.

The cards were returned from Hewlett-Packard factory at the beginning of November 1982. However, problems were encountered with the scanning cards. In fact, undesirable noise levels were generated. This was particularly noticeable when the double channel acquisition system was operated at the 500 samples/second x channel rate. At the same time a significant shift of the base line was observed, as well, at that sampling rates.

A first and important improvement of the double channel acquisition system was, however, achieved by us on November, 1982 through a better grounding of the two photodetectors. Nevertheless, the shifting of the baseline and the ±16% noise error level were considered too big for accurate bubble detection. It is important to mention that the basis for the error calculation is a typical 10mV

deviation that is normally observed when a bubble is recorded by the EG&G photodetectors-laser beam device. At this point, we requested the assistance of the Electronic Shop, Faculty of Engineering Science. Following their views an operational amplifier was built and hooked between the photodetectors and the multiprogrammer. The operational amplifier had two functions: - to bring down the impedance of the input signal, - to amplify this signal approximately one hundred times. With this last improvement the base line shift was eliminated and the noise reduced to ± 4.5%. More details of the experimental results showing the remarkable performance of the data acquisition system developed for this project are given on the sections 3.3 and 3.4 of the present report.

Finally, it is important to mention that two 256 K memory extensions and an advanced Basic 2.0 language were purchased from Hewlett-Packad on September, 1982 and March, 1983 respectively to significantly increase the capability of the duration of our bubble detection runs. In fact, the data acquisition system, as originally designed, could only be operated around 8 seconds before being saturated by the information coming from the probes located in the three-phase bidimensional fluidized bed. However,those improved 4 channels could be sampled at 500 samples/channel x sec during several minutes.

3.2 Development of the Absorption Photometric System

The first bubble photometric system used in the bidimensional fluidized bed was based on an absorption technique: two lasers

crossing the bed and two photodetectors sensing the exit beams (Figure 1). This system was completed with the appropriate beam optical attenuators that prevent the saturation of the photodetectors. The photometric system was also designed in such a way that three options might be chosen to process the laser signal obtained from the photodetectors/attenuator combination:

- Option 1: Direct reading from the powermeter using the instantaneous digital display of the powermeter.

- Option 2: Analog display of the perturbation generated by the laser oscillation on the screen of the oscilloscope. In this case it is necessry to attach the pulse viewing adaptor to the back of the photodetector and to install an appropriate resistor to the pulse adaptor.

- Option 3: Transformation of the analog signal leaving the photodetectors into a digital form and storage of it in the microprocessor. The analog signal obtained from the two EG&G Electro-Optics detectors may be converted into a digital signal by means of the high speed A/D multiprogrammer (HP-6940B) and processed later on in an HP9826 data processor.

The complete debugging of the absorption photometric system was completed by August, 1982. Some typical results obtained for the two detectors spaced 6cm are reported in Figures 16, 17, 18 and 19. These results are discussed in detail on Section 4.1 of the present report.

3.3 Development of the Fiber Optic Photometric System

A major objective of the present program was to investigate the possible application of a photometric technique based on the use of a fiberoptic sensor to three phase fluidized bed units. With such a purpose a custom made U-shaped single core silica fiber (400μm diameter) was designed in March, 1983 and used as the bubble sensor in the following phases of the research program. The design of the optical fiber probe was based on the difference of refraction indexes between the gas phase and the liquid phase. According to Snell's law the angle of total reflection is bigger in the liquid than that in the air. If this principle is applied to a fiber having a U-shape the fiber has to be bent as follows: the radius of curvature of the U has to be large enough so that the angle of incidence at the turning point is bigger than the angle of total reflection when the same fiber is exposed to air. If this condition is met, the source light is conserved in the fiber. However, the U has to be, at the same time, curved in such a way that the radius is small enough to secure an angle of incidence at the turning point smaller than the angle of total reflection for the same fiber dipped in water. Then, with this

U design the source light will be lost in water and conserved when exposed to air. Therefore, a significant difference can be seen at the detecting end of the fiber each time a gas bubble contacts the U probe.

A single core silica optical fiber of 400μm diameter was bent in a U shape, according to the principles mentioned above. The radius of the U was approximately 0.5 mm at the tip of the probe. (Figure 4). The fiber was then placed in a stainless steel tube so that only the tip of the U bend was exposed to the fluidized bed.

Four fiber probes were used in the bidimensional column. Two of the probes were located vertically at a separation of 1.27 cm. The two others were positioned horizontally on both sides of the upper one, leaving a space of 1.27 cm between them (Figure 5). All the probes were placed on a plexiglass window which can easily be removed from the wall of the column to modify the probe separation. The plexiglass window with the four probes was located in the bidimensional column at 44 cm. from the grid. Several changes were introduced, however, in the plexiglass windows holding the probes in the cylindrical column (Section 3.7) in order to allow the location of a bigger number of U-shaped sensors (six instead of four), a more detailed description of bubble phenomena and a better assessment of probe performance (probe-bubble interactions).

The bubble detection system was completed by a helium-neon laser beam. (Spectra Physics Unit, 15 mW). The laser was focused on one end of the fiber and was guided through the U-shape tip to the other end. The perturbation of the returning light generated when gas bubbles contacted the probe, was detected by the photodetector (EG&G). The analog signal from the photodetector was first sent to an operational amplifier for impedance matching, later on to high speed A/D converter for digitizing and finally to a microprocessor HP9826 for storage and data analysis. The characteristics of the A/D interface-microprocessor facility are described on the Section 3.1 of the present report.

The development of the fiber optic system included the purchase and the installation of an optical bench. It is important to mention that the purpose of using an optical bench was to achieve a good alignment of the laser and the optical fibers. The first configuration of the optical bench, completed in February, 1983, consisted of two parts, the emitting side and the receiving side. The emitting side components are described below: a) mounting slides in which the laser was placed. Its position could be adjusted either horizontally or vertically, b) lens holders with a beam splitter and a reflector where the source laser beam was divided into two parallel equal power beams, c) lens holders with convex lenses where the two laser beams were focused and directed into the optical fibers, d) fiber holders on which the optical fibers were fixed and positioned to receive the laser beams. The laser beams were then

guided into the fluidized bed by the optical fibers. The perturbation of laser intensities were detected on the receiving bench side where fiber holders and optic holders with concave lenses were used before the laser beam reached the EG&G photodetectors.

In May 1983, an important modification of the emitting side of the optical bench was undertaken in order that the bench could contain four optical fibers at an affordable cost compatible with the project budget. This new, less expensive configuration consisted of a single concentrated laser beam directly focused on four bunched optical fibers. This new arrangement for the emitting side showed an excellent performance, during all the systematic runs, in both the bidimensinal and the cylindrical column.

3.4 Design and Modifications of the Bidimensional Column and the Liquid Circuit

The various components of the liquid circuit of the bidimensional column (2.44 cm x 66 cm x 2.54 cm) were designed and fully assembled as shown in Figure 6 on March 1982. Water flows through a centrifugal pump, a flow-meter, a steel "wind-box" and a perforated plate grid into the two-dimensional fluidized bed. Four pipes collect the water overflowing at the top of the column and take it back to a plastic storage 150 gallon capacity tank. A second line allows a by--pass of the fluidized bed, returning directly a fraction of the pumped water to the storage tank. In order to prevent a sandblasting

effect of the pump by the solid particles, a special filter was made with a plexiglass support covered by a 200 mesh stainless steel screen. At the same time an antivibration pad located underneath the pump was used to isolate the pump from the floor avoiding the transmissions of vibrations to the various laboratory instruments and computer equipment. Moreover, a technician of the Building and Services Department of the University of Western Ontario did the appropriate electrical jobs to hook up the pump to the three-phase electrical supply box of our laboratory. Finally, the required valves, brass and ABS fittings, connectors and pipes to complete the water circuit, described in Figure 6, were purchased and installed in April, 1982.

However, in August 1982, three important changes were introduced in the original liquid circulation system

- In order to avoid a frequent blockage of the screen filter, positioned at the inlet of the centrifugal pump, the pump was lifted up by a few centimeters. A more stable operation was achieved with this modification.

- An overflow pipe was installed in the storage tank for safety reasons as well as to maintain a constant liquid level at the pump inlet.

- A piece of reinforced tube was installed also between the centrifugal pump and the flowmeter providing some extra

flexibility for the piping system. It is important to point out as well that several modifications of the two dimensional bed injectors (I.D.:0.94 cm) were done in July 1982 in order to suit the needs of the present program.

- Stainless steel screens were placed inside the stainless steel tubes (bubble injectors) instead of having them at their top as was the case in the original design. At the same time four additional bubble injectors were installed and distributed evenly across the bed. Bubble injector holders with O-ring type seals were manufactured to allow a quick change of the bubble injector position. More specifically, the bidimensional fluidized bed was modified as it is described in the next paragraph. First, the perforated support plate was redesigned for better performance and uniform fluidization. These improvements were achieved with a grid plate having 0.317 cm holes (Open Area/Total Area = 0.018). With this type of design the grid pressure drop is around 43% of the bed pressure drop. Secondly, the bubble injection system was improved as follows: a) a stainless steel screen (200 mesh) was placed inside each bubble injector at 10 cm.from the exit of the nozzle to eliminate any effect of the screen on bubble formation. A total of five identical injectors were fixed to the grid plate, b) O-ring seals, one for each bubble injector, were placed on the grid support plate. By pushing the injectors more or less inside the bed, the bubble injection level can be varied at will, c) a tee and a ball valve were installed at the inlet of each bubble

injector with the purpose of easily draining the liquid that could leak from the fluidized bed into the gas injector.

3.5 Design of a Minifluidized Bed for the Calibration of the Laser Beam Absorption

A small fluidized bed was designed and built on January 1983 to measure the absorption of the laser beam in various liquid-solid suspensions. It had a square (2.54 cm x 2.54 cm) section and was made of plexiglass. Figures 7 and 8 show the main characteristics of the bed which is constituted by four components:- a wind box (height: 2.54 cm) - a flow stabilizing section (height: 1.27 cm) - a liquid-solid fluidized bed (height: 7.6 cm) - an overflow section (height: 3.80 cm). Screens were located between sections in order to confine the particle motion to the fluidized bed itself and to avoid,at the same time, particle entrainment. In this way, during the calibration experiments, the weight of solid particles trapped in the mini-fluidized bed is kept close to a constant value. Knowing the weight of the particles in the bed and the volume of the fluidized bed section, one can estimate the average particle concentration in the liquid-solid suspension for each calibration run. The calibration unit has also other features. For instance, a plexiglass rod of 0.63 cm may be moved laterally reducing the effective thickness of the liquid-solid suspension seen by the laser. Thus, if the laser beam is focused on one end of the plexiglass rod the absorption of the beam could be calibrated by means of a variable thickness of

liquid-solid suspension. For instance, if the rod is positioned 1.27 cm from the walls at the centre line of the fluidized bed, the thickness of fluidized bed, seen by the laser, will be the half of the total thickness available.

However, due to the fact that a direct measurement of pressure profiles in the fluidized bed was implemented and could directly provide, with no extrapolation uncertainties, the hold-up of the different phases, both in liquid-solid and gas-liquid-solid fluidization (Section 4.3), the minifluidized bed calibration technique was not used in the following phases of the program.

3.6 Development of a Pressure Measurement System

The development of the pressure measurement system was undertaken considering the crucial importance of obtaining pressure profiles in three phase fluidized beds in conjunction with bubble measurements. Because pressure profiles allow the estimation of the hold-ups of the different phases (Section 4.3), the bubble data obtained from a specific run, could then be related to the general fluid dynamic state of the bed. The pressure measurement system developed by us was constituted by three components: - a switching valve, - a pressure transducer, - a power supply and a controller. The purpose of the switching valve was to allow a single pressure transducer to serve multiple channels of pressure taps. Otherwise, one pressure transducer would be needed for each pressure tap which will involve

an unaffordable cost for our project budget. With such a purpose a fluid switch wafer valve with twelve channels was purchased from Scanivalve in March, 1983. It is important to mention that the wafer mechanism is switched internally, in the Scanivalve device, by a solenoid drive. The pressure transducer was used to measure absolute pressures along the longitudinal axis of the fluidized bed. With such a purpose, the pressure transducer was connected to the common channel of the fluid switch wafer and it was employed to measure the pressure of each tap as the wafer turned around periodically. The voltage signal generated in the pressure transducer was digitalized and stored by the data acquisition system developed as part of the present project and described in Section 3.1. of this report. The transducer manufactured by Data Instruments has an accuracy of ± 0.25 at full pressure capacity. It is interesting to mention as well that a calibration of the pressure transducer was performed, obtaining the results shown in Figure 9 which confirmed the high performance of this device. Finally, a 24V DC power supply was built in the Electronic Shop, Faculty of Engineering Science, University of Western Ontario. This power supply was controlled by a repeated-cycle timer which activates the solenoid drive of the fluid switch wafer. The period of excitation can be adjusted in the device from virtually continuous to a minimum of thirty seconds, so as to leave enough time for pressure equilibration after switching from one channel to another. Another important feature of this device consists of the possible application of the same timer as a controller of the solenoid valve for single bubble experiments.

It is important to mention that the pressure measuring system was used in two phase and three phase fluidized bed systems. The performance of the multipoint pressure measuring system was found to be satisfactory. For instance pressure profiles as the ones described in Figure 10, where a microprocessor report is given, were determined on a systematic basis obtaining for each operating condition the fluidized bed height, the fraction of solids, the fraction of liquid and the fraction of gas. These results are described in Section 4.3 of the present report.

3.7 Design of a Cylindrical Fluidized Bed Column

A cylindrical fluidized bed was designed and built in July-August 1983, for the second phase of this contract. The colum was made out of plexiglass with an internal diameter of 20.3 cm and a height of 334 cm. The fluidized bed consisted of three sections. The first one was the liquid distribution section which ensures an even distribution of liquid and gas. The second section consisted of three interchangeable columns where the measuring probes could be positioned at different axial locations along the fluidized bed. The upper section of the system was the gas-liquid disengaging section where the liquid was collected and recycled back to the storage tank. It is important to mention that an overflow weir insured an approximately constant liquid level in the fluidized bed.

More specifically, the liquid distributor box (Figure 11) had an internal diameter of 20.3 cm and 15.4 cm in depth. There were three injectors mounted on the bottom of this box. These injectors were made out of stainless steel tube (I.D.= 1.57 cm). They were located at 5.1 cm from the center and with 120 degree circumferential separation. Concerning the characteristics of the liquid injectors it is important to mention that the end of each injector was sealed having six 0.635 cm lateral holes evenly distributed around the tube. These injectors entered 10.2 cm inside the distribution box where the liquid was dispersed radially.

At the same time four gas nozzles (I.D. = 0.94 cm) were used to introduce the gas into the fluidized bed. These nozzles were made out of stainless tube and mounted on the bottom plate of the distribution box (Figure 11). One of them was located at the center and the other three were positioned at 6.78 cm from the center with 120 degree circumferential separation. The gas nozzles passed through the distribution box and the perforated plate and could be moved easily in the axial direction sogas bubbles could be generated at different levels. Both gas and liquid injectors were arranged in a staggered form in order that the fluidizing streams were distributed uniformly across the bed (Figure 11).

Moreover, with the purpose of distributing the liquid flow and supporting the bed, a perforated plate was placed above the distributing section. There were fifty-four holes of 0.158 cm arranged in a 2.54 cm triangular pitch. A 100 mesh screen was placed on top of

the perforated plate to prevent grid leakage. Both the screen and the perforated plate were made out of stainless steel to prevent corrosion.

The cylindrical fluidized bed consisted of three sections. However, the "measuring windows" holding the optical fiber probes (Figures 12 and 13) were built only in one of them: "the test section". Because the three sections were interchangeable, the relative position of the "windows" could be easily modified, the bubble phenomena could be studied, inside the bed, at different positions from the grid.

The "test section" was 91.2 cm. in length and it had a series of pressure taps (eighteen) positioned along the walls of the column. The design of the measuring windows, located in the "test section" and supporting the U-shaped optical fibers, was similar to that used in the bi-dimensional bed (Section 3.3). However, some important modifications were introduced to the original "window" design for the cylindrical column. The diameter of the "window" was 5.08 cm and the distance between two adjacent probes was 0.952 cm (Figure 14). At the same time the "measuring windows" were mounted in pairs, on opposite sides (facing each other), at different bed levels (Figure 12 and 13). Each "window" had five ports both to support and to align the U-shaped probes (Figure 14). It is important to mention as well that the positions of the probes was not the same for the two opposite "windows". The U-shaped probe positions were horizontal for one "window" and vertical for the other one. This type of probe

distribution (Figure 14) allowed the bubble measurement on five points at a given level and at least one point before and one after the bubble contacted the horizontal row of probes.

Concerning the second section of the fluidized bed column, described in Figure 15, it is possible to observe that the main characteristics (diameter and height) were the same as those of the "test section". The only difference was that the "measuring windows" were omitted in this section of the column. The third section had 60 cm. in length and six pressure taps spaced 10 cm.

The disengaging section was situated on top of the fluidized bed where the liquid was collected and recycled back to the liquid storge tank. It is important to point out that the entrained particles were kept inside the fluidized bed by a screen fixed in the overflow weir. Here again a 100 mesh stainles steel screen was used. The disengaged gas was vented from the top of the column. Finally, it is interesting to mention that on top of the overflow weir, there was another section of column, a safety device to be used in case an uncontrolled liquid level built up in the fluidized bed.

4.0 Experimental Results

4.1 Bubble Measurements in Three-Phase Fluidized Beds Using the Absorption Photometric Technique. Bidimensional Column.

The first series of runs using the absorption photometric techniques, - two laser beams crossing the bidimensional plexiglass column (Figure 1) - were completed in December 1982. These runs were oriented to a full test of the double channel data acquisition system in conjunction with the bidimensional three-phase fluidized bed in operation. The following liquid and gas superficial velocities were used:

V_ℓ = 1.28 cm/s Vg = 2.10 cm/s

V_ℓ = 1.51 cm/s Vg = 3.50 cm/s

Typical results for the lower and upper channels are reported in Figures 16 and 18. It is possible to observe there that the noise level in those experiments was reduced enough to be compatible with a detailed analysis of bubble phenomena in a three-phase fluidized bed. It is important to mention, however, that further modifications of the data acquisition system in December, 1982 reduced the ± 4.5% noise band (Figures 16 and 18) to ±1.5%.

It is interesting to point out on Figure 16 and 18 a clear biunivocal correspondance between the signals of the two channels, i.e. a bubble signal at the lower channel can be easily identified by the signal shape at the upper channel. Particularly in the case of the absorption photometric technique the use of the two photodetectors, located 7.6 cm apart, allowed a good estimation of bubble velocities.

Figures 17 and 19 give an example of the signals involved on bubble velocity calculations. In those figures the time scale was expanded to report the accuracy and bubble detail obtained with our data acquisition system. The second group of runs (systematic runs) using the absorption photometric technique, two laser beams (6 cm. apart) crossing the bidimensional bed, was developed in February, 1983. Sand particles having a 210μm average size were used as the solid. These runs involved two main operating conditions:

Condition 1 V_ℓ = 1.13 cm/s Vg = 4.38 cm/s

Condition 2 V_ℓ = 1.51 cm/s Vg = 7.30 cm/s

It may be observed that a typical relationship interrelating bubble velocity and the bubble characteristic dimension (bubble cord in the axial direction) was found (Figure 20). Moreover, it is important to mention that the slopes of the straight lines, in the $\log V_b$ - $\log \ell$ diagram are in the range of values reported in the literature for three-phase fluidized beds (Section 4.2) for correlations involving bubble sizes and bubble velocities. In summary, the experiments in the bidimensional column involving the absorption photometric techique, allowed us, during the first phase of the present contract, to successfully develop the data acquisition facility and the laser-optic-photodetector system.

4.2 Bubble Measurements in Three-Phase Fluidized Beds using the U-Shaped Fiber Optic Probe. Bidimensional Column

4.2.1 The data obtained from the four U-shaped fiber optics probes, whose geometry and design was described in Section 3.3, was processed on an HP8926 microprocessor using the computer programs reported on the Appendices 2 and 3. Glass beads of 335 μm were used as the solid phase in these systematic runs. Typical square wave signals recorded when a gas bubble crossed the probes is shown in Figure 21 and 22. The bubble velocity and axial bubble length (bubble cord) were acquired from the signals coming from the two central probes. This analysis involved the definition of the starting and the ending points of each signal. With this information, the mean value (estimated with the first statistical moment) and the duration of each signal were calculated. Then the bubble velocity was evaluated considering the distance between the two probes and dividing it by the separation of the two mean values. Once the bubble velocity was obtained the axial bubble lengths were calculated from the duration of either signal. An average bubble length was then defined.

A careful screening of the experimental data was performed. Only the signals coming from the central probes and showing a standard deviation of the square waves smaller than 10% were accepted for further analysis. With this constraint, virtually all the bubbles selected were travelling in a straight upward fashion. In addition, the signals coming from the two lateral probes were used as guidelines

in selecting suitable bubble signals and were also employed in the process of estimating the central buble cord. Assuming, as a first approximation, that the bubbles have a cap of spherical shape (assumption to be verified later on) the shape and size of the bubble were reconstructed using the top three probes (Figure 23). The equations employed to perform the central bubble cord estimation, based on geometric considerations, were:

- Central Bubble Cord

$$L = R - (y - b_1) \tag{1}$$

- Radius of the Spherical Cap

$$R = (x^2 + y^2)0.5 \tag{2}$$

- Characteristic Dimensions of the Spherical Cap

$$x = [(a_4{}^2+b_4{}^2)b_3 - (b_3{}^2+a_3{}^2)b_4]/$$

$$[2(a_4b_3 - a_3b_4)] \tag{3}$$

$$y = (a_3{}^2+b_3{}^2 - 2a_3x)/2b_3 \tag{4}$$

4.2.2 Relatively high liquid and gas flow rates were used to test the fiber optic sensor in the bidimensional column. The superficial liquid

velocity ranged from 0.75 to 2.26 cm/s while the superficial gas velocity was fixed at 1.9 cm/sec. The observed variations of bubble velocity with respect to the axial bubble length are shown in Figure 24. Since relatively high liquid fluidization velocities were employed, in a bed constituted of fine particles, the effect of the liquid flow rate was quite low. In fact the data taken under a variety of conditions appeared to be bunched around a single straight line. Linear regression analysis was applied to obtain the relationship between the bubble velocity and the axial bubble length. The correlation obtained is as follows:

$$V_b = \alpha \, \ell^{\beta} \qquad (5)$$

$\alpha = 37.92$ $\beta = 0.6592$

regression correlation: 0.7512

Standard deviation: 17.38 cm/s

The bubble data were further treated considering three separate bubble groups generated under different liquid velocities: V_ℓ = 0.752 cm/s, V_ℓ = 1.504 cm/s, V_ℓ = 2.256 cm/s (Table 1, Runs 1a, 2a and 3a). The correlation of the bubble velocity with the measured axial bubble length showed different α and β values. An important result was that the β parameters were progressively increasing with the liquid velocity ranging from 0.462 to 0.749. The lowest β is close to the 0.5 power predicted through the Davies-Taylor relationship and to the β found by Henriksen and Ostergaard (1974). The highest β is well within the values of β for the three phase

fluidized beds (Kim et al. 1977). At the same time it was noticed that the correlation of the data was improved with the increase of the liquid velocity. In fact, the regression coefficients reported in Table 1 changed from 0.5473 to 0.8764 when V_ℓ was varied from 0.752 cm/s to 2.256 cm/s. As mentioned above, the correction of the measured bubble length to obtain the central bubble cord was attempted in the present study based on the assumption that the shape of the bubble was a spherical cap. When performing this correction the information obtained from diferent operating conditions was also treated separately in Runs 1, 2 and 3. The summary of these results and the resulting coefficients α and β for V_b correlation is shown in Table 1 under the labels 1b, 2b and 3b. For all three runs the regression coefficients did not improve when the correlation of V_b with the bubble central cord, estimated through the spherical cap bubble shape, was intended. This possibly indicates the lack of adequacy of the spherical cap assumption for the bubbles considered here. At the same time with the bubble cap radius, the bubble included angle was estimated and the gas bubbles were classified into three groups according to their shape: 1) $100° < \theta < 140°$, 2) $140° < \theta < 360°$ and 3) $\theta > 360°$ (slug type, $L > 2R$). This classification was considered because 100° - 140° is the typical reported included angle, for air bubbles in three phase fluidized bed (Henriksen and Ostergaard (1974)). The results obtained are given in Table 2, which shows the dominant occurrence of bubbles of groups 2 and 3. In fact, the bubbles recorded showed that the bubbles with $\theta > 140°$ were 9 out of 11 in Run 1; 16 out of 19 in Run 2 and 7 out of 9 in Run 3.

Moreover, the relative abundance of the slug type bubbles of group 3 ($L > 2R$), 45% for Run 1, 37% for Run 2 and 33% for Run 3 also suggests, on this series of runs, the weakness of the spherical cap assumption in approximating the bubble shape. The relative small distance (40 cm) between the bubble gas injector and the plexiglass window, holding the four U-shaped fiber optic probes, could possibly explain the types of bubble shapes observed in the present contribution.

4.3 Hold-Up Estimation for the Different Phases in Three-Phase Fluidized Beds Using the Pressure Profiles Obtained with the Data Acquisition System. Bidimensional Column

The individual hold-ups of the different phases (gas, liquid and solid) in three-phase fluidization may be determined using the following set of equations:

$$\varepsilon_s = \frac{M_s}{A\, H_b\, \rho_s} \quad \text{(fraction of solids)} \qquad (6)$$

$$\varepsilon g = \frac{\rho_\ell\left(1 - \frac{M_s}{A\, H_b \rho_s}\right) + \frac{M_s}{A\, H_b} - \frac{\Delta P_b}{H_b} \cdot \frac{g_c}{g}}{(\rho_\ell - \rho g)} \quad \text{(fraction of gas)} \qquad (7)$$

$$\varepsilon_\ell = \frac{\frac{\Delta P_b}{H_b} \cdot \frac{g_c}{g} - \rho_g\left(1 - \frac{M_s}{\rho_s H_b \rho_s}\right) - \frac{M_s}{A\, H_b}}{(\rho_\ell - \rho_g)} \quad \text{(fraction of liquid)} \qquad (8)$$

The derivation of these equations are given in Appendix 5 of the present report. It may be observed that those expressions involve several parameters such as Ms (mass of catalyst), A (cross sectional area of the column), H_b (height of the bed), ρ_s (density of the solid), ρ_g (density of the gas), ρ_ℓ (density of the liquid) and $\frac{\Delta P_b}{H_b}$ (pressure drop per unit length). Some of these parameters are known, for the case of our experiments: Ms = 7000 g., A = 167.7 cm^2 ρ_s=2.5 g/cm^3, ρ_ℓ=1.09cm^3, ρ_g=1.55.$10^3 g/cm^3$. The others, H_b and $\frac{\Delta P_b}{H_b}$, must be determined experimentally. In fact, using the data acquisition system developed by us, for measuring pressure profiles in fluidized beds (Section 3.6), and the computer routine of Appendix 4, the height of the dense fluidized bed was defined. For instance, Figure 10 shows that with the pressure data points obtained at different bed levels and with a numerical regression technique the characteristic $\frac{\Delta P_b}{H_b}$ straight lines (above the bed and in the bed itself) were defined. The intersection of the two straight lines gives, for the operating condition V_ℓ = 1.504 cm/s and Vg = 1.519 cm/s of Figure 10, an H_b = 42.22 cm. The other parameter required for εg and ε_ℓ estimations, $\frac{\Delta P_b}{H_b}$, was calculated with the slope of the straight line between 0-42.2 cm. Consequently with this method it is possible to estimate εg = 0.1832, ε_ℓ= 0.4214 and ε_s = 0.3955 for the case reported in Figure 10.

4.4 Bubble Measurement in Three-Phase Fluidized Beds Using the U-Shaped Probes. Cylindrical Column

Several modifications were introduced to the U-shaped probe arrangement when the runs in the bidimensional column were completed and the bubble measurements in the cylindrical column were tackled. Those modifications are described in Section 3.7 and Figure 14. Probes 1 and 2, separated 0.952 cm. recorded bubbles and allowed the measurement of both bubble velocities and bubble characteristic lengths. In the same way that it was done for data obtained in the bidimensional column, only the square waves resulting from the fiber optic probes, showing a second statistical moment (variance) differing in less than 10%, were considered for further processing. This means that only the bubbles ascending essentially upwards were selected for the estimation of V_b. For the bubbles fulfilling those conditions, the first statistical moment (mean) was calculated. Later on, the bubble velocity was evaluated dividing the probe separation by the time difference between the two means. Finally the bubble characteristic length (bubble cord) was asessed multiplying V_b by the duration of the square waves.

Figure 31 is an example of an HP9826 microprocessor report where the typical square waves recorded by the U-shaped probe - photodetector - microprocessor facility in the cylindrical bed are shown. The different characteristic times (mean, start, end of the perturbation) are given too. Finally, in Figure 31, the V_b and ℓ values assessed with those time parameters are given at the bottom of the HP9826 microprocessor report.

It is important to stress that the same type of data acquisition technique was used in each of the systematic runs conducted in the bidimensinal column during the present program. Figures 25, 27 and 29 were then generated using the equations (6),(7) and (8) and the computer method reported on the previous paragraph. In those figures it is possible to observe how ε_ℓ, εg and $(\varepsilon_\ell + \varepsilon g)$ fractions vary with the liquid velocity V_ℓ for a given Vg value. For instance, the gas hold-up, εg tends to increase with V_ℓ. However, the effect is much more evident for Vg = 1.519 cm/s and Vg = 1.898 cm/s than for Vg = 2.278 cm/s. In opposite, the liquid fraction ε_ℓ steadily increase with V_ℓ for the various Vg considered. This gives a combined $(\varepsilon_\ell + \varepsilon g)$ term always growing with V_ℓ. Because the relationship between $(\varepsilon_\ell + \varepsilon g)$ and ε_s, $\varepsilon_s = 1 - \varepsilon_\ell - \varepsilon g$, a decreasing solid hold-up or in other words an expanded bed will result when V_ℓ increases. The last observations were certainly confirmed in Figures 26, 28 and 30 where the total height of the bed, H_b, against the Reynolds number, for a solid particle suspended in a liquid stream ($Re_\ell = (V_\ell . dp . \pi_\ell)/\mu_\ell$), were reported. It may be observed in those figures a progressive growth of H_b with Re_ℓ.

Then as a consequence of our systematic studies in the bidimensional column, using the pressure transducer data acquisition system, correlations are now available for estimating the volumetric fractions (hold-ups) occupied by the various phases in a three-phase fluidized bed constituted by water, air and 335μm glass particles.

4.5 Bubble Frequency in Three-Phase Fluidized Bed. Cylindrical Column.

Another important application of the U-shaped probe, consisted of its use for the evaluation of the bubble frequencies at different positions in the three-phase fluidized bed. It is important to point out that this type of application has an extreme interest to evaluate, for instance, the adequacy of the grid design and the gas distribution in a three-phase fluidized bed.

In fact, during the periods of data acquisition in the cylindrical column probes 1 and 2 (Figure 14) recorded the bubbles for periods of about 120-240 seconds. Some of those square waves, fulfilling special conditions in terms of their variance (Section 4.4) were also selected for V_b and ℓ evaluations. However, the entire bubble spectra, fromm both the upper and lower channel, as given for example in Figures 33, 34, 35 and 36, were employed for estimating the bubble frequency. The signals of Figures 33, 34, 35 and 36 corresponded to the signals coming from the U-shaped probes. They were observed when bubbles were generated by a single bubble injector located in the center of the grid at 52.5 cm from the sensor position. It is apparent from Figure 32 and Table 3, which summarizes the bubble frequency results that the region of high bubble frequency is limited to a r/R_c ratio between 0-0.25. Outside this region of the bed the bubble frequency decreased sharply certainly indicating the convenience of a multiple gas injector device for uniform gas distribution.

A logic following step in our program was to employ the U-shaped probes for assesing the performance of a multiple gas injector in a three-phase fluidized bed. Basically the same gas flow used for one injector was now split in four gas flows and fed to four injectors, positioned in the grid of the bed with the configuration given in Figure 11. Again, with the information coming from the lower and upper channels (probes 1 and 2) the bubble frequencies were estimated. The various results under the form of bubble spectra are given in Figures 38, 39, 40, 41, 42, 43, 44, 45, 46, 47, 48, 49 and 50. Figure 37 and Table 4 summarize those results. It is shown that a better gas distribution, more uniform bubble frequency with radial position, is obtained with the four injectors. However, it can also be observed in Figure 37 that the superficial liquid velocity, V_ℓ, strongly affect the bubble distribution function. In fact, increasing V_ℓ from 0.389 cm/s to 1.556 cm/s, the state of the bed changed from a bed showing a well distributed gas to a bed with a much higher gas flow in the center region.

In brief, it is proved through those runs that the U-shaped probe-microprocessor unit not only has the versatility to be used to determine bubble velocities, bubble cords, hold-ups of the different phases (gas,solid, liquid), but it also has the peculiar ability to allow the evaluation of effective gas distribution in the cross section of the bed. This certainly permits the direct assessment of the performance of a given gas injector configuration for a given set of operating conditions. All this represents a key advantage for a probe that could be implemented for large industrial three-phase fluidized bed reactors.

4.6 Correlations of Bubble Velocity with Respect to the Characteristic Bubble Length in Three-Phase Fluidized Bed. Cylindrical Column.

A significant effort was done at the end of the present program to derive correlations between the bubble velocity and the characteristic bubble length from the data obtained in the cylindrical column. A first attempt involved the development of correlations for each one of the particular operating conditions studied. The various cases are presented in Figure 51 (single gas injector positioned at $r/R_c = 0$) and Figure 52, 53, 54, 55 (multiple gas injectors located in the grid with the distribution described in Figure 11). It is possible to observe, both in those figures and Table 5, that the β parameter laid in a narrow range 0.40-0.42, approaching the 0.5 value given by Davies-Taylor theory. Those β parameter values between 0.40-0.42, are certainly lower than the β's ($\beta = 0.659$) obtained for similar conditions in the bidimensional column. (Section 4.2). This fact makes us believe that the wall effect was a significant one for the experiments conducted in the bidimensional bed. This possibility is also supported by two observations:

- It was apparent from the bubble spectra that bubbles have a much more stable path in the cylindrical column than in the bidimensional bed. In the latter case bubbles tend to swing frequently making bubble detection a much more difficult task.
- The regression coefficients obtained for the different runs in the cylindrical column reported in Figures 52, 53, 54 and 55, ranged between 0.79 - 0.91 (Table 5). This is a higher regression correlation coefficient that the 0.751 value obtained in the bidimensional bed.

All those findings certainly fully support the strategy selected for the present program involving first a preliminary development of the U-shaped probe in a bidimensional column and later on an extensive testing of the sensor in a cylindrical fluidized bed.

Finally, it is important to mention as well that the observed trends described above concerning β and the regression coefficients were confirmed when the different V_b and ℓ values, obtained for the various liquids flows and type of injectors, were plotted together (Figure 56 and 57). The resulting correlation showed a similar β value (β = 0.425-0.429) with respect to the ones obtained for the individual conditions, as well as a similar correlation coefficient (correlation coefficient = 0.84). This seemed to confirm that for the conditions analyzed in the present program, the liquid flow rate and the gas injector configuration have little effect on the $V_b = \alpha \ell^{\beta}$ correlations derived for the cylindrical three phase fluidized bed.

5.0 ACTIONS INDICATED IN THE ORIGINAL WORK STATEMENT NOT COMPLETED

5.1 "Use of Coal Particles" (Item 1)

Instead of coal particles of 250 μm, sand (210 μm) and glass beads (335 μm) of similar size were used in the experiments. Because this modification does not affect significantly the fluid dynamics of the bed, we decided in consultation with Dr. D. Liu, CANMET Scientific Authority, that this change was suitable for the present program.

5.2 "Use of CO_2 or a denser gas".(Items 6 and 7)

The various runs of the present program were conducted with air instead of CO_2 or denser gases. This direction was taken to quickly generate a significant amount of data to show the peculiar versatility of the U-shaped fiber optic sensor. With this exploratory strategy in mind several actions not included in the original proposal were undertaken: a) the development of a powerful data acquisition system (interface-microprocessor facility) able to be implemented, in conjunction with the U-probes, in a large scale hydrocracking unit (Sections 3.1, 3.3 and 3.6), b) the use of several fiber optic sensors (only two were proposed originally) to characterize the bubble shapes in three phase fluidized beds (Section 4.2), c) the use of the same data acquisition system, developed to measure bubble velocities, to assess bed heights and hold-ups (Section 4.3), d) the application of the U-shaped probe to determine the radial distribution of the bubble frequency in order to test the adequacy of a given grid design in an industrial three phase fluidized bed (Section 4.5).

5.3 "Development of a Mathematical Model for a hydrocracking reactor". (Items 8 and 16).

Concerning these two actions we would like to state the following:

- The preliminary development of the hydrocracking reactor model was completed in April 1983 and described in detailed in the Progress Report No. 6.

- Following the suggestions of Dr. D. Liu, Scientific Authority, the full development of the hydrocracking reactor model was not undertaken. This direction was taken considering Dr. Liu's concerns that a completion of this task could interfere with confidential aspects of the CANMET process.

6.0 REPORT OF THE RESULTS OF THE PROGRAM

Considering the technical success achieved during the present program developing the U-shaped optical fiber probe for three-phase fluidized bed reactors one presentation was coordinated for 1983 [de Lasa et al. (1983). In this presentation the main characteristics of the U-shaped fiberoptic sensor as well as its ability to measure bubble phenomena was described. The possibility of using a multiple U-shaped probe arrangement to characterize bubble shapes was also reported. At the same time, in September, 1983, a manuscript entitled "Bubble Measurement in Three-Phase Fluidized Beds Using a U-Shaped Optical Fiber" was sent to the Canadian Journal of Chemical Engineering in view of publication. The paper was accepted in November, 1983. The paper will be published in the Canadian Journal of Chemical Engineering in the April 1984 issue.

7.0 FURTHER RESEARCH PLANNED IN THREE PHASE FLUIDIZED BEDS

Further actions, going beyond the objectives of the present program, are currently being undertaken to employ the U-shaped sensor in fluidized beds

constituted by larger particles (bigger than 210-335 μm) and various operating conditions. We plan to report the results of this new phase of research in two communications (Lee et al. (1984a), (1984b)).

8.0 CONCLUSIONS

- A novel multiple fiber optic device was successfully designed and its capability for measuring bubble characteristics (bubble length, central bubble cord and bubble velocities) in three-phase fluidized beds was fully confirmed. The multiple fiber optic device was extensively tested in both bidimensional and cylindrical columns.

- Each one of the probes of this promising bubble sensor was bent into a special U geometry in order to appropriately balance the light transmitted and reflected each time that a bubble contacted the probes.

- An auxiliary data acquisition system was also successfully developed in order to process the data obtained from the probes. The same data acquisition system was employed, in combination with a pressure transducer and a Scanivalve to systematically estimate the hold-ups of the gas, liquid and solid phases. In this way, the crucial hold-up information, giving the overall fluid dynamic state of the bed, was derived.

- The entire bubble spectra, as recorded by the U-shaped probes in the cylindrical columns was also employed to assess the variation of the bubble frequency with the bed radial position. This peculiar ability of our U-shaped probe-data acquisition system, establishing the distribution of the gas in the bed for a given configuration of gas injectors, is of extreme importance for the operation of industrial three-phase fluidized bed reactors.

- The significant technical results of the present program encouraged us to apply the fiber optic sensor, based on a U-shaped configuration to strongly absorging media (case of the heavy oil). In fact a program has been recently proposed by us to Energy, Mines and Resources (de Lasa and Bergougnou, 1983) to secure the continuation of the the present research effort. This future research activity will involve an extensive test of the U-shaped probe under special conditions - hot fluidized bed (600°C) using nitrogen as the fluidizing media - that will mimic the operation of the CANMET hydrocracking process.

9.0 ACKNOWLEDGEMENTS

We wish to thank the generous funding of this research by Energy, Mines and Resources Canada. The significant support of the Natural Sciences and Engineering Research Council (NSERC) and the University of Western Ontario, which provided the funds for the components of the data acquisition system (microprocessor-multiprogrammer), is also very much appreciated

The contractual supervision and the positive criticism of Dr. Dirkson Liu and Dr. David Patmore from CANMET deserve special acknowledgement. Particularly, we would like to thank Dr. Dirkson Liu who suggested to us in January, 1983 the possibility of bending fiber optics to develop a bubble sensor.

The kind assistance of the following staff members of the Faculty of Engineering Science at the University of Western Ontario is greatly appreciated: Mr. R. Kaeger, Mr. H. Cook and Mr. R. Stuart (Engineering Shop), Mr. E. Price and Mr. A. Dieroff (Engineering Stores); Mrs. A. Leitch (Secretarial Services), Mr. J. Watkinson and T. Hunt (Electronic Shop).

10.0 NOTATION

a_1 abscissa of point 1 (Figure 4) (cm)

a_2 abscissa of point 2 (Figure 4) (cm)

a_3 abscissa of point 3 (Figure 4) (cm)

a_4 abscissa of point 4 (Figure 4) (cm)

A	cross sectional area of the column (cm^2)
b_1	ordinate of point 1 (Figure 4) (cm)
b_2	ordinate of point 2 (Figure 4) (cm)
b_3	ordinate of point 3 (Figure 4) (cm)
b_4	ordinate of point 4 (Figure 4) (cm)
dp	particle size (μm)
g	gravity acceleration (cm/s)
H_b	total height of the bed (cm)
ℓ	measured axial bubble length (cm)
L	bubble central cord (cm)
M_s	total mass of solid particles (Kg)
r	radial position in the cylindrical column (cm)
R	radius of the spherical cap (cm)
R_c	radius of the cylindrical column (cm)
Re_ℓ	Reynolds of the particle immerse in a liquid phase: $(V_\ell . \rho_\ell . dp)\mu$
V_b	relative velocity of the bubble with respect to the liquid (cm/s)
V_ℓ	superficial liquid velocity (cm/s)
Vg	superficial gas velocity (cm/s)
x	characteristic abscissa giving the distance between the central probe and the center of the circumference containing the spherical cap (Figure 4) (cm)
y	characteristic ordinate giving the distance between the central probe and the center of the circumference containing the spherical cap (Figure 4)(cm)

α coefficient of the bubble velocity correlation (eq. 5)

β coefficient of the bubble velocity correlation (eq. 5)

ρ_g density of the gas (g/cm^3)

ρ_ℓ density of the liquid (g/cm^3)

ρ_s density of the solid (g/cm^3)

ΔP_b pressure drop (KPa)

θ bubble included angle

ε_g volumetric fraction of gas (cm^3 gas/cm^3 reactor)

ε_ℓ volumetric fraction of liquid (cm^3 liquid/cm^3 reactor)

ε_s volumetric fraction of solids (cm^s solid/cm^3 reactor)

μ_ℓ viscosity of the liquid (g/(cm.s))

9.0 BIBLIOGRAPHIC REFERENCES

- de Lasa, H.I., S.L.P. Lee and M.A. Bergougnou, "Application of a Photometric Technique to the Study of Three-Phase Fluidized Beds". Proceedings CSChE Meeting Vol. 2, Toronto (1983).
- de Lasa, H.I., S.L.P. Lee and M.A. Bergougnou, "Bubble Phenomena in Three-Phase Fluidized Beds Using a U-Shaped Optical Fiber". Accepted Canadian Journal of Chemical Engineering, November (1983).
- de Lasa, H.I. and M.A. Bergougnou, "Development of a U-Shaped Fiber Optic Sensor for Three-Phase Fluidized Beds Used in the Hydrocracking of Heavy Oils". Research Proposal Submitted to the EMR Research Agreement Program on November (1983).
- Henrikson, H.K. and K. Ostergaard, "Characteristics of large two-dimensional air bubbles in liquids and in three-phase fluidized beds". The Chem. Eng. J., 7, 141-46 (1974).
- Ishida, M., A. Nishiwaki, and T. Shirai, "Movement of Solid Particles around Bubbles in Three-Dimensional Fluidized Bed at High Temperatures". "Fluidization". Ed. by J. Grace and J. Matsen, Plenum Press. 357-64 (1980).
- Ishida, M. and H. Hatano, "The behaviour of gas and solid particles in a gas-solid fluidized bed detected by optical fiber probes". Proceedings Fourth International Fluidization Conference, Japan 181-8 (1983).
- Kim, S.D., C.G.J. Baker, and M.A. Bergouignou, "Bubble characteristics in three phase fluidized beds". Chem. Eng. Sci, 32, 1299-306, (1977).

- Lee, S.L.P., H.I. de Lasa and M.A. Bergougnou, "A U-Shaped Fiber Optic Probe to Study Three-Phase Fluidized Beds" Submitted for the AIChE Meeting, Fluidization Session, San Francisco (1984a).
- Lee, S.L.P., H.I. de Lasa, and M.A. Bergougnou. "Bubble Phenomena in Three-Phase Fluidized Beds Viewed by a U-Shaped Fiber Optic Probe'. Submitted for the 15th Annual Meeting Fine Particle Society, Florida (1984b).
- Park, W.H., W.K. Kang, C.E. Capes, and G.L. Osberg, "The properties of bubbles in fluidized beds of conducting particles as measured by an electroresistivity probe". Chem. Eng. Sci., 24, 851-65 (1969).
- Rigby, G.R., G.P. van Blockland, W.H. Parks, and C.E. Capes, "Properties of bubbles in three phase fluidized beds as measured by an electroresistivity probe". Chem. Eng. Sci. 25, 1729-41 (1970).
- Stewart, P.S.B. and J.F. Davidson, "Three-phase fluidization: water, particles and air". Chem. Eng. Sci. 1 , 319-21 (1964).

Appendix No. 1

Hewlett-Packard 9826 Microprocessor Program

"Bubble Detection Using a Single Data Acquisition Channel"

```
!TEST PROGRAM PL11 FOR BUBBLE OBSERVATION"
OPTION BASE 1
COM INTEGER N,Ttot,J
INTEGER V(18000),B(5,2)
N=18000
INPUT "RETRIEVE(1) OR NEW EXPERIMENT(2)?",P1
IF P1=2 THEN 120
INPUT "FILE NAME OF DATA ?",Name$
INPUT "PROTECT CODE ?",R$
N$=Name$&"<"&R$&">"
ASSIGN @Path TO N$
ENTER @Path;V(*)
ASSIGN @Path TO *
INPUT "FILE NAME OF TIME ?",Time$
INPUT "PROTECT CODE ?",R$
T$=Time$&"<"&R$&">"
ASSIGN @Path TO T$
ENTER @Path;Ttot
ASSIGN @Path TO *
DISP Ttot
WAIT 5
BEEP 244.14,.1
DISP "DATA HAS BEEN RETRIEVED FROM ";Name$
WAIT 3
GOTO 265
IMAGE #,W
OUTPUT 12 USING 120;-3920
CONTROL 12,3;8192
BEEP 244.14,.5
BEEP 486.28,.1
DISP " PRESS CONTINUE TO START"
PAUSE
Tin=TIMEDATE
ENTER 12 USING 120;V(*)
Ttot=(TIMEDATE-Tin)*1000
DISP "TOTAL MEASURING TIME",Ttot
WAIT 3
INPUT "ASSIGN FILE NAME !!",File$
INPUT "PROTECT CODE ?",R$
F$=File$&"<"&R$&">"
CREATE BDAT F$,18000,2
ASSIGN @Path TO F$
OUTPUT @Path;V(*)
ASSIGN @Path TO *
!ROTECT File$,R$
INPUT "ASSIGN FILE NAME FOR TIME",Time$
INPUT "PROTECT CODE ?",R$
T$=Time$&"<"&R$&">"
CREATE BDAT T$,1,2
ASSIGN @Path TO T$
OUTPUT @Path;Ttot
ASSIGN @Path TO *
BEEP 244.14,.3
DISP "DATA STORED ON ",File$
WAIT 3
DISP "DATA MASSAGE TIME !!!"
END
```

```
280   IF A>=2048 THEN A=A-4096
285   V(I)=ABS(A-.05)*100
290   NEXT I
295   BEEP 244.14,.3
315   DISP "PICKING BUBBLES !!!"
320   Base=.25
325   J=1
330   I=0
335   IF I=N THEN 500
340   I=I+1
345   IF (V(I)/100.-Base)>.5 THEN
350   B(J,1)=I
355   GOTO 370
360   END IF
365   GOTO 335
370   IF I=N-4 THEN 500
375   I=I+5
380   IF (V(I)/100.-Base)<1 THEN 335
385   IF I=N THEN 500
390   I=I+1
395   IF (V(I)/100.-Base)>5 THEN 445
400   IF I=N-1 THEN 500
405   I=I+2
410   IF (V(I)/100.-Base)<2.25 THEN 335
415   IF I=N-1 THEN 500
420   I=I+2
425   IF (V(I)/100.-Base)>5 THEN 445
430   IF I=N-1 THEN 500
435   I=I+2
440   IF (V(I)/100.-Base)<5 THEN 335
445   IF I=N THEN 500
450   I=I+1
455   IF (V(I)/100.-Base)<0 THEN
460   B(J,2)=I
465   GOTO 480
470   END IF
475   GOTO 445
480   IF I<18000 THEN
485   J=J+1
490   GOTO 335
495   END IF
500   J=J-1
505   BEEP 244.14,.3
510   DISP "DATA HAS BEEN SCANNED WITH CRITERIA 5"
515   WAIT 3
535   PRINTER IS 701
540   PRINT "BEGINNING                    END"
545   FOR K=1 TO J
550   PRINT "B(";K;",1 )=";B(K,1);"      B(";K;",2 )=";B(K,2)
555   NEXT K
560   PRINTER IS 1
580   INPUT "PLOTTING(1) OR LISTING(2) ?",C
585   ON C GOTO 590,600
590   CALL Plotting(V(*),B(*))
595   GOTO 605
600   CALL Listing(V(*),B(*))
605   INPUT "FINISH(1) OR MORE(2) ?",X
610   IF X=2 THEN 580
615   END
```

```
630  SUB Plotting(INTEGER V(*),B(*))
635  COM INTEGER N,Ttot,J
636  Ttot=Ttot/1000.
640  INPUT "FULL SCHEME(1) OR PARTIAL PLOT(2)?",P5
645  IF P5=2 THEN 830
665  PRINT CHR$(12)
670  GINIT
675  GRAPHICS ON
680  WINDOW -200,1800,-10,50
685  AXES 200,10.
690  DEG
695  LDIR 30
700  FOR I=-200 TO 1800 STEP 200
705  MOVE I-80,-7
710  LABEL I
715  NEXT I
720  LDIR 0
725  FOR I=-10 TO 50 STEP 10
730  MOVE -180,I-1
735  LABEL I
740  NEXT I
745  Tspace=Ttot/N
750  MOVE 0,0
755  FOR I=1 TO N
760  X=Tspace*I
765  A=V(I)/100.
770  DRAW X*100,A
775  NEXT I
780  MOVE 500,40
785  LABEL "VOLTAGE(mV) vs. TIME(cSec)"
790  INPUT "HARD COPY(1) OR CRT ONLY(2)",K
795  IF K=2 THEN 815
800  PRINT IS 701
805  DUMP GRAPHICS
810  PRINT IS 1
815  INPUT "DETAIL PLOTTING(1) OR SKIP(2) ?",W1
820  GCLEAR
825  IF W1=2 THEN 1120
830  INPUT "AUTO PLOT(1) OR MANUAL(2) ?",P4
850  IF P4=2 THEN
855  INPUT "TIME RANGE ?",R1,R2
860  GOTO 915
865  END IF
870  FOR K=1 TO J
890  R1=.001*(B(K,1)-2)
895  R2=.001*(B(K,2)+2)
915  R22=R2*100
920  R00=(R1-.1*(R2-R1))*100
925  R33=R1*100
930  R11=(R2-R1)*10
935  GINIT
940  GRAPHICS ON
945  DEG
946  PRINT CHR$(12)
950  WINDOW R00,R22,-2,10
955  AXES R11,2,R33,0
960  LDIR 30
965  FOR I=R33 TO R22 STEP R11
970  MOVE I,-2
```

```
980   NEXT I
985   LDIR 0
990   FOR I=-2 TO 10 STEP 2
995   MOVE R00,I
1000  LABEL I
1005  NEXT I
1010  MOVE R33,0
1015  R111=R1*1000
1020  R222=R2*1000
1025  Tspace=Ttot/N
1030  FOR I=R111 TO R222
1035  X=Tspace*I
1040  A=V(I)/100.
1045  DRAW X*100,A
1050  NEXT I
1055  R33=(R1+.2*(R2-R1))*100
1060  MOVE R33,8
1065  LABEL "VOLTAGE(mV) vs. TIME(cSec)"
1070  INPUT "HARD COPY(1) OR CRT DISPLAY(2) ?",Aa
1075  IF Aa=2 THEN 1095
1080  PRINTER IS 701
1085  DUMP GRAPHICS
1090  PRINTER IS 1
1095  IF P4=1 THEN 1115
1100  INPUT "FINISH(1) OR ANOTHER RANGE(2) ?",Kk
1105  IF Kk=2 THEN 855
1110  GOTO 1120
1115  NEXT K
1120  GCLEAR
1125  SUBEND
1130  ! ****************************************
1140  SUB Listing(INTEGER V(*),B(*))
1145  COM INTEGER N,Ttot,J
1146  Ttot=Ttot/1000.
1150  INPUT "HARD COPY(1) OR CRT LISTING(2) ?",P7
1155  INPUT "AUTO LISTING(1) OR MANUAL(2) ?",P6
1160  IF P7=2 THEN 1170
1165  PRINTER IS 701
1170  IF P6=2 THEN
1175  INPUT "TIME RANGE ?",P1,P2
1180  INPUT "TIME SPACING ?",P3
1181  PRINTER IS 1
1182  INPUT "HARD COPY(1) OR CRT LISTING(2) ?",P8
1183  IF P8=2 THEN 1186
1184  PRINTER IS 701
1185  GOTO 1225
1190  END IF
1195  FOR K=1 TO J
1210  P1=.001*(B(K,1)-2)
1215  P2=.001*(B(K,2)+2)
1220  P3=.001
1221  PRINT B(K,1),B(K,2)
1225  P11=1000*P1
1230  P22=1000*P2
1235  P33=1000*P3
1240  FOR I=P11 TO P22 STEP P33
1245  A=V(I)/100.
1250  PRINT A
1255  NEXT I
```

```
1270  INPUT "FINISH(1) OR ANOTHER RANGE(2) ?",S
1275  IF S=2 THEN 1175
1280  GOTO 1287
1285  PRINT "END OF BUBBLE #":K
1286  NEXT K
1287  PRINTER IS 1
1290  SUBEND
```

Appendix No. 2

Hewlett-Packard 9826 Microprocessor Program

"Data Acquisition Program for Bubble Measurement in Bi-dimensional Three Phase Fluidized Bed Using Four U-Shaped Optical Fiber Probes"

Code of the Program: 4PROB-ACQ1

```
! DATA ACQUISITION PROGRAM, WITH ALL THE DATA AND CONDITIONS STORED
! EXTENDED BASIC BIN "ADQ_D" REQUIRED
OPTION BASE 1
N=10500
INTEGER A(10506,4) BUFFE-
S.001=4096
S.004=16384
S.007=28672
IMAGE #,N
Cu=-4096
Ubl=126
Dte=64
Sve=32
Tme=16
J=0
S=2000
P=1
B=1.E-5
P1=2*(2*S+B)
F=INT(P1)
Sact=INT(2*(2*F+6))
P=2.0
INPUT "*** RUN NUMBER OF THE FIRST DATA FILE ?",Ran1
INPUT "*** RUN NUMBER OF THE LAST DATA FILE ",Ran2
INPUT "*** NAME OF THE FILE ?",Name$
INPUT "*** PROTECT CODE ?",P$
INPUT "*** DATE ? ( MONTH, DAY, YEAR )",Date
INPUT "*** LIQUID VELOCITY ? ( GPM )",Vliq
Vliq=INT(2502.49*Vliq)  ! CONVERT INTO SI UNIT OF M/SEC WITH SCALE FACTOR
1000
INPUT "*** GAS VELOCITY ? ( SCFM )",Vgas
INPUT "*** PRESSURE OF GAS ? ( PSI )",Press
Vgas=INT(96.6*(14.3+Press)*Vgas  ! unit of m/sec with scale factor of 1000
base on 740 mmHg
Press=INT(689.12*Press)  ! CONVERT INTO SI UNIT OF Pa,N/(M**2) WITH SCALE
FACTOR OF 1/10
INPUT "*** INITIAL BED HEIGHT ? ( INCHES FROM GRID )",Bini
Bini=INT(250*Bini)  ! CONVERT INTO SI UNIT OF M WITH SCALE FACTOR OF 10000
INPUT "*** WEIGHT OF SOLIDS ? (Gram)",Weight
INPUT "*** INJECTOR USED ? ( NUMBER )",Inject
INPUT "*** INJECTOR POSITION ? ( INCHES FROM GRID )",Posinjec
Posinjec=INT(250*Posinjec)  ! CONVERT INTO SI UNIT OF M WITH SCALE FACT
OF 10000
INPUT "*** LOWER PROBE POSITION ? ( INCHES FROM GRID )",Probel
INPUT "*** UPPER PROBE POSITION ? ( INCHES FROM GRID )",Probeu
Probel=INT(250*Probel)  ! CONVERT INTO SI UNIT OF M WITH SCALE FACTOR OF
10000
Probeu=INT(250*Probeu)  ! CONVERT INTO SI UNIT OF M WITH SCALE FACTOR OF
10000
INPUT "* POWER LEVEL OF LOWER PROBE IN AIR ( mW ) ",Plow
Plowair=100*Plow  ! SCALE FACTOR OF 100
INPUT "*** POWER LEVEL OF UPPER PROBE IN AIR ",Pup
Pupair=100*Pup  ! SCALE FACTOR OF 100
INPUT "* POWER LEVEL OF LOWER PROBE IN WATER ? (mW)",Plow
Plowater=100*Plow  !SCALE FACTOR OF 100
INPUT "* POWER LEVEL OF UPPER PROBE IN WATER (mW) ",Pup
Pupwater=100*Pup  ! SCALE FACTOR OF 100
BEEP
DISP "******* PRESS CONTINUE TO START *******"
PAUSE
DISP "******* DATA ACQUISITION !!! *******"
```

```
280     FOR Run=Run1 TO Run2
        GOSUB Data_acq
        V(N+1,1)=Sact
295     V(N+1,2)=Date
300     V(N+1,3)=Vlig
305     V(N+1,4)=Vgas
310     V(N+2,1)=Press
315     V(N+2,2)=Rini
320     V(N+2,3)=Weight
325     V(N+2,4)=Inject
330     V(N+3,1)=Posiinjec
335     V(N+3,2)=Ppropl
340     V(N+3,3)=Pprobu
345     Num$=VAL$(Run)
350     N$=Name$&Num$&"<"&P$&">"
355     CREATE BDAT N$,4*(N+6),2
360     ASSIGN @Path TO N$
365     TRANSFER @Buff TO @Path;COUNT 100048,WAIT
370     ASSIGN @Path TO *
375     ASSIGN @Source TO *
380     ASSIGN @Buff TO *
385     PRINT Name$&Num$;" STORED"
390     NEXT Run
395     DISP "DATA ACQUISITION COMPLETED"
400     STOP
405 Data_acq: !
410     OUTPUT 12 USING 45:Cw+Sye
415     OUTPUT 12 USING 45:Slot1+3072+R
        OUTPUT 12 USING 45:Slot'+P
        OUTPUT 12 USING 45:Slot7+C0
430     OUTPUT 12 USING 45:Cw+Sye+Isi+Tme
435     OUTPUT 12 USING 45:Slot4
440     ASSIGN @Source TO 12;WORD
445     ASSIGN @Buff TO BUFFER V(*);WORD
450     TRANSFER @Source TO @Buff;COUNT 100048,WAIT
455     OUTPUT 12 USING 45:Cw+Sye+Dte
460     OUTPUT 12 USING 45:Slot1+P
465     OUTPUT 12 USING 45:Slot1+3072
470     RETURN
475     END
```

Appendix No. 3

Hewlett-Packard 9826 Microprocessor Program

"Data Processing Program for Bubble Measurement Using the Data Acquisition Program 4 PROB-ACQ1"

Code of the Program: VIVA 7

```
!  VIVA7 ON JULY 10,1983
! FOR PROCESSING DATA OBTAINED FROM "4PROB_ACQ"
! BASE LINES ON ALL CHANNELS ARE SHIFTED TO ZERO
! DIFFERENT CRITERIA SET FOR EACH PROBE
! DATA REJECTED IF NOT REACH REQUIRED CRITERION WITHIN 4 POINTS
! RESULT CAN BE PRINT OUT ON PAPER OR DISPLAYED ON CRT FIRST WITH OPTION 0
F CHECKING AGAIN
! DATA CAN BE RESTORED ON NEW FILE IN COMPACT FORM TO SAVE STORAGE SPACE
OPTION BASE 1
COM N,Disk,Mon,Date,Year
N=12500
ALLOCATE INTEGER V(N+6,4),B(100,2,4),D(100,4),C(4),Crit(4)
!
! INPUT OLD FILE NAME AND RETRIEVE FROM DISK
!
INPUT "NUMBER OF DISK ?",Disk
INPUT "NAME OF DATA FILE ?",Name$
INPUT "PROTECT CODE ?",R$
N$=Name$&"<"&R$&">"
ASSIGN @Path TO N$
ENTER @Path;V(*)
ASSIGN @Path TO *
!
! SELECT BASE LINES FOR DATA PROCESSING
!
DISP "SELECTING BASE LINES"
FOR J=1 TO 4
Sum=0.
I1=1
I2=30
FOR I=I1 TO I2
Sum=Sum+FNVbs(V(I,J))
NEXT I
Base(J)=Sum/30
Square=0.
FOR I=I1 TO I2
Square=Square+(FNVbs(V(I,J))-Base(J))^2
NEXT I
IF Square>5 THEN
I1=I1+30
I2=I2+30
Sum=0.
GOTO 150
END IF
NEXT J
!
! PICK UP PEAKS
!
! SET CRITERION FOR EACH PROBE
Crit(1)=20
Crit(2)=20
Crit(3)=20
Crit(4)=10
DISP "PICKING BUBBLES !!!"
FOR J=1 TO 2
Cr1=.3*Crit(J)
Cr2=.5*Crit(J)
Cr3=.7*Crit(J)
Cr4=Crit(J)
C(J)=1
```

```
300     I=0
305     IF I>=N THEN 455
310     I=I+1
315     IF FNVconv(V(I,J),Base(J))>Cr1 THEN
320     B(C(J),1,J)=I
325     GOTO 340
330     END IF
335     GOTO 305
340     IF I>=N THEN 455
345     I=I+1
350     IF FNVconv(V(I,J),Base(J))<Cr2 THEN 305
355     IF I=N THEN 455
360     I=I+1
365     IF FNVconv(V(I,J),Base(J))>Cr4 THEN 400
370     IF I=N THEN 455
375     I=I+1
380     IF FNVconv(V(I,J),Base(J))<Cr3 THEN 305
385     IF I>=N THEN 455
390     I=I+1
395     IF FNVconv(V(I,J),Base(J))<Cr4 THEN 305
400     IF I=N THEN 455
405     I=I+1
410     IF FNVconv(V(I,J),Base(J))<Cr1 THEN
415     B(C(J),2,J)=I
420     GOTO 435
425     END IF
430     GOTO 400
435     IF I<N THEN
440     C(J)=C(J)+1
445     GOTO 305
450     END IF
455     C(J)=C(J)-1
460     NEXT J
465     GOTO 660
470     !
475     ! PRINT DATE OF EXPERIMENT
480     ! PRINT BEGINNING AND END OF BUBBLES
485     !
490     Mon=INT(V(N+1,2)/1000)
495     Date=INT((V(N+1,2)-1000*Mon)/10)
500     Year=V(N+1,2)-1000*Mon-10*Date
505     PRINTER IS 701
510     PRINT CHR$(10),CHR$(10)
515     PRINT " *** DATE OF EXPERIMENT: ";Mon;"/";Date;"/198";Year
520     PRINT ""
525     PRINT " *** DISK NUMBER: ";Disk
530     PRINT ""
535     PRINT " *** FILE NAME: ";Name$
540     PRINT CHR$(10),CHR$(10)
545     PRINT "                              LOWER CHANNEL"
550     PRINT ""
555     PRINT "BEGINNING OF BUBBLE                  END OF BUBBLE"
560     FOR K=1 TO C(1)
565     PRINT "Blc(";K;",1 )=";B(K,1,1)/500.;"Sec      Blc(";K;",2 )=";B(K,2,1)/50
0.;"Sec"
570     NEXT K
575     PRINT ""
580     PRINT "*** SCANNING CRITERION :";Cri(1)
585     PRINT ""
590     PRINT ""
595     PRINT "                              UPPER CHANNEL"
```

```
600     PRINT ""
605     PRINT "BEGINNING OF BUBBLE                END OF BUBBLE"
610     FOR K=1 TO C(2)
615     PRINT "Buc(":K;")=":B(K,1,2)/500.;"Sec      Buc(":K;")=":B(K,4,2)/50
0.;"Sec"
620     NEXT K
625     PRINT ""
630     PRINT "*** SCANNING CRITERION :":Crit(2)
635     PRINTER IS 1
640     !
645     ! CHOOSE METHOD OF DATA SHOWING
650     !
655     !INPUT "PLOTTING(1) OR LISTING(2) ?",C
660     I=1
665     ON I GOTO 670,680
670     CALL Plotting(V(*),B(*),C(*),D(*),Crit(*),Base(*),Name$)
675     GOTO 685
680     CALL Listing(V(*),B(*),C(*),D(*),Crit(*),Base(*),Name$)
685     !INPUT "FINISH(1) OR MORE(2) ?",X
690     X=1
695     IF X=2 THEN 655
700     END
705     ! ************************************
710     !
715     SUB Plotting(INTEGER V(*),B(*),C(*),D(*),Crit(*),REAL Base(*),Name$)
720     COM N,Disk,Mon,Date,Year
725     REAL Deno,Mean,Tm(40,2),Var(40,2),Sdv(40,2)
730     INTEGER Stor(40,2)
735     Ttot=4.*N/V(N+1,1)
740     !INPUT "FULL SCHEME(1) OR PARTIAL PLOT(2)?",P5
745     P5=2
750     IF P5=2 THEN 1080
755     !
760     ! PLOT DATA THROUGH THE WHOLE TIME RANGE
765     !
770     PRINT CHR$(12)
775     GINIT
780     GRAPHICS ON
785     W1=INT(Ttot)
790     W2=.1*W1
795     WINDOW -W2,W1,-10,50
800     AXES W2,1,0,0,5,5,3
805     DEG
810     LDIR 90
815     FOR I=0 TO W1 STEP W2
820     MOVE I-W1/20,-7
825     LABEL I
830     NEXT I
835     LDIR 0
840     FOR I=0 TO 20 STEP 5
845     MOVE -.8*W2,I-1
850     LABEL I
855     NEXT I
860     FOR I=25 TO 50 STEP 5
865     MOVE -.8*W2,I-1
870     LABEL I-25
875     NEXT I
880     Tspace=4./V(N+1,1)
885     MOVE 0,0
890     FOR I=1 TO N
895     X=Tspace*I
```

```
900     DRAW (.FNVconv(V(I,1),Base(1))
905     NEXT I
910     MOVE 0,25
915     DRAW W ,25
920     MOVE 0,25
925     FOR I= TO N
930     X=Space*I
935     DRAW (.FNVconv(V(I,2),Base(2))+25
940     NEXT I
945     MOVE .2*W1,45
950     LABEL "Response of probe #1 & #2"
955     MOVE .3*W1,-10
960     LABEL "real time, second"
965     LDIR 90
970     MOVE -.05*W2,0
975     LABEL "lower probe,mV"
980     MOVE -.05*W2,25
985     LABEL "upper probe,mV"
990     !INPUT "HARD COPY(1) OR CRT ONLY(2)",X
995     X=1
1000    IF X=2 THEN 1060
1005    PRINTER IS 701
1010    PRINT CHR$(12)
1015    PRINT CHR$(10),CHR$(10)
1020    PRINT " *** DATE OF EXPERIMENT: ";Mon;"/";Date;"/";Year
1025    PRINT ""
1030    PRINT " *** DISK NUMBER: ";Disk
1035    PRINT ""
1040    PRINT " *** FILE NAME: ";Name$
1045    PRINT CHR$(10),CHR$(10)
1050    DUMP GRAPHICS
1055    PRINTER IS 1
1060    !INPUT "DETAIL PLOTTING(1) OR SKIP(2) ?",W1
1065    W1=1
1070    GCLEAR
1075    IF W1=2 THEN 3150
1080    !
1085    ! BOTH CHANNELS PLOTTED ON THE SAME GRAPHICS
1090    !
1095    M=1
1100    FOR I1=1 TO C(1)
1105    FOR I2=M TO C(2)
1110    IF B(I2,1,2)<B(I1,1,1) THEN 1160
1115    IF B(I2,1,2)<=B(I1,1,1)+20 THEN
1120    ! IF BUG(I2,1)<=BLG(I1,1)+80 THEN !FOR LOW FLOW RATE
1125    D(M,1)=B(I1,1,1)
1130    D(M,3)=B(I1,2,1)
1135    D(M,2)=B(I2,1,2)
1140    D(M,4)=B(I2,2,2)
1145    M=M+1
1150    GOTO 1165
1155    END IF
1160    NEXT I2
1165    NEXT I1
1170    M=M-1
1175    !
1180    ! DOUBLE PLOTTING
1185    !
1190    !INPUT "AUTO PLOT(1) OR MANUAL (2) ?",P1
1195    P1=1
```

```
1200  IF R1<>2 THEN
1205  INPUT "TIME RANGE ?",R1,R2
1210  R1=INT(R1*V(N+1,1)/4)
1215  R2=INT(R2*V(N+1,1)/4)
1220  D(K,3)=R2-10
1225  D(K,2)=R1+10
1230  GOTO 1630
1235  END IF
1240  !
1245  ! SELECT QUALIFIED DATA AND PRINT OUT
1250  !
1255  FOR K=1 TO 4
1260  T1=D(K,1)
1265  T3=D(K,3)
1270  T2=D(K,2)
1275  T4=D(K,4)
1280  Vmaxic=FNVconv(V(T1,1),Base(1))  ! PICK UP MAXIMUM VALUES
1285  FOR T=T1+1 TO T3
1290  A=FNVconv(V(T,1),Base(1))
1295  IF A>Vmaxic THEN
1300  Vmaxic=A
1305  END IF
1310  NEXT T
1315  Vmaxuc=FNVconv(V(T2,2),Base(2))
1320  FOR T=T2+1 TO T4
1325  A=FNVconv(V(T,2),Base(2))
1330  IF A>Vmaxuc THEN
1335  Vmaxuc=A
1340  END IF
1345  NEXT T
1350  IF Vmaxuc>Vmaxic THEN
1355  Vmax=Vmaxuc
1360  ELSE
1365  Vmax=Vmaxic
1370  END IF
1375  GOTO 1390
1380  Devia=ABS(1-Vmaxic/Vmaxuc)  ! CHECK CONSISTANCY OF MAXIMUM VALUES
1385  IF Devia>.2 THEN 2860
1390  Duraic=T3-T1   ! CHECK CONSISTANCY OF DURATIONS
1395  Durauc=T4-T2
1400  GOTO 1415
1405  Devia=ABS(1-Duraic/Durauc)
1410  IF Devia>.2 THEN 2860
1415  Areaic=0.  ! CHECK CONSISTANCY OF SIGNAL SHAPES
1420  Areauc=0.
1425  Tic=T1
1430  Tuc=T2
1435  !
1440  ! SKIP THE FIRST FEW POINTS
1445  !
1450  FOR T=Tic TO Tic+2
1455  Areaic=Areaic+FNVconv(V(T,1),Base(1))
1460  NEXT T
1465  FOR T=Tuc TO Tuc+2
1470  Areauc=Areauc+FNVconv(V(T,2),Base(2))
1475  NEXT T
1480  !
1485  ! INTEGRATE AND CHECK POINT BY POINT
1490  !
1495  Tic=Tic+3
1500  Tuc=Tuc+3
```

```
1505  Areaic=Areaic+FNVconv(V(Tic,1),Base(1))
1510  Areauc=Areauc+FNVconv(V(Tuc,2),base(2))
   5  GOTO 1530
1520  Devia=ABS(1-Areaic/Areauc)
1525  IF Devia>.2 THEN 2860
1530  IF Tic=T3 THEN
1535  FOR T=Tuc+1 TO T4
1540  Areauc=Areauc+FNVconv(V(T,2),Base(2))
1545  NEXT T
1550  GOTO 1620
1555  END IF
1560  IF Tuc=T4 THEN
1565  FOR T=Tic+1 TO T3
1570  Areaic=Areaic+FNVconv(V(T,1),Base(1))
1575  NEXT T
1580  GOTO 1620
1585  END IF
1590  Tic=Tic+1
1595  Tuc=Tuc+1
1600  GOTO 1505
1605  !
1610  ! DOUBLE PLOTTING
1615  !
1620  R1=D(K,1)-10
1625  R2=D(K,4)+10
1630  R11=R1*4/V(N+1,1)
1635  R22=R2*4/V(N+1,1)
1640  R33=.1*(R22-R11)
1645  R00=R11-R33
   50 GINIT
1655  GRAPHICS ON
1660  DEG
1665  PRINT CHR$(12)
1670  Vmax=5*(INT(INT(Vmax)/5)+1)
1675  WINDOW R00,R22,-Vmax/5,Vmax
1680  AXES R33,Vmax/10,R11,0,1,2,3
1685  LDIR 90
1690  FOR I=R11 TO R22 STEP R33
1695  MOVE I,-.8*Vmax/5
1700  LABEL DROUND(I,4)
1705  NEXT I
1710  LDIR 0
1715  FOR I=0 TO Vmax STEP Vmax/5
1720  MOVE R11-.8*R33,I-2
1725  LABEL I
1730  NEXT I
1735  MOVE R11,0
1740  FOR I=R1 TO D(K,3)+10
1745  X=I*4./V(N+1,1)
1750  DRAW X,FNVconv(V(I,1),Base(1))
1755  NEXT I
1760  MOVE 4.*(D(K,2)-10)/V(N+1,1),0
1765  FOR I=D(K,2)-10 TO R2
1770  X=I*4./V(N+1,1)
1775  DRAW X,FNVconv(V(I,2),Base(2))
1780  NEXT I
1785  R44=(R11+.2*(R22-R11))
1790  MOVE R44,.9*Vmax
1795  LABEL "Response of probe #1 & #2"
1800  MOVE R11+3*R33,-Vmax/5
1805  LABEL "real time, second"
```

```
1810  LDIR 90
1815  MOVE R11-.55*R33.Vmax/5
1820  LABEL "probes' response, mV"
1825  INPUT "HARD COPY(1) or CRT DISPLAY(2) ?",Aa
1830  IF Aa=2 THEN 1920
1835  PRINTER IS 701
1840  PRINT CHR$(12)
1845  PRINT CHR$(10),CHR$(10)
1850  PRINT " *** DATE OF EXPERIMENT: ";Mon;"/";Date;"/'99";Year
1855  PRINT ""
1860  PRINT " *** DISK NUMBER: ";Disk
1865  PRINT ""
1870  PRINT " *** FILE NAME: ";Name$
1875  PRINT CHR$(10),CHR$(10)
1880  DUMP GRAPHICS
1885  !
1890  ! VELOCITY AND SIZE CALCULATION
1895  !
1900  PRINT CHR$(10),CHR$(10),CHR$(10)
1905  !
1910  ! CALCULATE MEAN & VARIANCE OF LOWER CHANNEL
1915  !
1920  Mean=0.
1925  FOR T=T1 TO T3
1930  Mean=Mean+T*ENVconv(V(T,1),Base(1))/Areal
1935  NEXT T
1940  Tm(K,1)=Mean/500.
1945  Var=0.
1950  FOR T=T1 TO T3
1955  Var=Var+(ENVconv(V(T,1),Base(1))*T^2)/Areal
1960  NEXT T
1965  Var(K,1)=(Var-Mean^2)/2.5E+5
1970  Sdv(K,1)=SQR(Var(K,1))
1975  !
1980  ! CALCULATE MEAN & VARIANCE OF UPPER CHANNEL
1985  !
1990  Mean=0.
1995  FOR T=T2 TO T4
2000  Mean=Mean+T*ENVconv(V(T,2),Base(2))/Areau
2005  NEXT T
2010  Tm(K,2)=Mean/500.
2015  Var=0.
2020  FOR T=T2 TO T4
2025  Var=Var+(ENVconv(V(T,2),Base(2))*T^2)/Areau
2030  NEXT T
2035  Var(K,2)=(Var-Mean^2)/2.5E+5
2040  Sdv(K,2)=SQR(Var(K,2))
2045  !
2050  ! PRINT MEAN,VARIANCE,VELOCITY & BUBBLE SIZE
2055  !
2060  GCLEAR
2065  PRINT "*** BUBBLE #";K
2070  PRINT ""
2075  PRINT "*** STARTING OF LOWER CHANNEL :";DROUND(D(K,1)/500.5);"Sec"
2080  PRINT "*** END OF LOWER CHANNEL :";DROUND(D(K,3)/500.5);"Sec"
2085  PRINT "*** DURATION OF BUBBLE :";Durat
2090  PRINT "*** MEAN=";DROUND(Tm(K,1),5);"Sec"
2095  PRINT "*** VARIANCE=";DROUND(Var(K,1),5);"Sec*Sec"
2100  PRINT "*** STANADAR DEVIATION=";DROUND(Sdv(K,1),5);"Sec"
2105  PRINT CHR$(10)
```

```
2110  PRINT "*** STARTING OF UPPER CHANNEL :";DROUND(D(K,2)/500,5);"Sec"
2115  PRINT "*** END OF UPPER CHANNEL :";DROUND(D(K,4)/500,5);"Sec"
2120  PRINT "*** DURATION OF BUBBLE :";Durauc
2125  PRINT "*** MEAN=";DROUND(Tm(K,2),5);"Sec"
2130  PRINT "*** VARIANCE=";DROUND(Var1(K,2),5);"Sec*Sec"
2135  PRINT "*** STANDARD DEVIATION=";DROUND(Sdv(K,2),5);"Sec"
2140  IF Aa=2 THEN
2145  DISP "*** Press CONTINUE for more !!!"
2150  PAUSE
2155  END IF
2160  Velo=DROUND(1.27/(Tm(K,2)-Tm(K,1)),4)
2165  ON ERROR GOTO 2840
2170  Simp=DROUND(1.27*500/(D(K,2)-D(K,1)),4)
2175  ON ERROR GOTO 2840
2180  PRINT CHR$(10),CHR$(10)
2185  PRINT "*** BUBBLE VELOCITY :";Velo;"cm/Sec     OR";Simp;"cm/Sec"
2190  Diam=DROUND(Velo*(Duralc+Durauc)/(2.*500),3)
2195  Dsimp=DROUND(Simp*(Duralc+Durauc)/(2.*500.),3)
2200  PRINT ""
2205  PRINT "*** AVERAGE BUBBLE SIZE :";Diam;"cm    OR";Dsimp;"cm"
2210  IF Sdv(K,1)>Sdv(K,2) THEN
2215  Devia=ABS(1-Sdv(K,1)/Sdv(K,2))
2220  ELSE
2225  Devia=ABS(1-Sdv(K,2)/Sdv(K,1))
2230  END IF
2235  IF Devia>.1 THEN
2240  PRINT ""
2245  PRINT "BUBBLE SWING TOO MUCH !!!"
2250  END IF
2255  IF Aa=2 THEN
2260  DISP "*** Press CONTINUE for more !!!"
2265  PAUSE
2270  END IF
2275  FOR J=3 TO 4
2280  IF Aa=2 THEN 2325
2285  PRINT CHR$(12)
2290  PRINT CHR$(10),CHR$(10)
2295  PRINT " *** DATA OF EXPERIMENT: ";Mon;"/";Date;"/'89";Year
2300  PRINT ""
2305  PRINT " *** DISK NUMBER: ";Disk
2310  PRINT ""
2315  PRINT " *** FILE NAME: ";Name$
2320  PRINTER IS 1
2325  R1=T1-10  ! PLOT CHANNEL 3 & 4 AS REFERENCES
2330  R2=T4+(T2-T1)+10
2335  Stor(K,1)=R1
2340  Stor(K,2)=R2
2345  R11=R1*4./V(N+1,1)
2350  R22=R2*4./V(N+1,1)
2355  R33=(R22-R11)/10
2360  R00=R11-R33
2365  GINIT
2370  GRAPHICS ON
2375  DEG
2380  WINDOW R00,R22,-Vmax/5,Vmax
2385  AXES R33,Vmax/10,R11,0,1,2,3
2390  LDIR 30
2395  FOR I=R11 TO R22 STEP R33
2400  MOVE I,-.8*Vmax/5
2405  LABEL DROUND(I,4)
2410  NEXT I
```

```
2415  LDIR 0
2420  FOR I=0 TO Vmax STEP Vmax/5
2425  MOVE R11-.8*R33,I-2
2430  LABEL I
2435  NEXT I
2440  MOVE R11,0
2445  FOR I=R1 TO R2
2450  X=I*4./V(N+1,1)
2455  DRAW X,FNVconv(V(I,J),Base(J))
2460  NEXT I
2465  R44=(R11+.2*(R22-R11))
2470  MOVE R44,.9*Vmax
2475  LABEL "Response of probe #";J
2480  MOVE R11+3*R33,-Vmax/5
2485  LABEL "real time, second"
2490  LDIR 90
2495  MOVE R11-.65*R33,5
2500  LABEL "probe response, mV"
2505  IF Aa=2 THEN
2510  GCLEAR
2515  GOTO 2560
2520  END IF
2525  PRINTER IS 701
2530  PRINT CHR$(10),CHR$(10),CHR$(10)
2535  PRINT "REFERENCE CHANNEL #";J
2540  PRINT ""
2545  PRINT "Original Base Line:";Base(J)
2550  PRINT CHR$(10)
2555  DUMP GRAPHICS
2560  Cr1=.3*Crit(J)
2565  Cr2=.5*Crit(J)
2570  Cr3=.7*Crit(J)
2575  Cr4=Crit(J)
2580  I=R1
2585  IF I>=R2 THEN 2715
2590  I=I+1
2595  IF FNVconv(V(I,J),Base(J))>Cr1 THEN
2600  B(K,1,J)=I
2605  GOTO 2620
2610  END IF
2615  GOTO 2585
2620  IF I>=R2 THEN 2715
2625  I=I+1
2630  IF FNVconv(V(I,J),Base(J))<Cr2 THEN 2585
2635  IF I=R2 THEN 2715
2640  I=I+1
2645  IF FNVconv(V(I,J),Base(J))>Cr4 THEN 2680
2650  IF I=R2 THEN 2715
2655  I=I+1
2660  IF FNVconv(V(I,J),Base(J))<Cr3 THEN 2585
2665  IF I=R2 THEN 2725
2670  I=I+1
2675  IF FNVconv(V(I,J),Base(J))<Cr4 THEN 2585
2680  IF I=R2 THEN 2715
2685  I=I+1
2690  IF FNVconv(V(I,J),Base(J))<Cr1 THEN
2695  B(K,2,J)=I
2700  GOTO 2725
2705  END IF
2710  GOTO 2680
2715  PRINT "*** BUBBLE DID NOT SHOW UP"
```

```
2720  GOTO 2790
2725  Duram=(Duraic+Durauc)/2.
2730  Dura=B(K,2,J)-B(K,1,J)
2735  Devia=ABS(1-Dura/Duram)
2740  PRINT CHR$(10)
2745  PRINT "*** STARTING OF PROBE #";J;": ";DROUND(B(K,1,J)/500,.4);" Sec"
2750  PRINT ""
2755  PRINT "*** END OF PROBE #";J;": ";DROUND(B(K,2,J)/500,.4);" Sec"
2760  PRINT ""
2765  PRINT "*** DURATION OF BUBBLE :";Dura
2770  IF Devia>.2 THEN
2775  PRINT ""
2780  PRINT "*** BUBBLE NOT DETECTED IN CENTRAL REGION"
2785  END IF
2790  PRINT CHR$(10),CHR$(10)
2795  IF Aa=2 THEN
2800  DISP "*** Press CONTINUE for more !!!"
2805  PAUSE
2810  END IF
2815  NEXT J
2820  IF Aa=2 THEN
2825  INPUT "RECONSIDER(1) or NEXT BUBBLE(2) ?",Aa
2830  IF Aa=1 THEN 1260
2835  END IF
2840  PRINTER IS 1
2845  IF P11=1 THEN 2860
2850  INPUT "FINISH(1) OR ANOTHER RANGE(2) ?",Kk
2855  IF Kk=2 THEN 1205
2860  NEXT K
  65  GCLEAR
2870  BEEP
2875  BEEP
2880  INPUT "*** STORE IN COMPACT FILE ? Yes (1) or No (2)",Ans
2885  IF Ans=2 THEN 3040
2890  Ntotal=0
2895  FOR L=1 TO M
2900  FOR J=1 TO 4
2905  FOR I=Stor(L,1) TO Stor(L,2)
2910  U(I-Stor(L,1)+Ntotal+1,J)=V(I,J)
2915  NEXT I
2920  NEXT J
2925  Ntotal=Ntotal+(Stor(L,2)-Stor(L,1)+1)
2930  NEXT L
2935  U(Ntotal+1,1)=V(N+1,1)
2940  U(Ntotal+1,2)=V(N+1,2)
2945  U(Ntotal+1,3)=V(N+1,3)
2950  U(Ntotal+1,4)=V(N+1,4)
2955  U(Ntotal+2,1)=V(N+2,1)
2960  U(Ntotal+2,2)=V(N+2,2)
2965  U(Ntotal+2,3)=V(N+2,3)
2970  U(Ntotal+2,4)=V(N+2,4)
2975  U(Ntotal+3,1)=V(N+3,1)
2980  U(Ntotal+3,2)=V(N+3,2)
2985  U(Ntotal+3,3)=V(N+3,3)
2990  INPUT "*** NAME FOR THE COMPACT DATA FILE ?",Ncp$
2995  INPUT "*** PROTECT CODE ?",P$
3000  DISP "*** Insert storage disk then press CONTINUE !!!"
3005  PAUSE
3010  Ncomp$=Ncp$&"comp"&"<"&P$&">"
3015  CREATE BDAT Ncomp$,4*(Ntotal+6),2
```

```
3020  ASSIGN @Path TO Ncomp$
3025  OUTPUT @Path:U(*)
3030  ASSIGN @Path TO *
3035  PRINT Name$;"HAS BEEN RESTORED ON";Ncomp$
3040  SUBEND
3045  ! ****************************************
3050  !
3055  SUB Listing(INTEGER V(*),B(*),C(*),D(*),Crit(*),REAL Base(*),Name$)
3060  COM N,Disk,Mon,Date,Year
3065  Ttot=4.*N/V(N+1,1)
3070  Tspace=4./V(N+1,1)
3075  INPUT "HARD COPY(1) OR CRT LISTING(2) ?",P7
3080  IF P7=1 THEN PRINTER IS 701
3085  INPUT "LOWER CHANNEL (1) OR UPPER CHANNEL (2) ?",Chan
3090  INPUT "AUTO PLOT (1) OR MANUAL (2) ?",C1
3095  IF C1=2 THEN
3100  INPUT "TIME RANGE ? t1,t2 ",P1,P2
3105  P1=P1*V(N+1,1)/4.-5
3110  P2=P2*V(N+1,1)/4.+5
3115  GOTO 3140
3120  END IF
3125  FOR K=1 TO C(J)
3130  P1=B(K,1,Chan)-5
3135  P2=B(K,2,Chan)+5
3140  PRINT ""
3145  IF Chan=2 THEN
3150  PRINT "UPPER CHANNEL :  BEGINNENG OF BUBBLE #";K
3155  GOTO 3170
3160  END IF
3165  PRINT "LOWER CHANNEL :  BEGINNING OF BUBBLE #";K
3170  FOR I=P1 TO P2
3175  A=V(I,Chan)/100.
3180  PRINT "V(";I;")=";A;"mV"
3185  NEXT I
3190  IF Chan=2 THEN
3195  PRINT "UPPER CHANNEL :  END OF BUBBLE #";K
3200  GOTO 3215
3205  END IF
3210  PRINT "LOWER CHANNEL :  END OF BUBBLE #";K
3215  IF C1=1 THEN 3235
3220  INPUT "FINISH (1) OR ANOTHER RANGE (2) ?",S
3225  IF S=2 THEN 3100
3230  GOTO 3240
3235  NEXT K
3240  INPUT "FINISH (1) OR THE OTHER CHANNEL (2) ?",C2
3245  IF C2=2 THEN 3085
3250  PRINTER IS 1
3255  SUBEND
3260  DEF FNVconv(INTEGER V,REAL Base)
3265  A=32768+V
3270  IF A>2047 THEN A=A-4096
3275  A=ABS(A*.05)-Base
3280  RETURN A
3285  FNEND
3290  DEF FNVbs(INTEGER V)
3295  A=32768+V
3300  IF A>2047 THEN A=A-4096
3305  A=ABS(A*.05)
3310  RETURN A
3315  FNEND
```

Appendix 4

Hewlett-Packard 9826 Microprocessor Program

"Data Acquisition and Data Processing Program for the Determination of the Pressure Profile in a Bidimensional Three-Phase Fluidized Bed".

Code of the Program: PRESS-5

```
5     ! PRESSURE MEASUREMENT PRESS_5 ONLY FORCED REGRESSION IS USED AND BACK CHE
CKING IS PERFORMED
10    ! FIVE SECOND OF DATA ACQUISITION FOR EACH CHANNEL
15    ! REGRESSION AND PLOTTING ARE PROGRAMMED IN SEPARATED SUBROUTINES
20    ! POROTITIES OF EACH PHASE ARE CALCULATED
25    OPTION BASE 1
30    COM Bset,Beye,Vliq,Vgas,Wp
35    N=500
40    M=12*N
45    INTEGER P,Q
50    ALLOCATE INTEGER U(N),V(M+9)
55    ALLOCATE REAL E(M+9),X(12),Pcorr(12)
60    ALLOCATE REAL Beta(2),Alpha(2),Rcor(2),Se(2)
65    X(1)=1.91    ! PRESSURE TAP POSITION, CM FROM GRID
70    X(2)=6.99
75    X(3)=14.61
80    X(4)=22.23
85    X(5)=37.47
90    X(6)=52.71
95    X(7)=67.95
100   X(8)=83.19
105   X(9)=98.43
110   X(10)=113.67
115   X(11)=128.91
120   X(12)=144.15
125   Pcorr(1)=3.2383
130   Pcorr(2)=2.7401
135   Pcorr(3)=1.9928
140   Pcorr(4)=1.2455
145   Pcorr(5)=-.2491
150   Pcorr(6)=-1.7437
155   Pcorr(7)=-3.2383
160   Pcorr(8)=-4.7329
165   Pcorr(9)=-6.2275
170   Pcorr(10)=-7.7221
175   Pcorr(11)=-9.25167
180   Pcorr(12)=-10.7113
185   INPUT "*** NEW EXPERIMENT (1) OR RETRIEVING (2) ? ***",D
190   IF D=2 THEN 595
195   INPUT "*** NUMBER OF DISK ?",Disk
200   Slot1=4096
205   Slot4=16384
210   Slot7=28672
215   IMAGE #,W
220   Cw=-4096
225   Isl=128
230   Dte=64
235   Sye=32
240   Tme=16
245   !INPUT "*** SAMPLING RATE ? ( 1 - 950/Second )",S
250   INPUT "*** TIME DELAY OF WAFER SWITCH ? ( 1 - 30 Sec)",Tde
255   S=100
260   INPUT "*** NAME OF THE FILE ?",Name$
265   INPUT "*** PROTECT CODE ?",P$
270   INPUT "*** DATE ? ( MONTH, DAY, YEAR )",Date
275   INPUT "*** LIQUID VELOCITY ? ( GPM )",Vliq
280   Vliq=INT(2632.49*Vliq)  ! CONVERT INTO SI UNIT OF M/SEC WITH SCALE FACTOR
OF 7E5
285   INPUT "*** GAS VELOCITY ? ( CFM )",Vgas
290   INPUT "*** PRESSURE OF GAS ? ( PSI )",Press
```

```
295   Vgas=196.6*(14.31+Press)*Vgas  ! unit of cm/sec with scale factor of 10000
based on 740 mmHg
300   Press=INT(689.12*Press)  ! CONVERT INTO SI UNIT OF Pa.N/(M*M) WITH SCALE
    FACTOR OF 1/10
305   INPUT "*** SETTLED BED HEIGHT ? ( INCHES FROM GRID )",Bset
310   Bset=INT(254*Bset)  ! CONVERT INTO SI UNIT OF M WITH SCALE FACTOR OF 10000
315   INPUT "*** WEIGHT OF SOLIDS ? (Gram)",Weight
320   INPUT "*** FLUIDIZED BED HEIGHT ? ( INCHES FROM GRID )",Bflu
325   Bflu=INT(254*Bflu)  ! CONVERT INTO SI UNIT OF M WITH SCALE FACTOR OF 10000
330   INPUT "*** INJECTOR USED ? ( NUMBER )",Inject
335   INPUT "*** INJECTOR POSITION ? ( INCHES FROM GRID )",Posiinjec
340   Posiinjec=INT(250*Posiinjec)  ! CONVERT INTO SI UNIT OF M WITH SCALE FACTO
R OF 10000
345   C0=0
350   IF S>250 THEN 410
355   IF S>25 THEN 395
360   IF S>3 THEN 380
365   B=.001
370   A=3
375   GOTO 420
380   B=.0001
385   A=2
390   GOTO 420
395   B=.00001
400   A=1
405   GOTO 420
410   B=.000001
415   A=0
420   P1=1/(2*S*B)
425   P=INT(P1)
430   Sact=INT(1/(2*P*B))
435   Tde=(Tde-5)*1.0256
440   R=2^A
445   BEEP
450   DISP "******* PRESS CONTINUE TO START *******"
455   PAUSE
460   DISP "******* DATA ACQUISITION !!! *******"
465   FOR Chan=0 TO 11
470   GOSUB Data_acq
475   PRINT "  *** CHANNEL # ";Chan+1;" ***"
480   FOR I=1 TO N
485   V(I+Chan*N)=U(I)
490   NEXT I
495   WAIT Tde
500   NEXT Chan
505   V(M+1)=Date
510   V(M+2)=Vliq
515   V(M+3)=Vgas
520   V(M+4)=Press
525   V(M+5)=Bset
530   V(M+6)=Weight
535   V(M+7)=Inject
540   V(M+8)=Posiinjec
545   V(M+9)=Bflu
550   N$=Name$&"<"&P$&">"
555   CREATE BDAT N$,M+9,2
560   ASSIGN @Path TO N$
565   OUTPUT @Path;V(*)
570   ASSIGN @Path TO *
575   GOTO 545
580   !
```

```
585   ! RETRIEVE FROM OLD FILE
590   !
595   INPUT "*** NUMBER OF DISK ?",Disk
600   INPUT "*** NAME OF THE OLD FILE ?",Name$
605   INPUT "*** PROTECT CODE ?",P$
610   N$=Name$&"<"&P$&">"
615   ASSIGN @Path TO N$
620   ENTER @Path;V(*)
625   ASSIGN @Path TO *
630   !
635   ! DATA PROCESSING
640   !
645   Mon=INT(V(M+1)/1000)
650   Date=INT((V(M+1)-1000*Mon)/10)
655   Year=V(M+1)-1000*Mon-10*Date
660   ALLOCATE Vavg(12),Pavg(12)
665   PRINTER IS 701
670   PRINT CHR$(10)
675   PRINT "*** DATE OF EXPERIMENT : ";Mon;"/";Date;"/ 19";Year
680   PRINT CHR$(10)
685   PRINT "*** DISK NUMBER : ";Disk
690   PRINT ""
695   PRINT "*** FILE NAME : ";Name$
700   PRINT ""
705   PRINT IS 1
710   FOR J=0 TO 5500 STEP 500
715   Chan=J/500+1
720   Sum=0.
725   FOR I=1 TO N
730   A=32768+V(I+J)
735   IF A>2047 THEN A=A-4096
740   E(I+J)=DROUND(ABS(A*.05),4)
745   Sum=Sum+E(I+J)
750   NEXT I
755   Vavg(Chan)=Sum/N
760   Pavg(Chan)=1.7238*Vavg(Chan)+Pcorr(Chan)  ! UNIT OF kPa
765   PRINT ""
770   PRINT "*** CHANNEL #";Chan
775   FOR I=1 TO 17 STEP 4
780   PRINT "V(";I;")=";E(I+J),"V(";I+1;")=";E(I+1+J),"V(";I+2;")=";E(I+2+J),"V(
";I+3;")=";E(I+3+J)
785   NEXT I
790   PRINT "*** AVERAGE VALUE=";Vavg(Chan),"PRESSURE=";Pavg(Chan);"kPa"
795   NEXT J
800   Bset=DROUND(V(M+5)/100.,4)
805   Beye=DROUND(V(M+9)/100.,4)
810   Vliq=DROUND(V(M+2)/7.E+3,4)
815   Vgas=DROUND(V(M+3)/1000.,4)
820   Np=V(M+6)
825   PRINT CHR$(12)
830   CALL Regr(P,Q,X(*),Pavg(*),Beta(*),Alpha(*),Rcor(*),Se(*),Hbed)
835   CALL Plot(P,Q,X(*),Pavg(*),Beta(*),Alpha(*),Rcor(*),Se(*),Hbed)
840   !
845 Data_acq: !
850   OUTPUT 12 USING 215:Cw+Sye
855   OUTPUT 12 USING 215:Slot1+3072+R
860   OUTPUT 12 USING 215:Slot1+P
865   OUTPUT 12 USING 215:Slot7+C0
870   OUTPUT 12 USING 215:Cw+Sye+Isl+Fne
875   CONTROL 12,3:Slot4
```

```
ENTER 12 USING 215:U(*)
OUTPUT 12 USING 215:Cw+Sve+Dte
OUTPUT 12 USING 215:Slot1+P
OUTPUT 12 USING 215:Slot1+3072
RETURN
END
!
! REGRESSION SECTION
!
SUB Regr(INTEGER P,Q,REAL X(*),Pavg(*),Beta(*),Alpha(*),Rcor(*),Se(*),Bbed
)
COM Bset,Beye,Vlig,Vgas,Hp
Bbed=Beye
FOR I=1 TO 12
IF X(I)>=Bbed THEN
P=I-1
Q=I
GOTO 975
END IF
NEXT I
Sx=0.
FOR I=1 TO P
Sx=Sx+X(I)
NEXT I
Sy=0.
FOR I=1 TO P
Sy=Sy+Pavg(I)
NEXT I
Ssqx=0.
FOR I=1 TO P
Ssqx=Ssqx+X(I)^2
NEXT I
Ssqy=0.
FOR I=1 TO P
Ssqy=Ssqy+Pavg(I)^2
NEXT I
Sxy=0.
FOR I=1 TO P
Sxy=Sxy+X(I)*Pavg(I)
NEXT I
!
! CALCULATE SLOPE OF REGRESSION LINE
Nume=P*Sxy-Sx*Sy
Deno=P*Ssqx-Sx^2
Beta(1)=DROUND(Nume/Deno,4)
Alpha(1)=DROUND((Sy-Beta(1)*Sx)/P,5)
!
! CALCULATE STANDARD ERROR OF ESTIMATE
Se(1)=0.
FOR I=1 TO P
Se(1)=Se(1)+(Pavg(I)-(Alpha(1)+Beta(1)*X(I)))^2
NEXT I
Se(1)=DROUND(Se(1)/(P-2),6)
!
! CALCULATE REGRESSION CORRELATION Rcor'f
Rn=P*Sxy-Sx*Sy
Rf=P*Ssqx-Sx^2
Rr=P*Ssqy-Sy^2
Rd=SQR(Rf*Rr)
Rcor(1)=DROUND(ABS(Rn/Rd),6)
!
```

```
1180  ! DILUTE PHASE REGRESSION
1185  !
1190  Sx=0.
1195  FOR I=0 TO 12
1200  Sx=Sx+X(I)
1205  NEXT I
1210  Sy=0.
1215  FOR I=0 TO 12
1220  Sy=Sy+Pavg(I)
1225  NEXT I
1230  Ssqx=0.
1235  FOR I=0 TO 12
1240  Ssqx=Ssqx+X(I) 2
1245  NEXT I
1250  Ssqy=0.
1255  FOR I=0 TO 12
1260  Ssqy=Ssqy+Pavg(I) 2
1265  NEXT I
1270  Sxy=0.
1275  FOR I=0 TO 12
1280  Sxy=Sxy+X(I)*Pavg(I)
1285  NEXT I
1290  !
1295  ! CALCULATE SLOPE FOF REGRESSION LINE
1300  Nume=(13-0)*Sxy-Sx*Sy
1305  Deno=(13-0)*Ssqx-Sx 2
1310  Beta(2)=DROUND(Nume/Deno,4)
1315  Alpha(2)=DROUND((Sy-Beta(2)*Sx)/(13-0),5)
1320  !
1325  ! CALCULATE STANDARD ERROR OF ESTIMATE
1330  Se(2)=0.
1335  FOR I=0 TO 12
1340  Se(2)=Se(2)+(Pavg(I)-(Alpha(2)+Beta(2)*X(I))) 2
1345  NEXT I
1350  Se(2)=DROUND(Se(2)/(11-0),6)
1355  !
1360  ! CALCULATE REGRESSION CORRELATION Rcor2
1365  Rn=(13-0)*Sxy-Sx*Sy
1370  Rf=(13-0)*Ssqx-Sx 2
1375  Rr=(13-0)*Ssqy-Sy 2
1380  Rd=SQR(Rf*Rr)
1385  Rcor(2)=DROUND(ABS(Rn/Rd),5)
1390  ! CALCULATE BED HEIGHT OF FORCED REGRESSION
1395  Hbed=DROUND((Alpha(2)-Alpha(1))/(Beta(1)-Beta(2)),4)
1400  IF Hbed<X(P) OR Hbed>X(0) THEN
1405  FOR I=1 TO 12
1410  IF ABS(Hbed-X(I))<1. THEN 1435
1415  NEXT I
1420  Bbed=Hbed
1425  GOTO 940
1430  END IF
1435  SUBEND
1440  !
1445  ! PLOTTING SECTION
1450  !
1455  SUB Plot(INTEGER P,Q,REAL X(*),Pavg(*),Beta(*),Alpha(*),Rcor(*),Se(*),Hbed
1460  COM Bset,Beye,Vlin,Vgas,HP
1465  PRINT CHR$(12)
1470  GINIT
```

```
1475  GRAPHICS ON
1480  WINDOW -30,150,100,130
1485  AXES 15,5,0,105
1490  DEG
1495  LDIR 0
1500  FOR I=0 TO 150 STEP 15
1505  MOVE I-7,102
1510  LABEL I
1515  NEXT I
1520  FOR I=105 TO 130 STEP 5
1525  MOVE -20,I-1
1530  LABEL I
1535  NEXT I
1540  MOVE 0,0
1545  FOR I=1 TO 12
1550  MOVE X(I),Pavg(I)
1555  GOSUB Symbol
1560  NEXT I
1565  Pbed=Beta(2)*Hbed+Alpha(2)
1570  Hbot=X(1)
1575  Pbot=Beta(1)*Hbot+Alpha(1)
1580  Htop=X(12)
1585  Ptop=Beta(2)*Htop+Alpha(2)
1590  MOVE Hbot,Pbot
1595  DRAW Hbed,Pbed
1600  DRAW Htop,Ptop
1605  MOVE 45,100
1610  LABEL "Height from Grid, cm"
1615  LDIR 90
1620  MOVE -22,110
1625  LABEL "Absolute Pressure, KPa"
1630  PRINTER IS 701
1635  PRINT CHR$(10),CHR$(10)
1640  DUMP GRAPHICS
1645  PRINT CHR$(10),CHR$(10)
1650  PRINT "*** AVERAGE PARTICLE SIZE : 250 E-6 meter"
1655  PRINT CHR$(10)
1660  PRINT "*** SETTLED BED HEIGHT :";Bset;" cm"
1665  PRINT ""
1670  PRINT "*** VISUAL FLUIDIZED BED HEIGHT :";Beye;" cm"
1675  PRINT ""
1680  PRINT "*** SUPERFICIAL LIQUID VELOCITY :";Vliq;" cm/Sec"
1685  PRINT ""
1690  PRINT "*** SUPERFICIAL GAS VELOCITY :";Vgas;" cm/Sec"
1695  PRINT ""
1700  PRINT "******  DENSE PHASE REGRESSION *** ***"
1705  PRINT "*** PRESSURE TAPS USED : FROM # 1 TO #";P
1710  PRINT "*** REGRESSION LINE :  P =";Beta(1);"* (height";") +";Alpha(1);" unit
s of KPa & cm"
1715  PRINT "*** REGRESSION CORRELATION :";Rcor(1)
1720  PRINT "*** STANDARD ERROR :";Se(1)
1725  PRINT CHR$(10)
1730  PRINT "******  DILUTE PHASE REGRESSION *** ***"
1735  PRINT "*** PRESSURE TAPS USED : FROM #";Q;"TO # 12"
1740  PRINT "*** REGRESSION LINE :  P =";Beta(2);"* (height";") +";Alpha(2);" unit
s of KPa & cm"
1745  PRINT "*** REGRESSION CORRELATION :";Rcor(2)
1750  PRINT "*** STANDARD ERROR :";Se(2)
1755  PRINT CHR$(10)
1760  PRINT "*** FLUIDIZED BED HEIGHT : ";Hbed;" cm"
1765  PRINT CHR$(10)
```

```
1770  PRINT ">>> POROSITIES IN FLUIDIZED BED <<<"
1775  Area=167.7     ! 26*2.54^2
1780  Dgas=1.5572E-3     ! density of gas at 740 mmHg
1785  Pors=Wp/(2.5*Area*Hbed)
1790  Porl=(-10.1974*Beta(1)-(1-Wp/(2.5*Area*Hbed))*Dgas-(Wp/(Area*Hbed)))/.9984
1795  Porg=1-Pors-Porl
1800  PRINT ""
1805  PRINT "*** POROSITY OF SOLID :";DROUND(Pors,4)
1810  PRINT ""
1815  PRINT "*** POROSITY OF LIQUID :";DROUND(Porl,4)
1820  PRINT ""
1825  PRINT "*** POROSITY OF GAS :";DROUND(Porg,4)
1830  PRINTER IS 1
1835  GCLEAR
1840  STOP
1845 Symbol:    ! SYMBOL DRAWING
1850  RPLOT -1,0
1855  RPLOT 1,0
1860  RPLOT 0,0
1865  RPLOT 0,.2
1870  RPLOT 0,-.2
1875  RETURN
1880  SUBEND
```

Appendix No. 5

Derivation of the equations (6), (7) and (8) that allow the estimation of the hold-up of the different phases in three-phase fluidization.

Determination of the Individual Hold-Ups εg, ε_ℓ, ε_s in Three Phase Fluidized Beds

The individual hold-ups of the different phases (gas, liquid and solid) may be determined as follows:

. The sum of the liquid hold-up + solid hold-up + gas hold-up = total volume 3 phase reactor.

$$\underbrace{V_{liquid}}_{cm^3 liq} + \underbrace{V_{gas}}_{cm^3 gas} + \underbrace{V_{solid}}_{cm^3 sol} = \underbrace{V_{total}}_{cm^3 total}$$

or

$$\frac{V_{liquid}}{V_{total}} + \frac{V_{liquid}}{V_{total}} + \frac{V_{solid}}{V_{total}} = 1$$

$$\varepsilon_\ell \left(\frac{cm^3 liq}{cm^3 tot}\right) \quad \varepsilon g \left(\frac{cm^3 gas}{cm^3 tot}\right) \quad \varepsilon_s \left(\frac{cm^3 sol}{cm^3 tot}\right)$$

$$\varepsilon_\ell + \varepsilon g + \varepsilon_s = 1$$

. The static pressure drop ΔP_b across the height of the bed of height H_b is given by the following equation:

$$\Delta P_b \left(\frac{Kg_f}{cm^2}\right) = H_b (cm) \frac{g(cm/s^2)}{g_c \left(\frac{Kg}{Kg_f} \cdot \frac{cm}{s^2}\right)} \quad . \; B$$

$$B = (\varepsilon_\ell \rho_\ell + \varepsilon g \rho_g + \varepsilon_s \rho_s)$$

$$\frac{cm^3 liq}{cm^3 tot} \quad \frac{g}{cm^3 liq} \quad \frac{cm^3 gas}{cm^3 t} \quad \frac{g}{cm^3 gas} \quad \frac{cm^3 s}{cm^3 t} \quad \frac{g}{cm^3 s}$$

ρ_s, ρ_ℓ and ρ_g are the densities of the solid, liquid and gas respectively and g is the gravity acceleration.

$$\Delta P_b = H_b \frac{g}{g_c} [\varepsilon_\ell \rho_\ell + \varepsilon_g \rho_g + \varepsilon_s \rho_s)]$$

. The solid hold-up may be calculated directly if the total mass of the particles in the bed is known. In fact M_s is normally a constant value for catalytic processes. M_s will be then the initial load of catalyst in the reactor.

$$M_s = V_s \rho_s = (\varepsilon_s A . H_b) \rho_s$$

Reactor
Cross Sectional Area

Then $$\varepsilon_s = \frac{M_s}{A H_b \rho_s}$$

. We may proceed to replace ε_s in the previous two equations and combine them to obtain ε_ℓ and εg.

$$\varepsilon_\ell + \varepsilon g + \varepsilon_s = 1$$

or

$$\varepsilon_\ell + \varepsilon g = 1 - \frac{M_s}{A H_b \rho_s}$$

$$\varepsilon_\ell \rho_\ell + \varepsilon g \rho_g + \varepsilon_s \rho_s = \frac{\Delta P_b \; g_c}{H_b \; g}$$

or

$$\varepsilon_\ell \rho_\ell + \varepsilon p \rho_g = \frac{\Delta P_b \; g_c}{H_b \; g} - \varepsilon_s \rho_s = \frac{\Delta P_b \; g_c}{H_b \; g} - \frac{M_s}{A \; H_b}$$

$$\varepsilon_\ell \rho_\ell + \varepsilon g \rho_g = \frac{\Delta P_b}{H_b} \frac{g_c}{g} - \frac{M_s}{A \; H_b}$$

$$\varepsilon_\ell = 1 - \frac{M_s}{A \; H_b \; \rho_s} - \varepsilon g \qquad \text{(A.5.1)}$$

and

$$\varepsilon_\ell = \left(\frac{\Delta P_b}{H_b} \frac{g_c}{g} - \frac{M_s}{A \; H_b} - \varepsilon g \rho_g\right) \frac{1}{\rho_\ell} \qquad \text{(A.5.2)}$$

Because the left hand side of the two previous expressions (A.5.1) and (A.5.2) is identical then

$$1 - \frac{M_s}{A H_b \rho_s} - \varepsilon g = \frac{\Delta P_b}{H_b} \frac{g_c}{g} \cdot \frac{1}{\rho_\ell} - \frac{M_s}{A H_b \rho_\ell} - \varepsilon g \frac{\rho_g}{\rho_\ell}$$

$$\rho_\ell - \frac{M_s}{A H_b} \frac{\rho_\ell}{\rho_s} - \varepsilon g \rho_\ell = \frac{\Delta P_b}{H_b} \frac{g_c}{g} - \frac{M_s}{A H_b} - \varepsilon g \rho_g$$

$$\rho_\ell \left(1 - \frac{M_s}{A H_b \rho_s} + \frac{M_s}{A H_b} - \frac{\Delta P_b}{H_b} \frac{g_c}{g}\right) = \varepsilon g (\rho_\ell - \rho_g)$$

$$\varepsilon g = \frac{\rho_\ell \left(1 \frac{M_s}{A H_b \rho_s}\right) + \frac{M_s}{A H_b} - \frac{\Delta P_b}{H_b} \frac{g_c}{g}}{(\rho_\ell - \rho_g)} \qquad \text{GAS HOLD-UP} \qquad \text{(A.5.3)}$$

- Using a similar method of substitution the ε_ℓ fraction may be defined as follows:

$$\varepsilon_\ell = \frac{\frac{\Delta P_b}{H_b} \frac{g_c}{g} - \rho_g \left(1 - \frac{M_s}{\rho_s H_b A}\right) - \frac{M_s}{H_b A}}{(\rho_\ell - \rho_g)} \qquad \text{LIQUID HOLD-UP} \qquad \text{(A.5.4)}$$

TABLE 1

CORRELATIONS FOR V_b and ℓ. BIDIMENSIONAL COLUMN

Run No.	Liquid Velocity (cm/s)	Method of Processing	α	β	No. of Bubbles	Regression Coef	Standard Deviation (cm/s)
1a	0.752	Measured	44.17	0.4620	11	0.5473	15.39
2a	1.504	Measured	40.52	0.6399	19	0.7458	17.72
3a	2.256	Measured	34.03	0.7494	9	0.8764	19.05
1b	0.752	Corrected	48.62	0.3643	11	0.4851	16.52
2b	1.504	Corrected	38.53	0.6406	19	0.7152	18.22
3b	2.256	Corrected	34.10	0.6952	9	0.8497	21.63
1a+2a+3a		Measured	37.92	0.6592	39	0.7512	17.38
1B+2b+3b		Corrected	38.51	0.6093	39	0.7182	18.52

TABLE 2

BUBBLE CLASSIFICATION. BIDIMENSIONAL COLUMN

Run No	No. of Bubbles $100° < \theta < 140°$	No. of Bubbles $140° < \theta < 360°$	No. of Bubbles $360° < \theta$
1	2	4	5
2	3	9	7
3	2	4	3

TABLE 3

BUBBLE FREQUENCIES IN A CYLINDRICAL THREE PHASE FLUIDIZED BED WITH A SINGLE BUBBLE INJECTOR

Liquid: Water, Gas: Air, Solid: Glass Beads 335μm, Vg = 1.769 cm/s, Injector Position: $r/R_c = 0$

Liquid Velocity c/ms	0.778	0.778	0.778	0.778
Probe Location, r/R_c	0	0.25	0.50	0.75
Sampling Time, S	240	120	120	120
Bubble Frequency 1/s	2.45	2.17	1.54	0.68

TABLE 4

BUBBLE FREQUENCIES IN CYLINDRICAL THREE PHASE FLUIDIZED BED WITH FOUR BUBBLE INJECTORS

Liquid: water, Gas: air, Solid: glass beads 335μm, Vg = 1.630cm/s,
Injector Position: See Figure 11

Liquid Velocity cm/s	1.556	1.556	1.556	1.556	1.167	1.167	1.167	1.167	0.778	0.778	0.778	0.778	0.389
Probes Location r/R_c	0	0.25	0.50	0.75	0	0.25	0.50	0.75	0	0.25	0.50	0.75	0
Sampling Time (s)	240	120	120	120	180	120	120	120	240	60	120	120	240
Bubble Frequency (1/s)	2.14	2.29	1.78	1.26	2.02	1.69	1.46	0.85	1.36	1.34	1.15	0.93	0.97

TABLE 5

CORRELATIONS FOR V_b AND ℓ. CYLINDRICAL COLUMN

Run	V_ℓ (cm/s)	Vg (cm/s)	Gas Injector	α	β	No. of Bubbles	Regression Coefficient	Standard Deviation (cm/s)	Reference Figure
1	0.778	1.769	1	57.22	0.4181	61	0.83377	17.26	51
2	0.389	1.630	4	44.77	0.4084	10	0.90706	7.77	52
3	0.778	1.630	4	60.21	0.4131	33	0.80249	15.0	53
4	1.167	1.630	4	52.07	0.4249	29	0.79179	14.93	54
5	1.556	1.630	4	58.33	0.455	65	0.89205	12.60	55
3+4+5	-	1.630	4	57.35	0.4291	127	0.84095	14.10	56
1+3+4+5	-	-	-	57.29	0.4247	188	0.84076	15.09	57

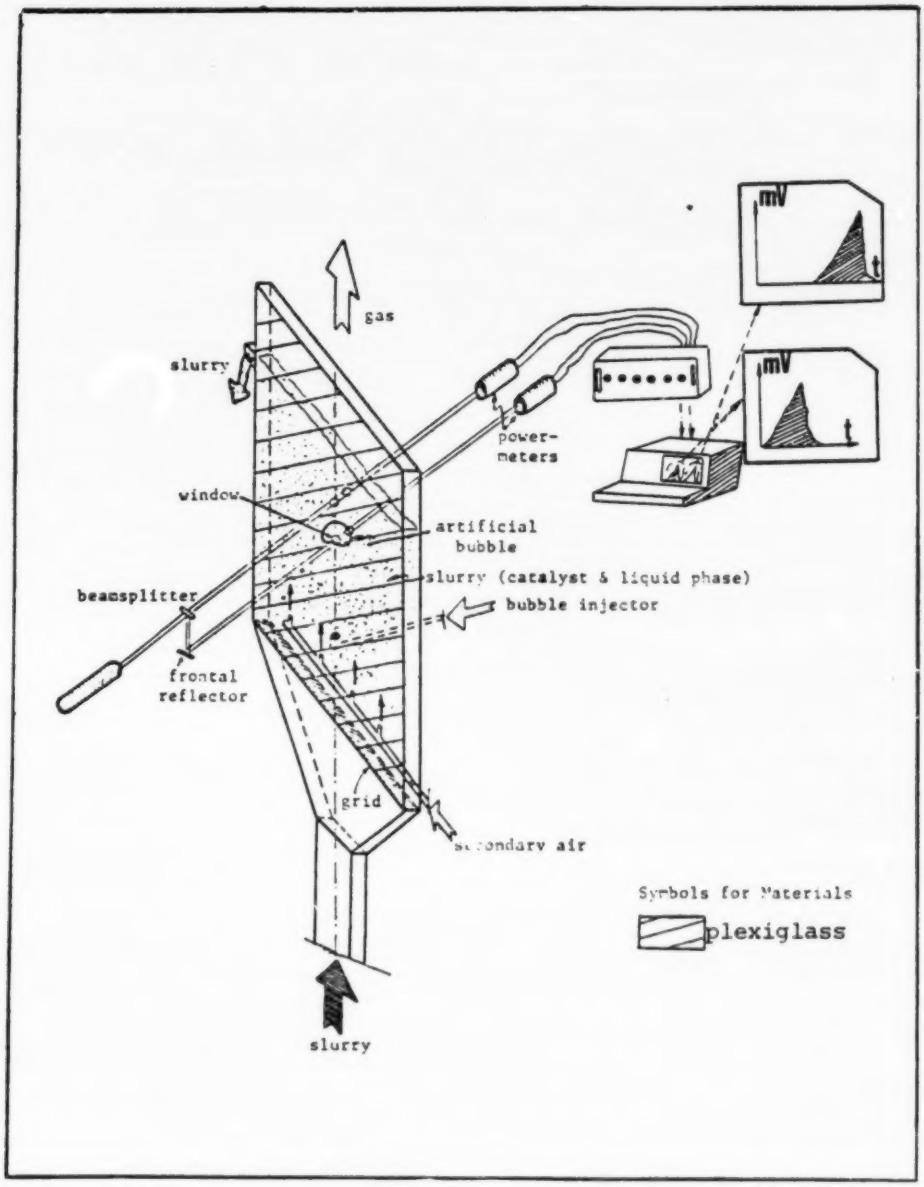

FIGURE 1. THREE-PHASE FLUIDIZED BED. COLD AND ATMOSPHERIC BIDIMENSIONAL COLUMN.

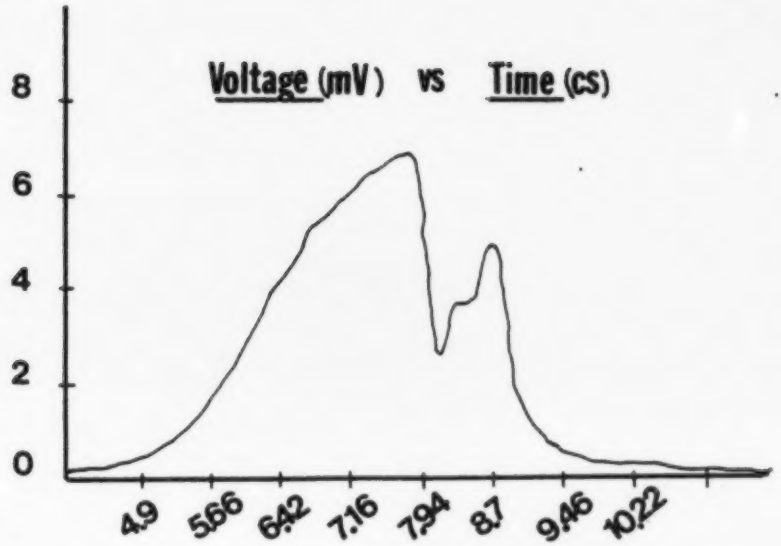

FIG. 2 OSCILLATION OF THE LASER WHEN A BUBBLE IS CROSSING THE BEAM (DATA ACQUISITION SYSTEM: 1 Channel, Column: Bidimensional, Detection System: Direct Laser Crossing the Column).

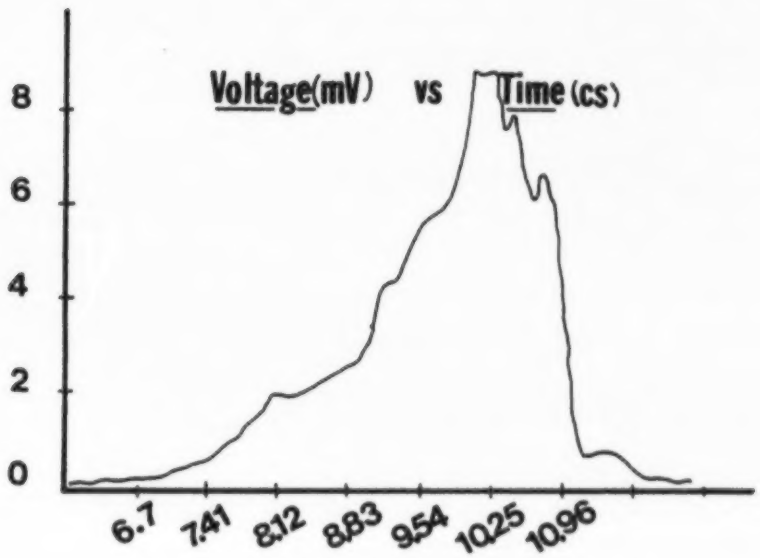

FIG. 3. OSCILLATION OF THE LASER WHEN A BUBBLE IS CROSSING THE BEAM (DATA ACQUISITION SYSTEM: 1 Channel, Column:Bidimensional, Detection System: Direct Laser Crossing the Column).

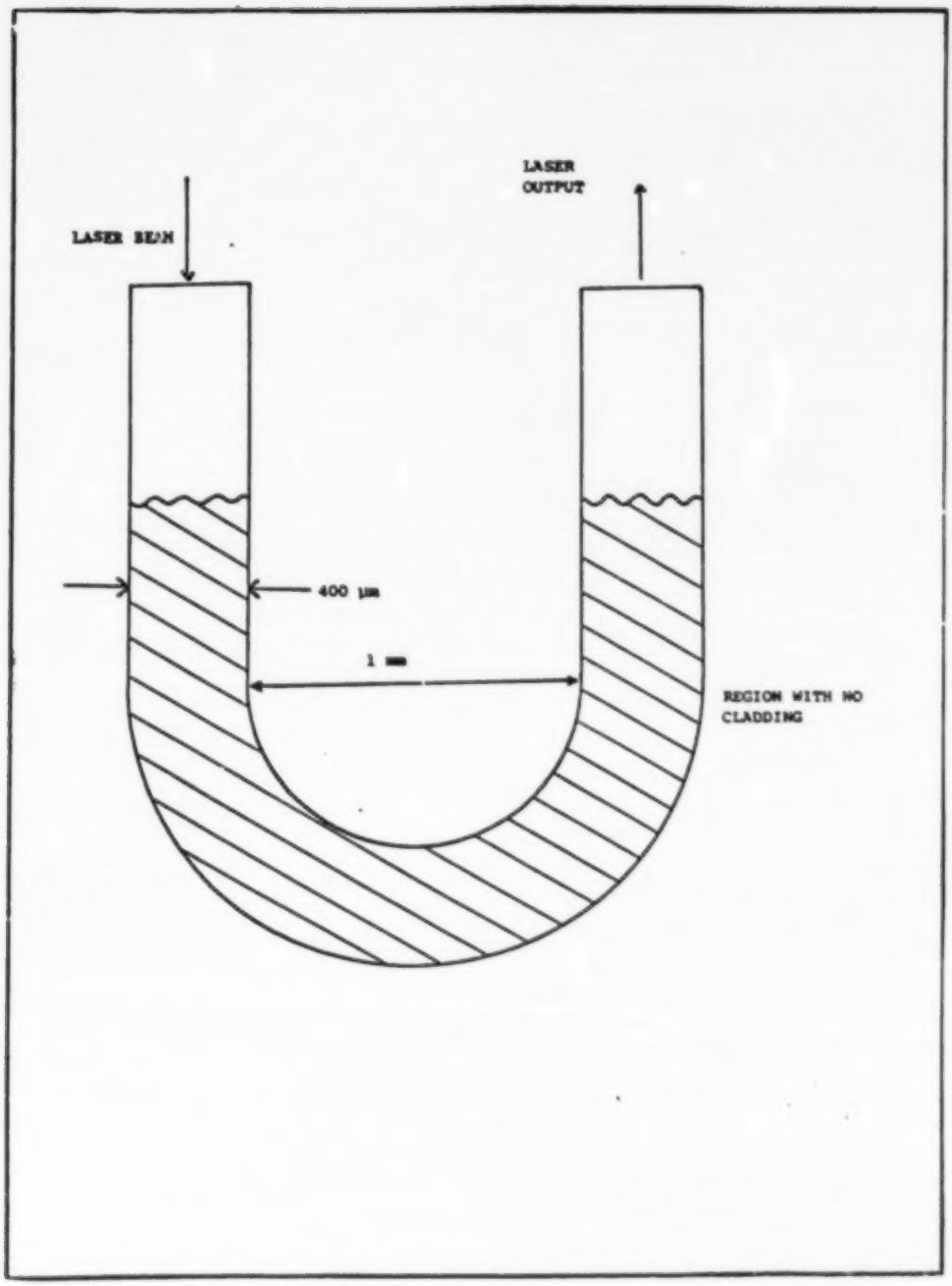

FIG. 4 FIBER OPTIC CONFIGURATION. THE SHADED AREA REPRESENTS THE SECTION OF THE PROBE WHERE THE CLADDING WAS REMOVED.

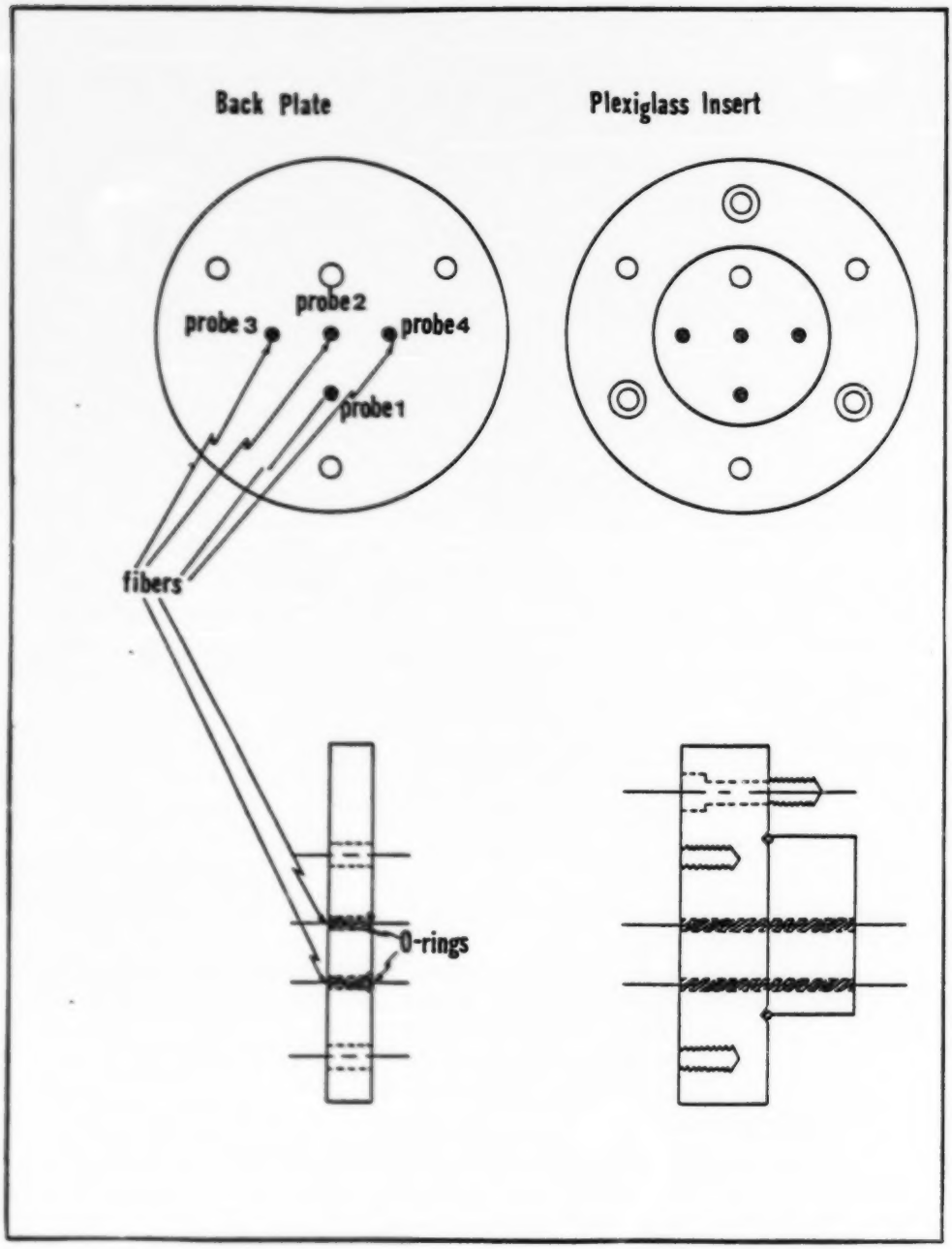

FIG. 5 SCHEMATIC REPRESENTATION OF THE PLEXIGLASS WINDOW HOLDING THE FIBRES IN THE BIDIMENSIONAL COLUMN.

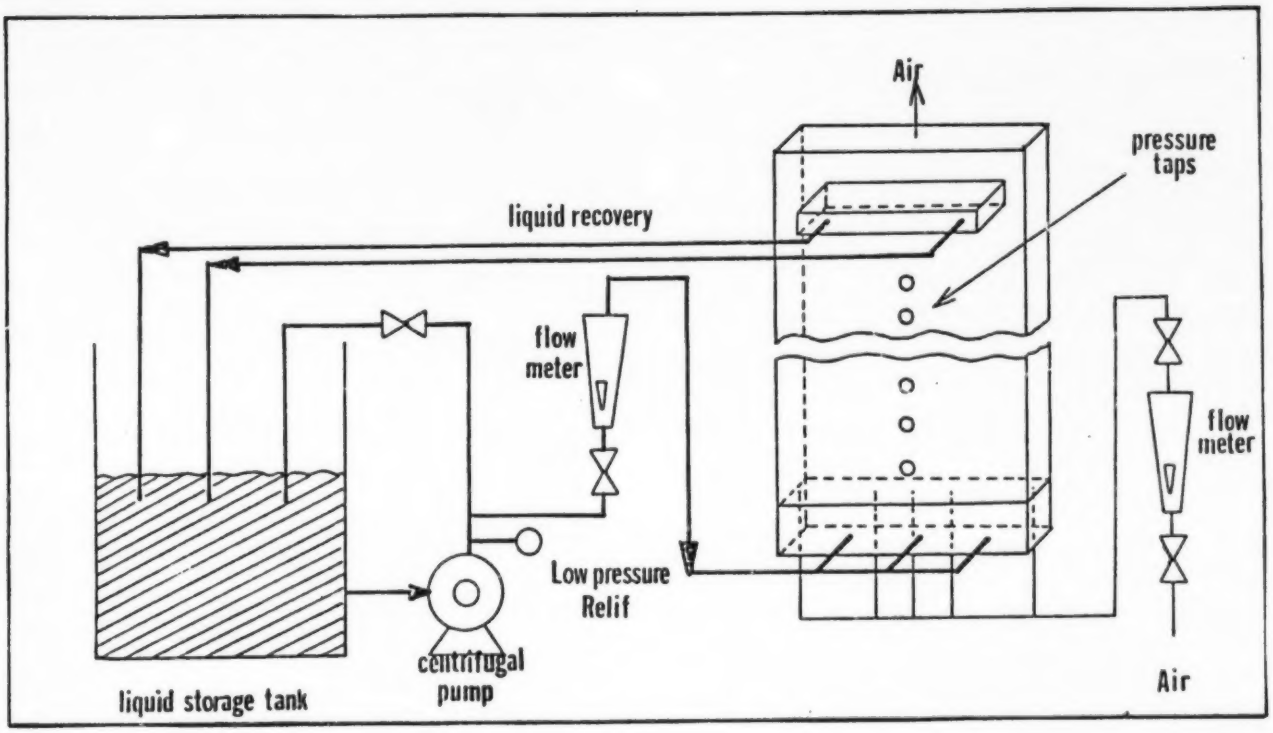

FIGURE 6 SCHEMATIC REPRESENTATION OF THE BI-DIMENSIONAL THREE-PHASE FLUIDIZED BED AND ACCESSORIES

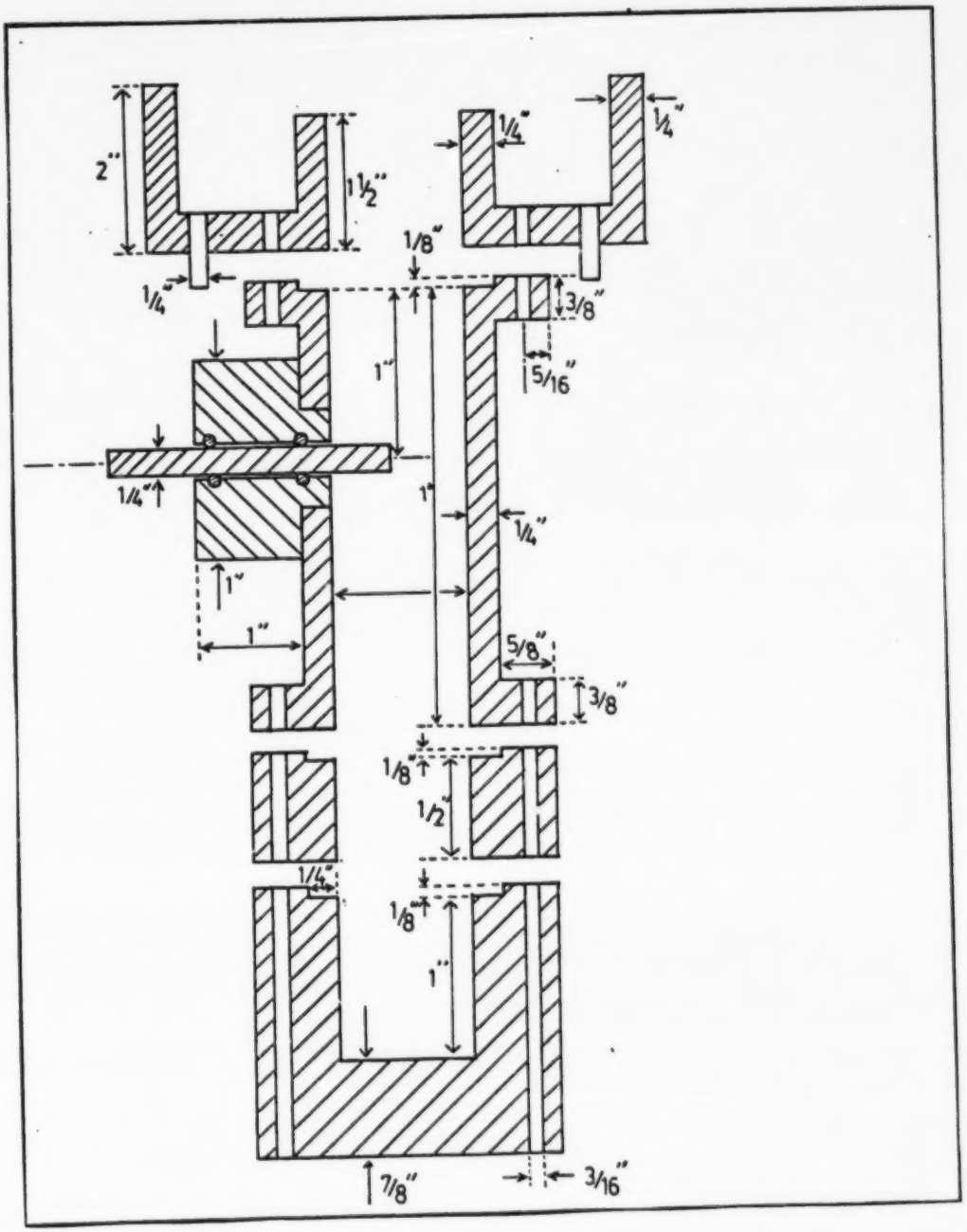

FIG. 7 MINIFLUIDIZED BED (LIQUID-SOLID) FOR LASER BEAM ABSORPTION CALIBRATION

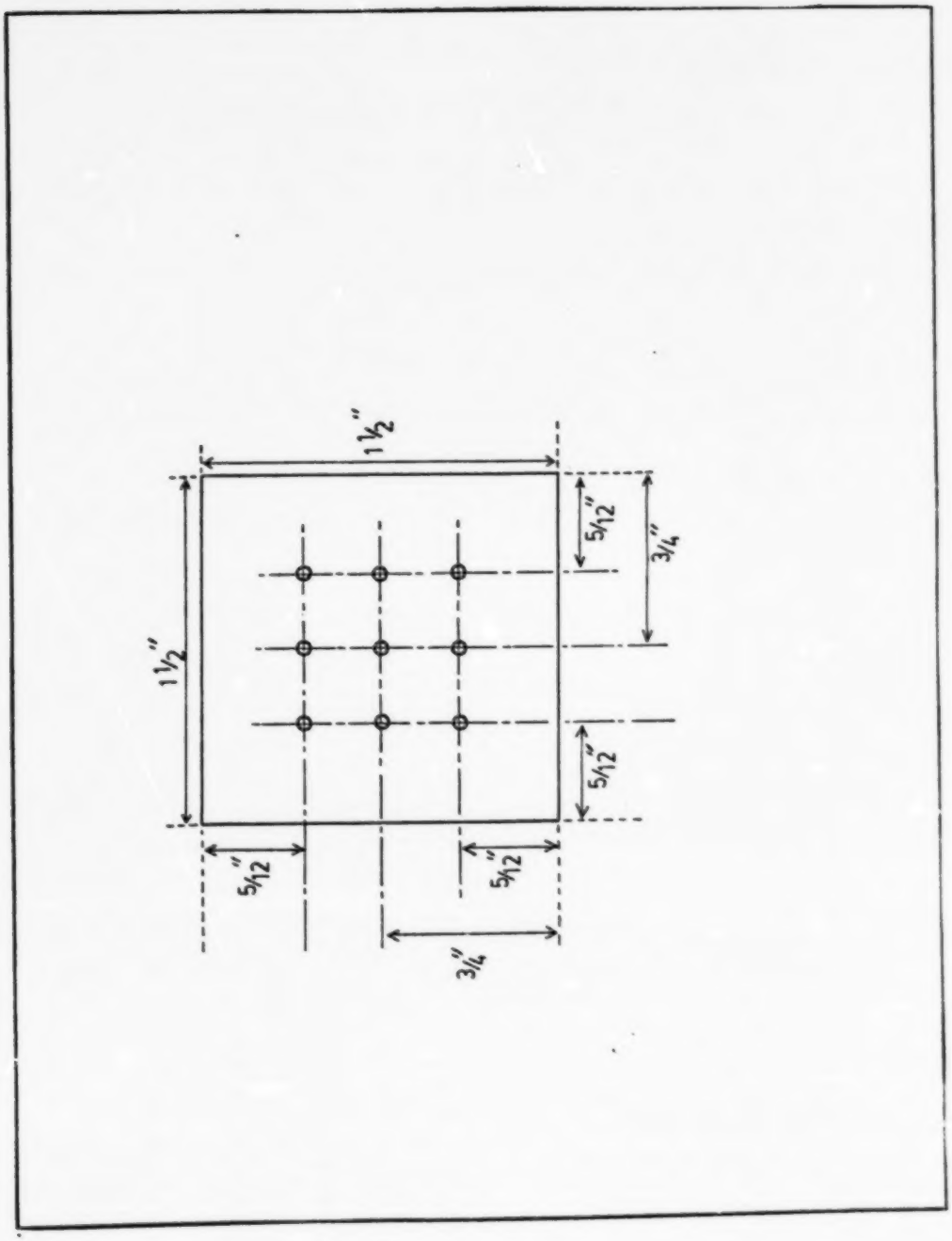

FIG. 8 VIEW OF THE GRID OF THE MINIFLUIDIZED BED

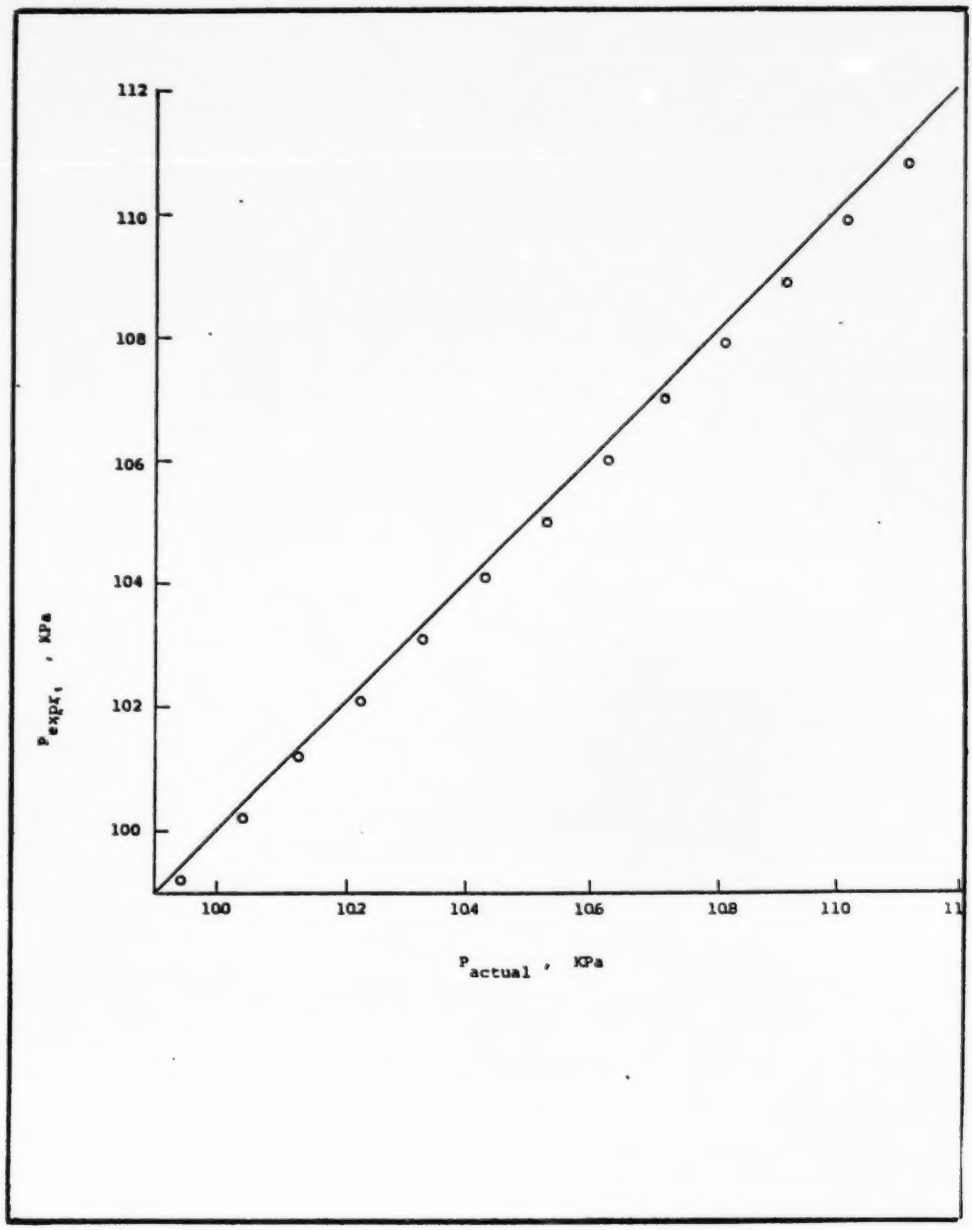

FIG. 9 CALIBRATION OF THE PRESSURE TRANSDUCER MANUFACTURED BY DATA INSTRUMENTS.

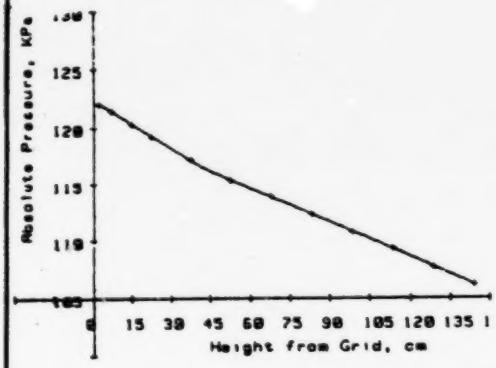


```
••• AVERAGE PARTICLE SIZE : 250 E-6 meter

••• SETTLED BED HEIGHT : 26.67   cm

••• VISUAL FLUIDIZED BED HEIGHT : 48.26   cm

••• SUPERFICIAL LIQUID VELOCITY : 1.504   cm/Sec

••• SUPERFICIAL GAS VELOCITY : 1.519   cm/Sec

•••••• DENSE PHASE REGRESSION ••• •••
••• PRESSURE TAPS USED : FROM # 1 TO # 5
••• REGRESSION LINE :  P =-.1383 * Xheight + 122.29          units of KPa & cm
••• REGRESSION CORRELATION : .999869
••• STANDARD ERROR : .00133894

•••••• DILUTE PHASE REGRESSION ••• •••
••• PRESSURE TAPS USED : FROM # 6 TO # 12
••• REGRESSION LINE :  P =-.1004 * Xheight + 120.69          units of KPa & cm
••• REGRESSION CORRELATION : .999954
••• STANDARD ERROR : .00121562

••• FLUIDIZED BED HEIGHT :  42.22  cm

>>> POROSITIES IN FLUIDIZED BED <<<

••• POROSITY OF SOLID : .3955

••• POROSITY OF LIQUID : .4214

••• POROSITY OF GAS : .1832
```

FIG. 10. MICROPROCESSOR REPORT SHOWING THE PRESSURE PROFILE IN THE FLUIDIZED BED AND THE DIFFERENT HOLD-UPS

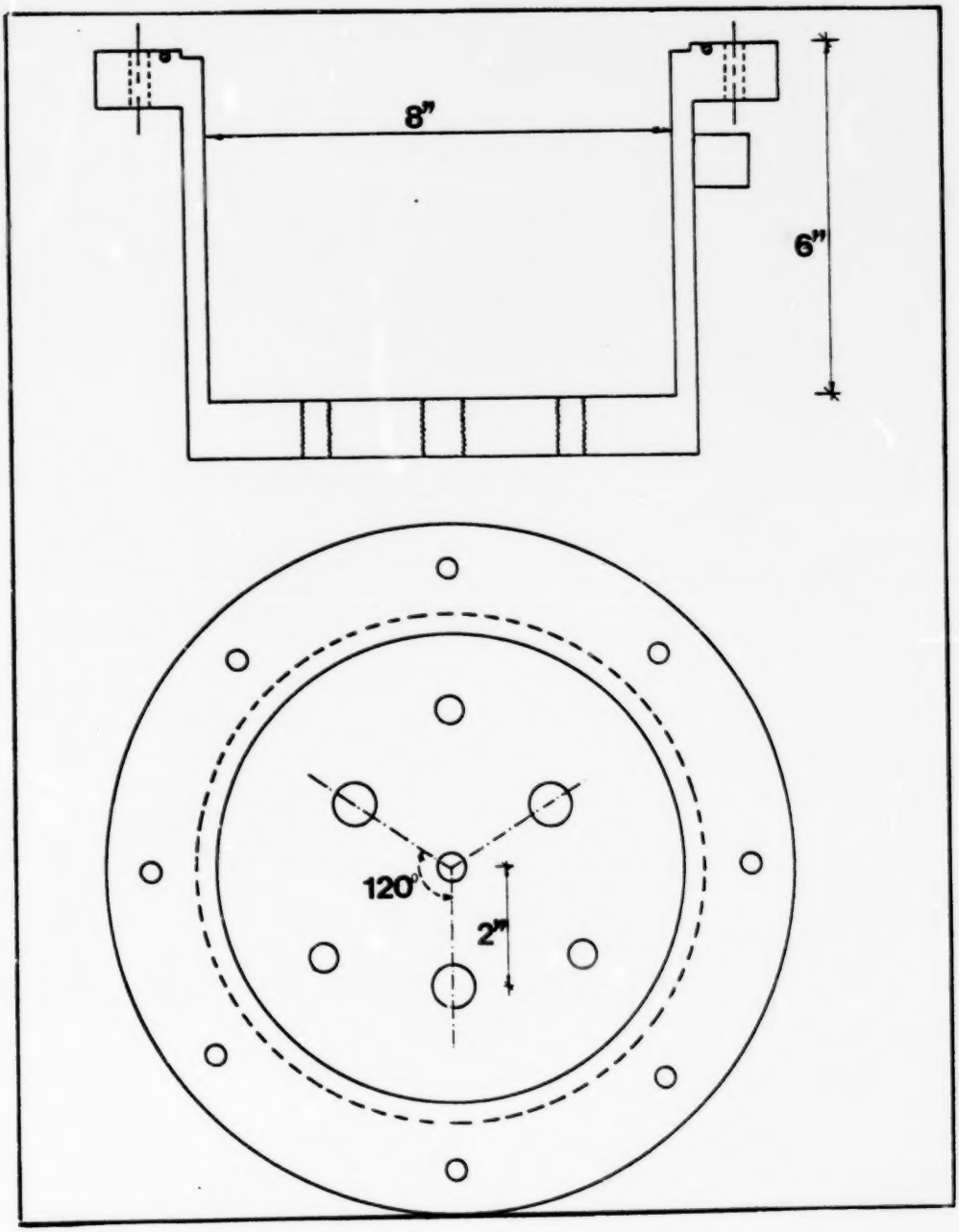

FIG. 11 SCHEMATIC REPRESENTATION OF THE CYLINDRICAL BED WIND-BOX.

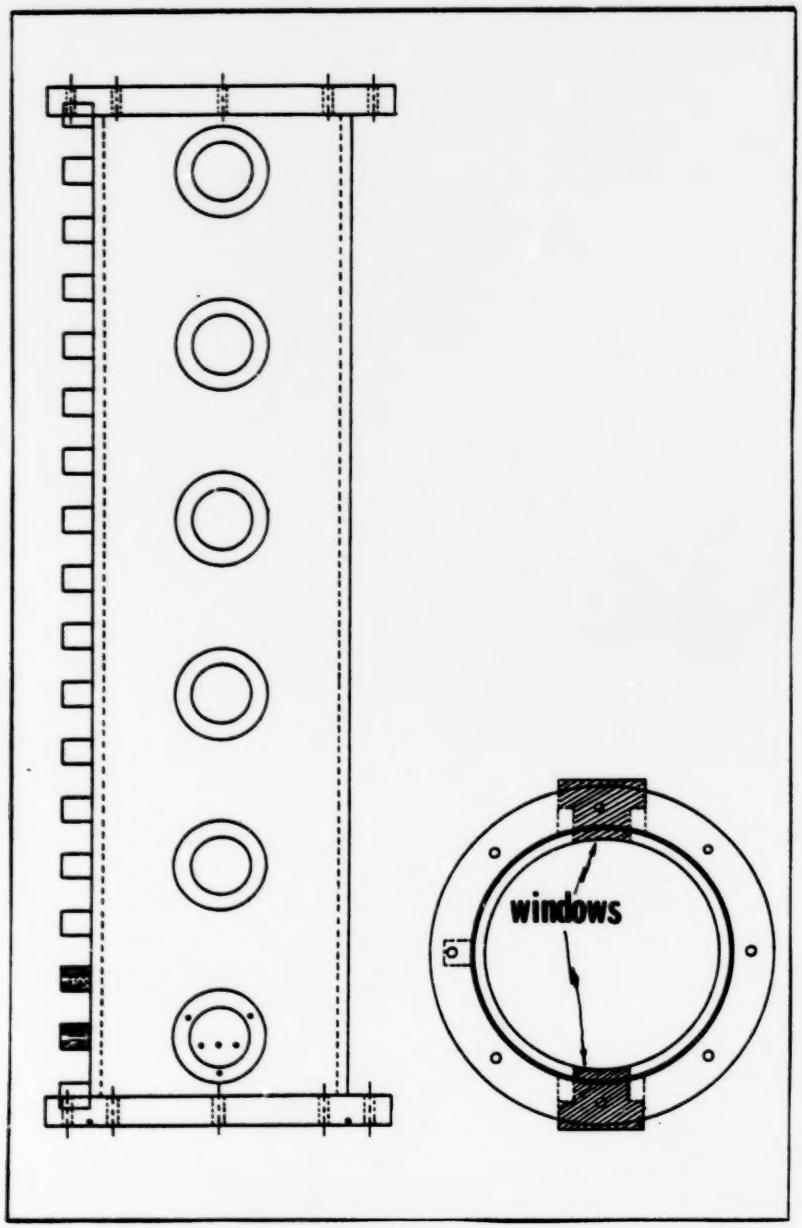

FIG. 12. SCHEMATIC REPRESENTATION OF THE "TEST SECTION" HOLDING THE "MEASURING WINDOWS" OF THE CYLINDRICAL FLUIDIZED BED. FRONT VIEW.

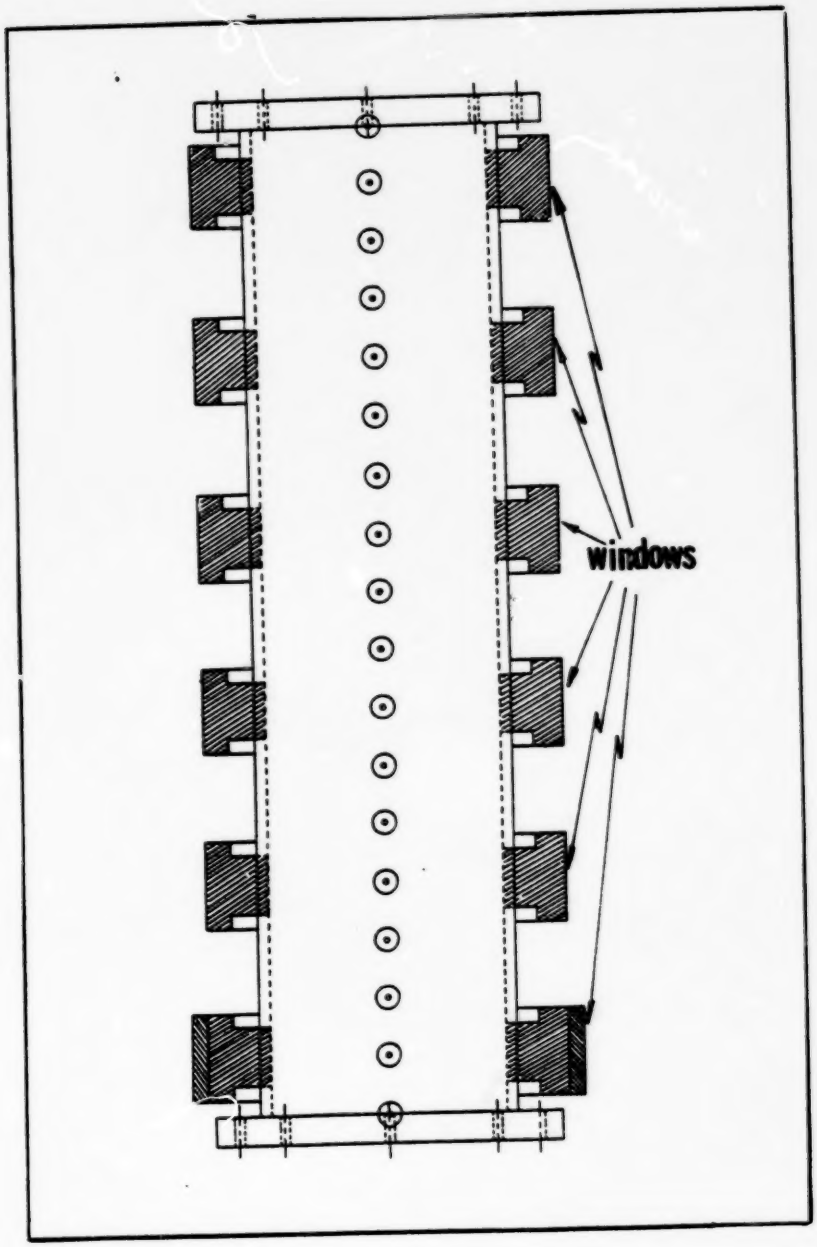

FIG. 13 SCHEMATIC REPRESENTATION OF THE "TEST SECTION" HOLDING THE "MEASURING WINDOWS", OF THE CYLINDRICAL FLUIDIZED BED. LATERAL VIEW.

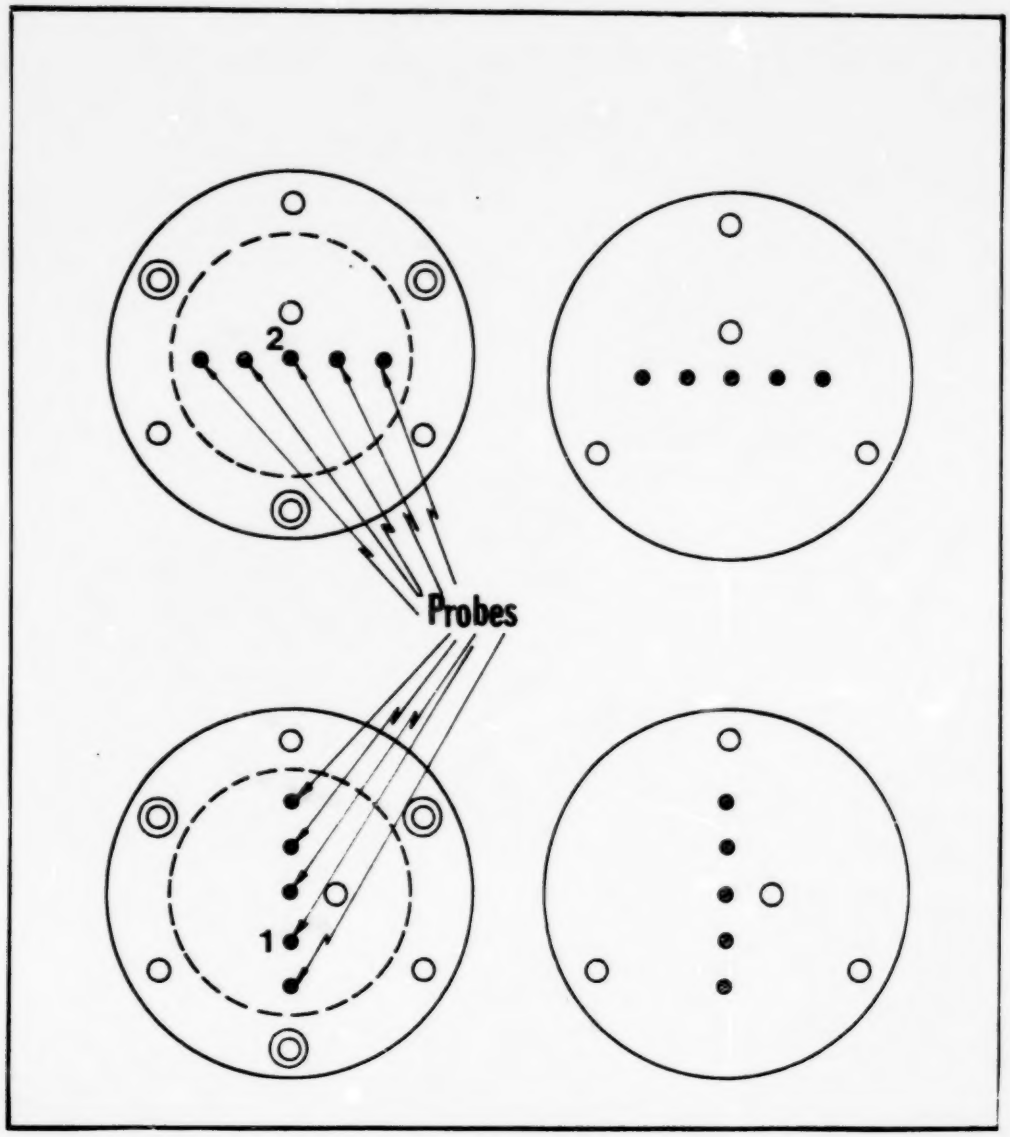

FIG. 14 SCHEMATIC REPRESENTATION OF THE "MEASURING WINDOWS" SHOWING THE HORIZONTAL AND VERTICAL POSITION OF THE PROBES.

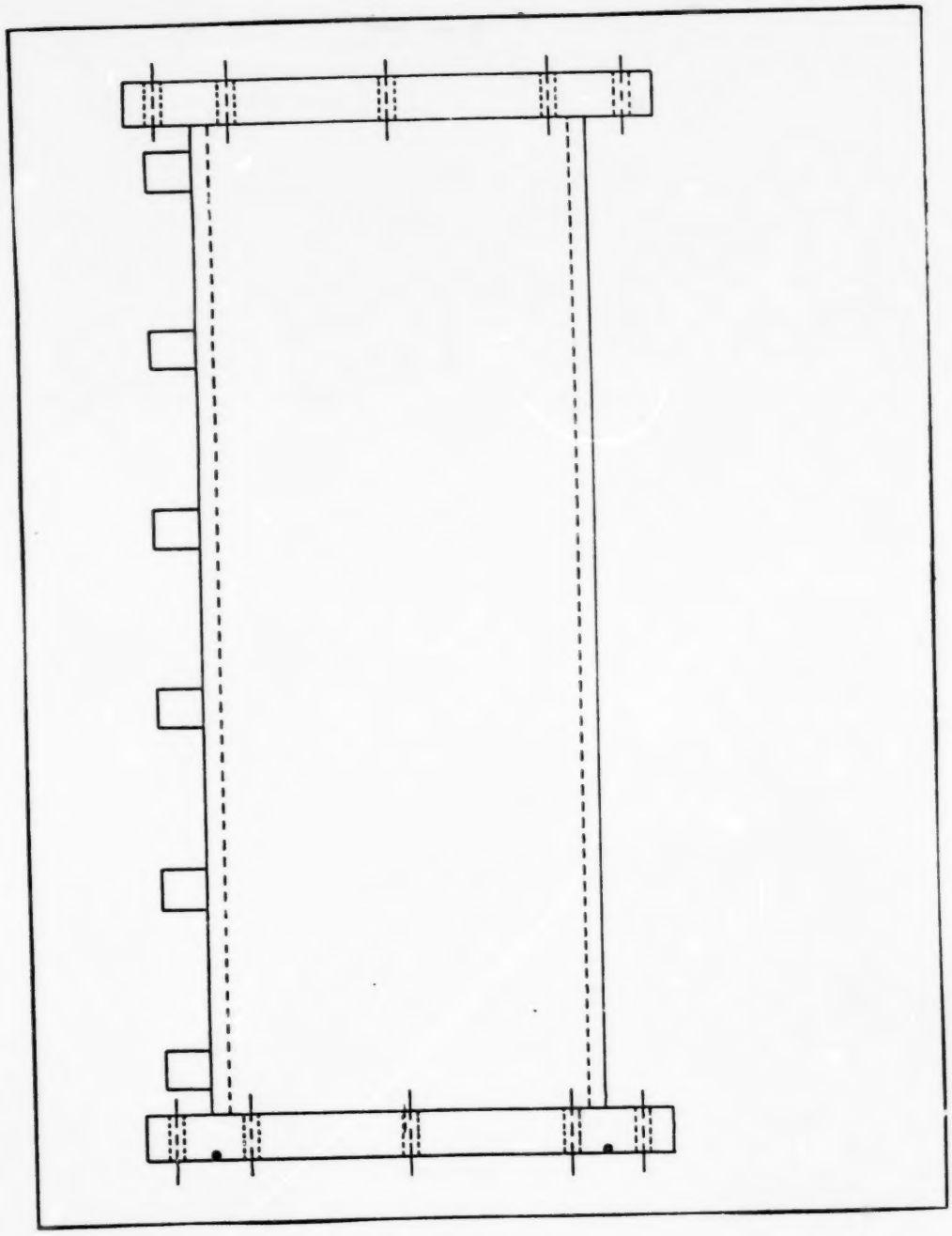

FIG. 15 SCHEMATIC REPRESENTATION OF ONE OF THE PLEXIGLASS SECTIONS (WITH NO WINDOWS) USED IN THE CYLINDRICAL BED.

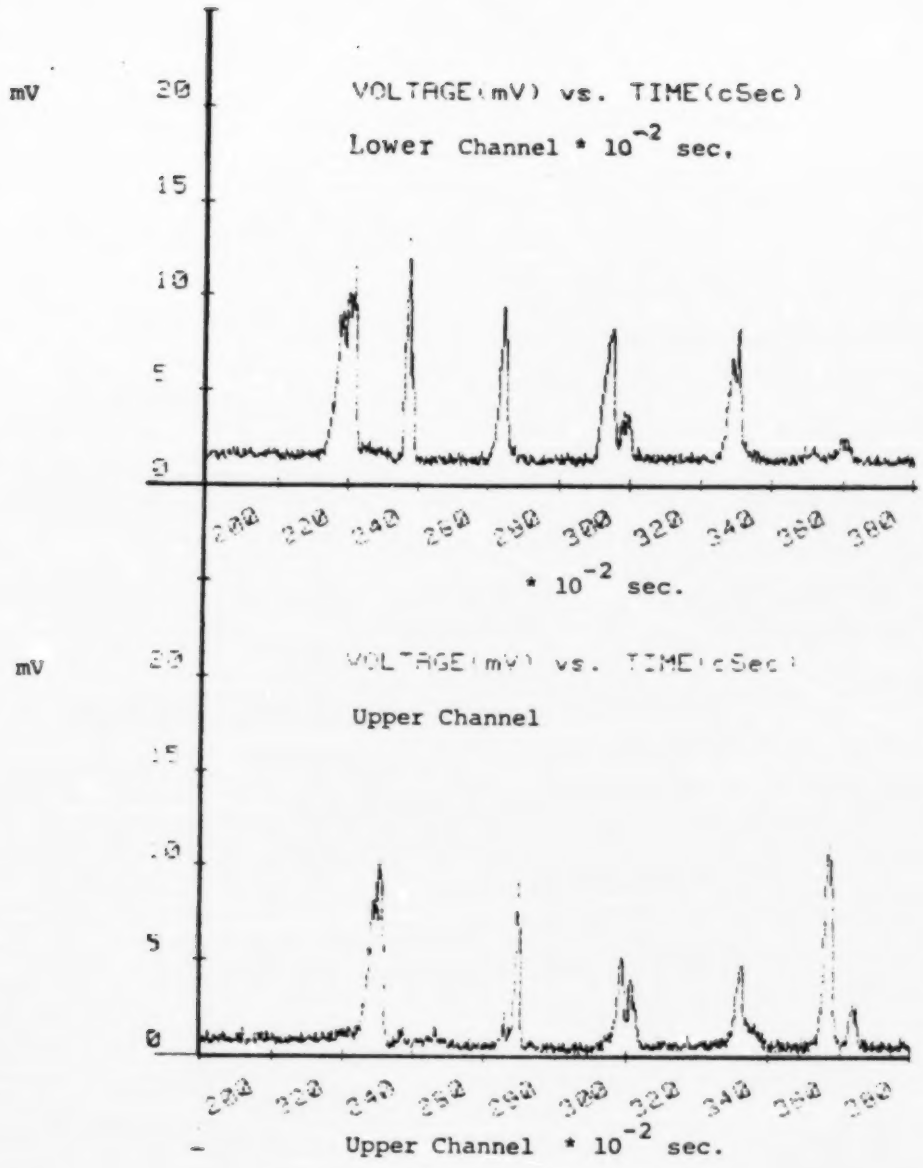

Fig. 16 RESPONSE OF PHOTODETECTORS AND OF THE DUAL CHANNEL DATA ACQUISITION SYSTEM

Vℓ : 1.28 cm/s
Vg : 2.10 cm/s

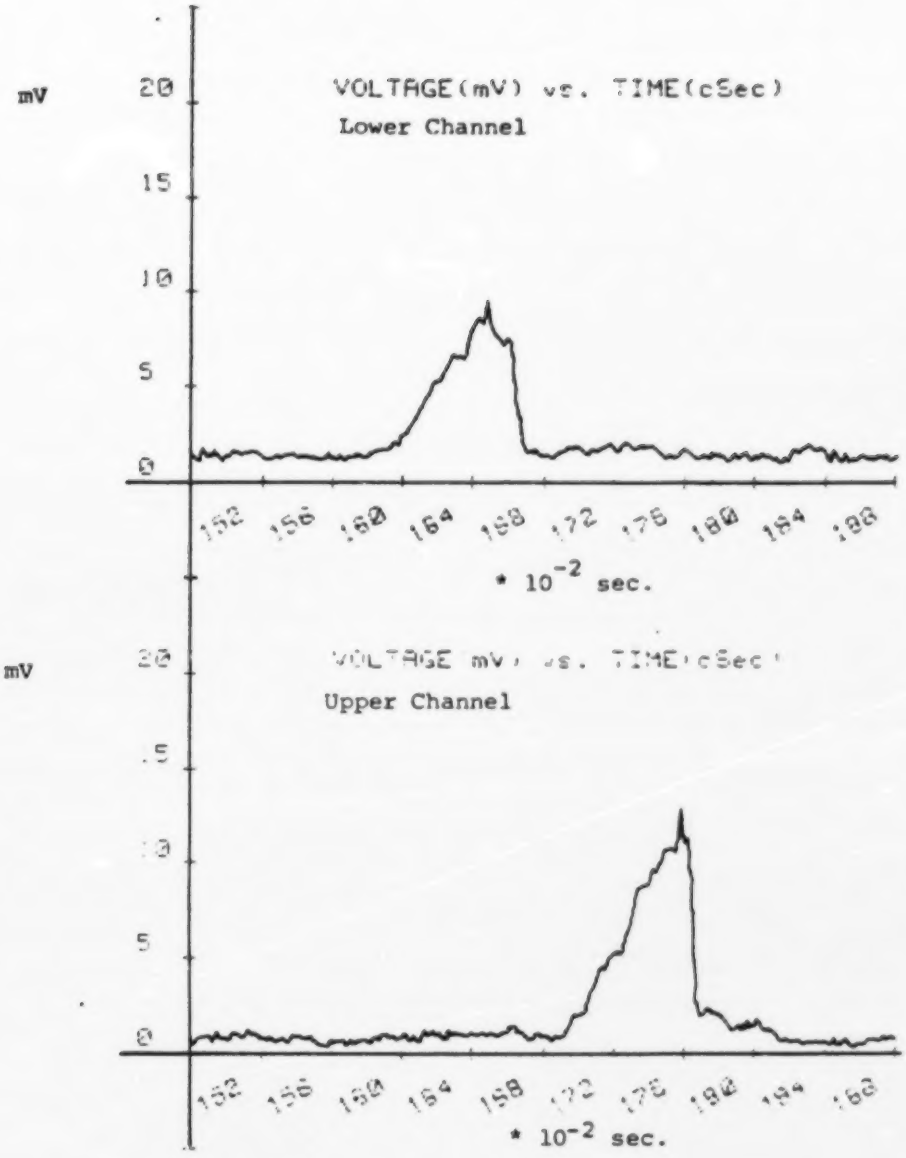

FIG. 17 RESPONSE OF PHOTODETECTORS AND OF THE DUAL CHANNEL DATA ACQUISITION SYSTEM

Vℓ : 1.28 cm/s

Vg : 2.10 cm/s

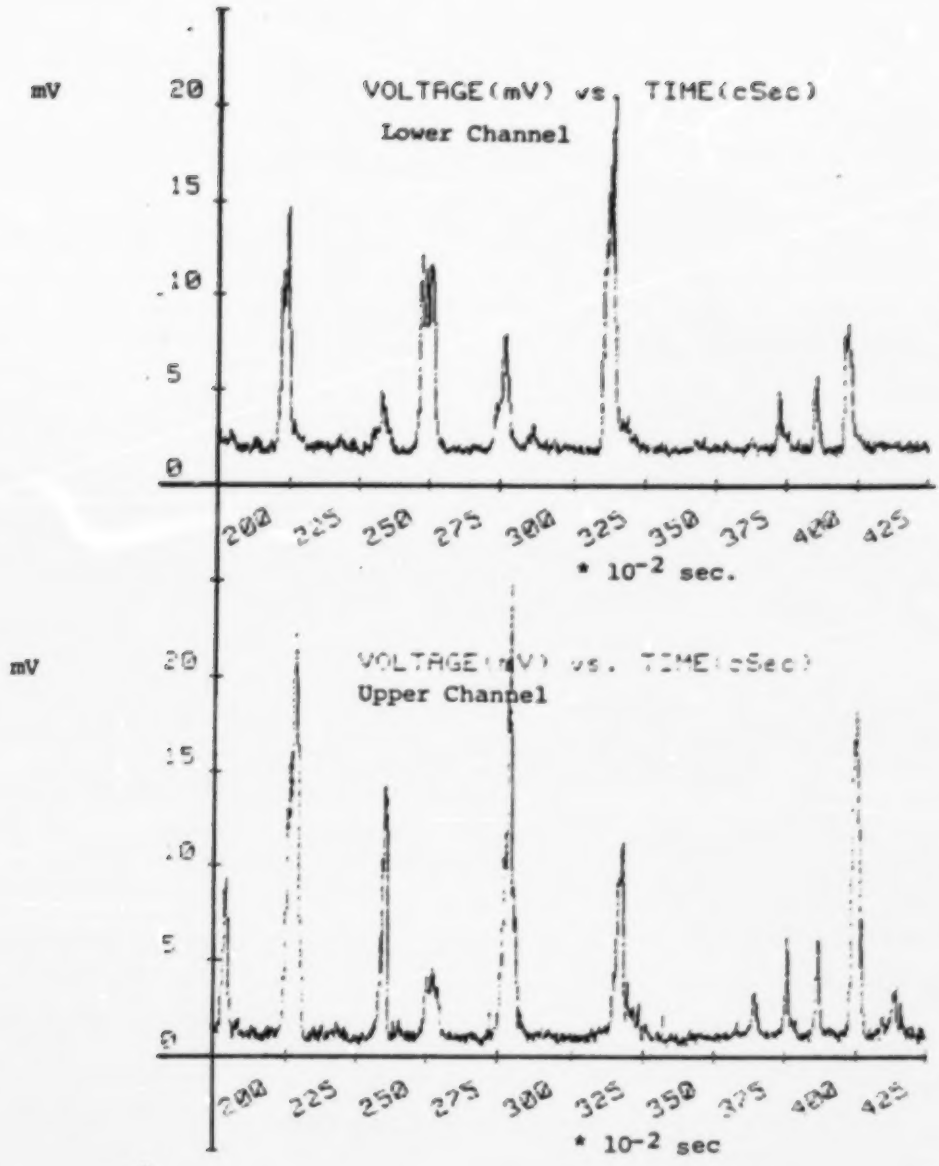

FIG. 18 RESPONSE OF PHOTODETECTORS AND THE DUAL CHANNEL DATA ACQUISITION SYSTEM.

V_ℓ : 1.51 cm/s

V_g : 3.50 cm/s

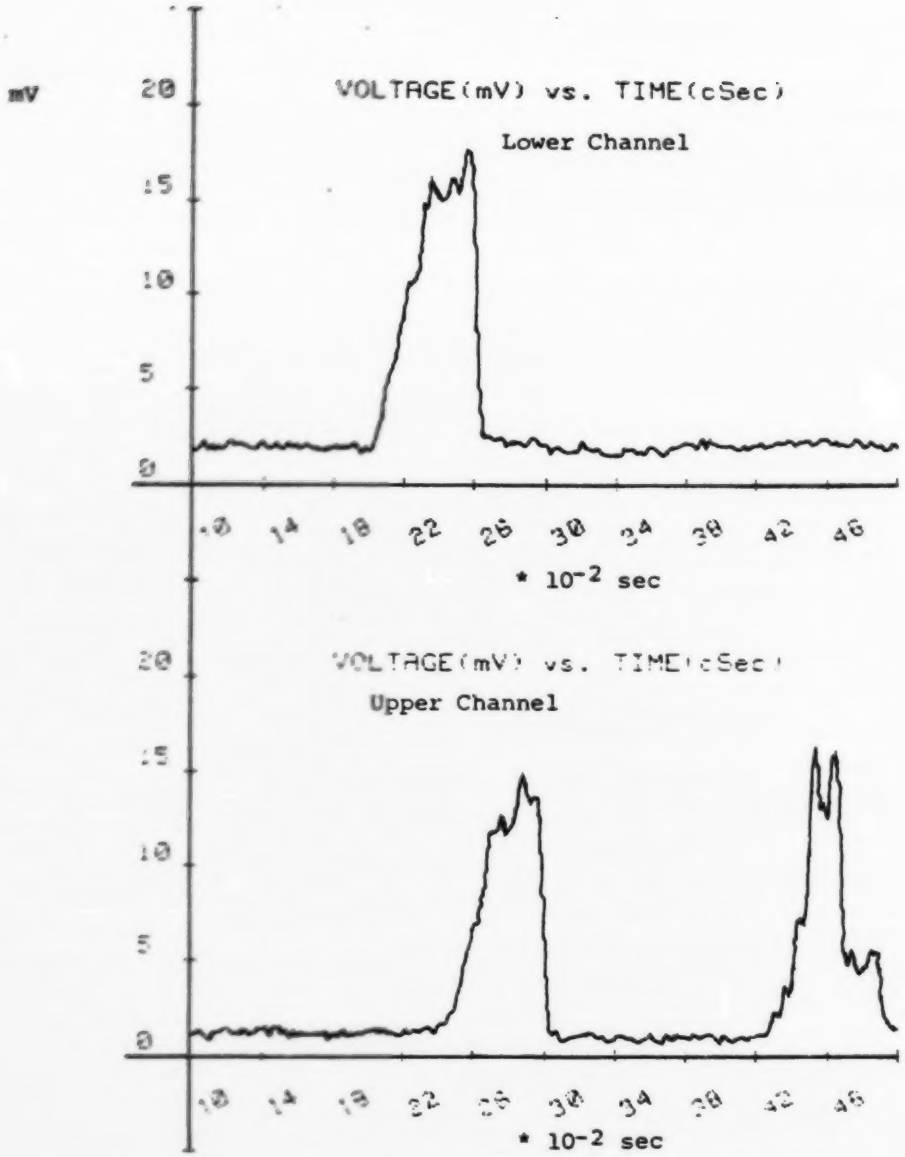

FIG. 19 RESPONSE OF PHOTODETECTORS AND THE DUAL CHANNEL DATA ACQUISITION SYSTEM

V_l : 1.51 cm/s

V_g : 3.50 cm/s

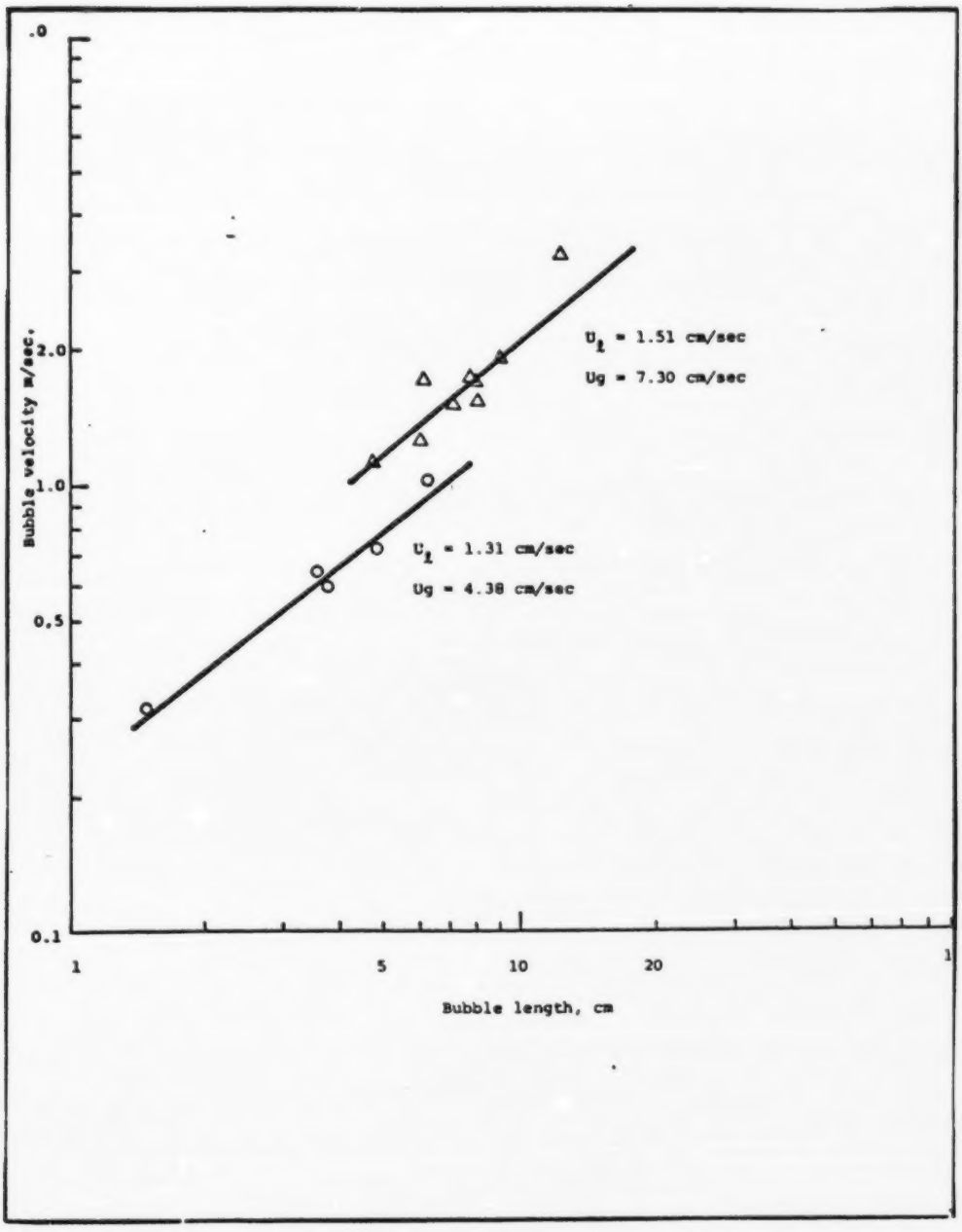

FIG. 20 RELATIONSHIP OF THE BUBBLE VELOCITY TO THE MEASURED AXIAL BUBBLE LENGTH ESTIMATED WITH THE ABSORPTION PHOTOMETRIC TECHNIQUE (Liquid: water, Gas: air, Solid: sand of 210μm average size)

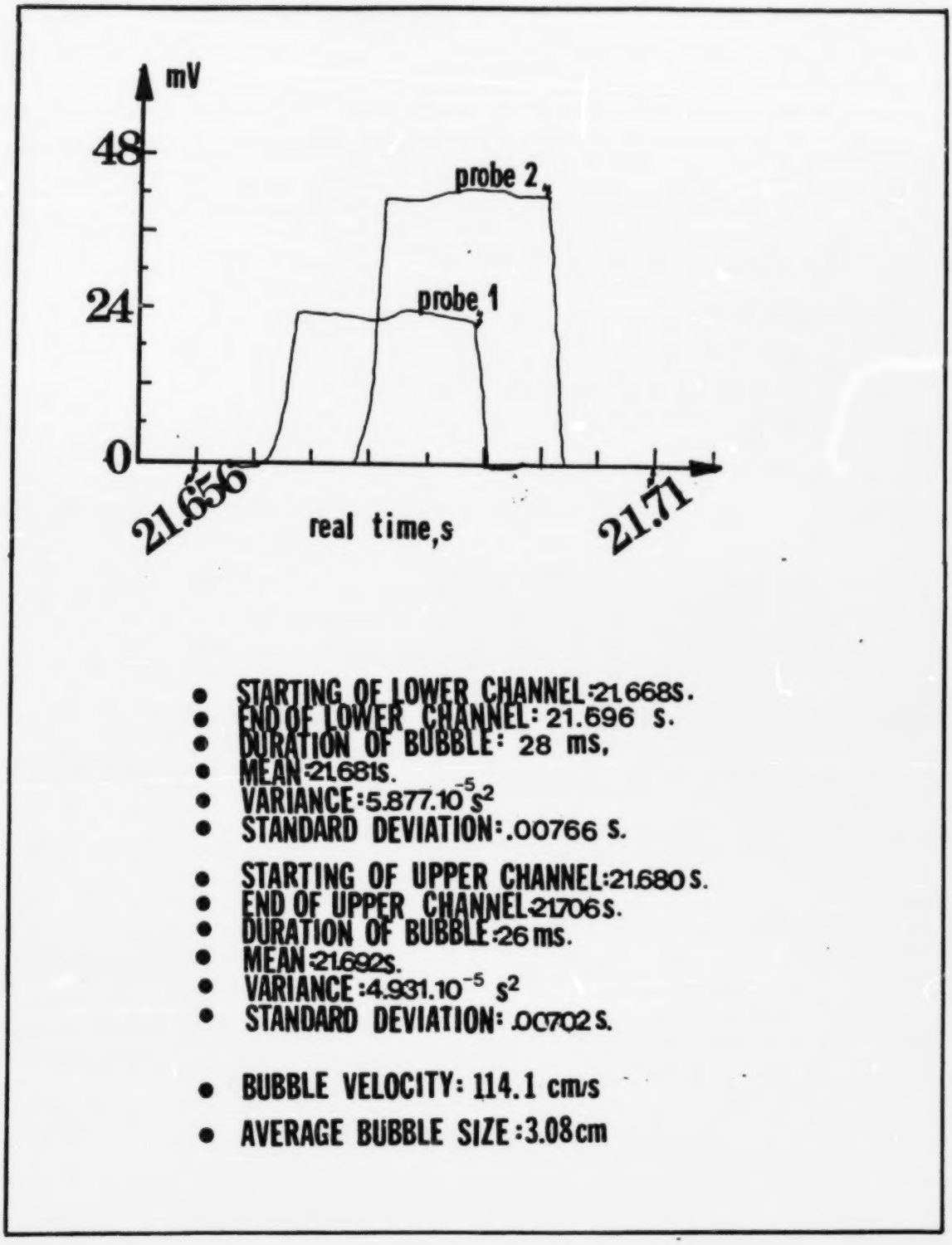

FIG. 21 TYPICAL SQUARE WAVE SIGNALS RECORDED BY THE U-SHAPED FIBER OPTIC SENSOR. PROBES 1 AND 2. BIDIMENSIONAL COLUMN

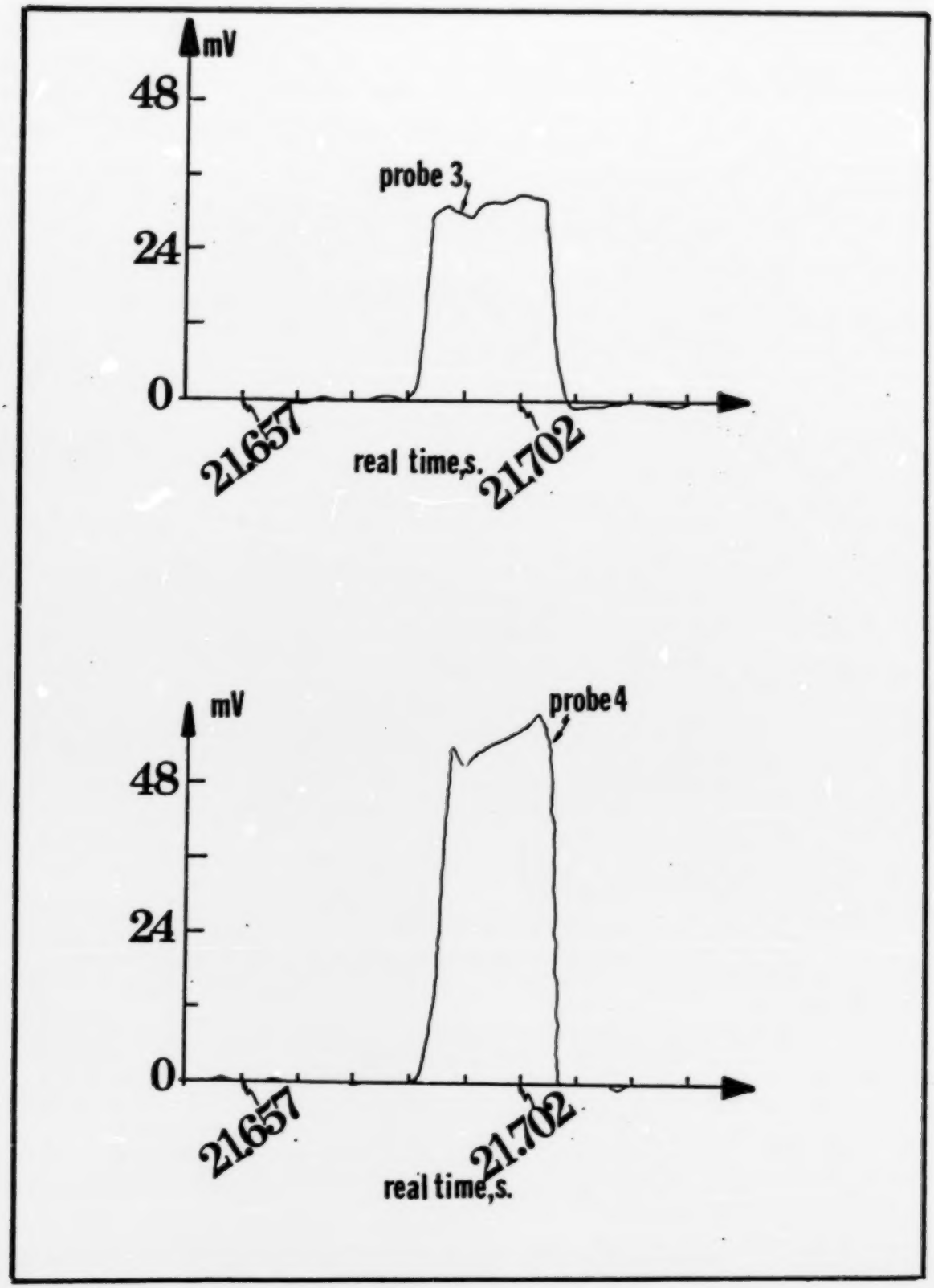

FIG. 22 TYPICAL SQUARE WAVE SIGNALS RECORDED BY THE FIBER OPTIC SENSOR. PROBES 3 AND 4. BIDIMENSIONAL COLUMN.

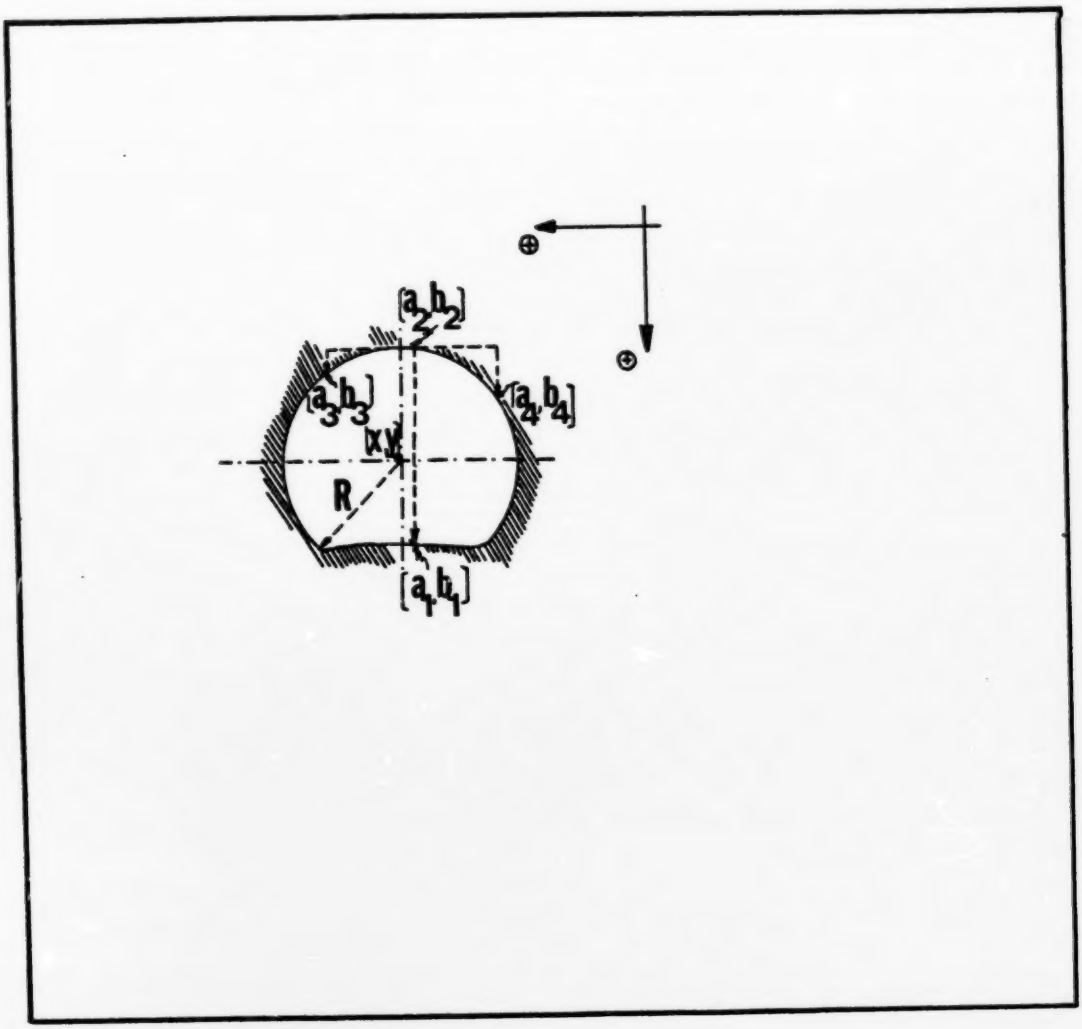

FIGURE 23 CAP OF SPHERICAL SHAPE SHOWING THE BUBBLE CHARACTERISTIC DIMENSIONS

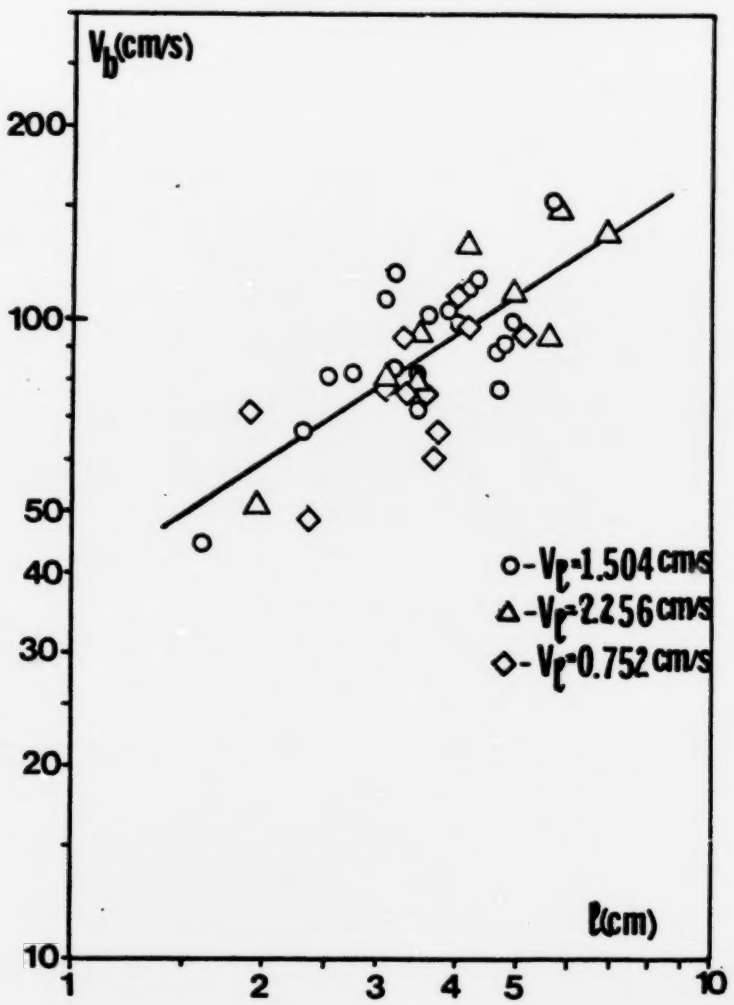

FIGURE 24 RELATIONSHIP OF THE BUBBLE VELOCITY TO THE MEASURED AXIAL BUBBLE LENGTH

Liquid: Water, Gas: Air, Solid: Glass Beads of 335 μm, Vg = 1.9 cm/s

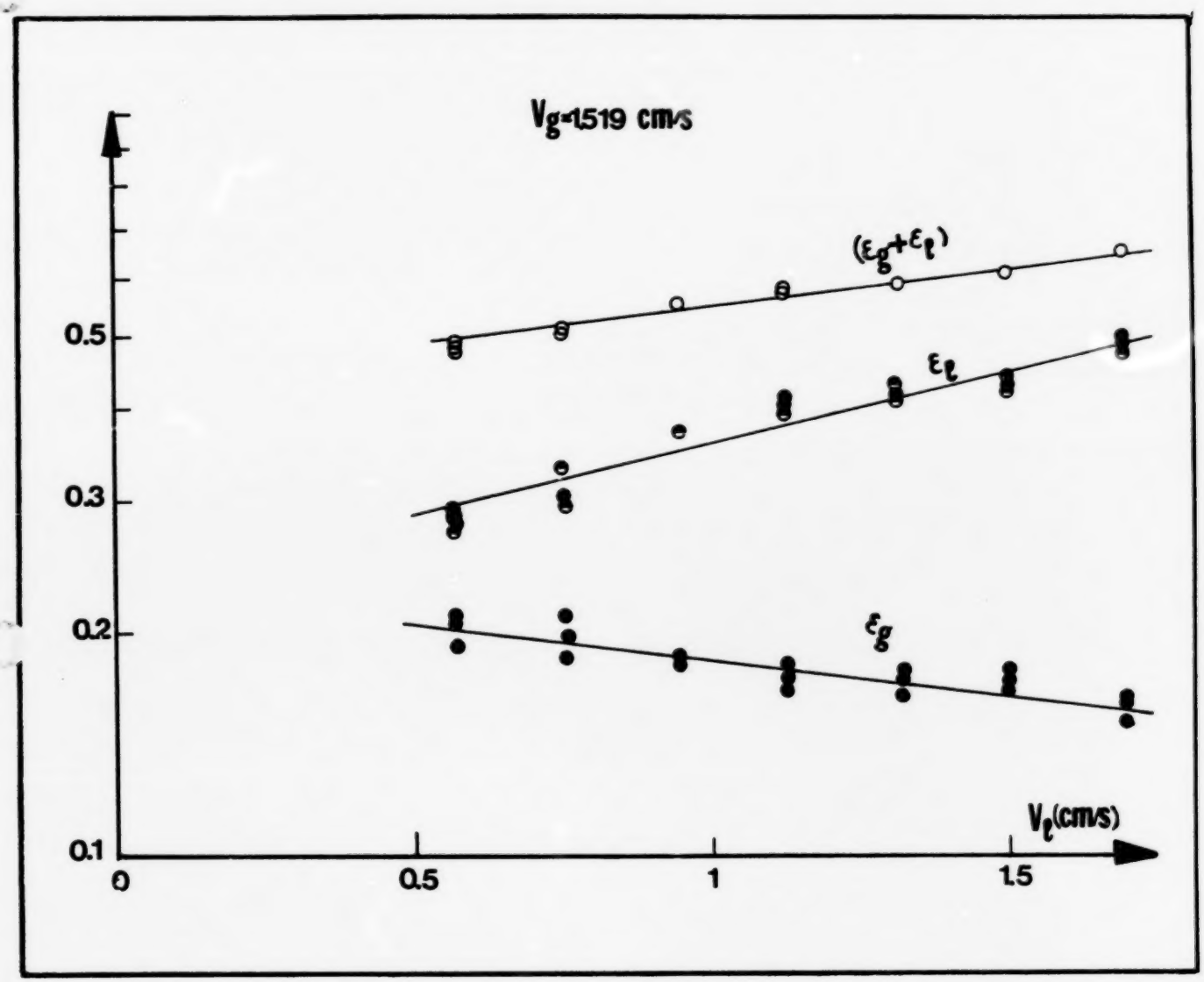

FIG. 25 VARIATION OF ε_ℓ, εg and $(\varepsilon_\ell + \varepsilon g)$ fractions with the velocity of the liquid.

Liquid: water, Gas: air, Solid: Glass beads of 335µm, Vg = 1.519 cm/s

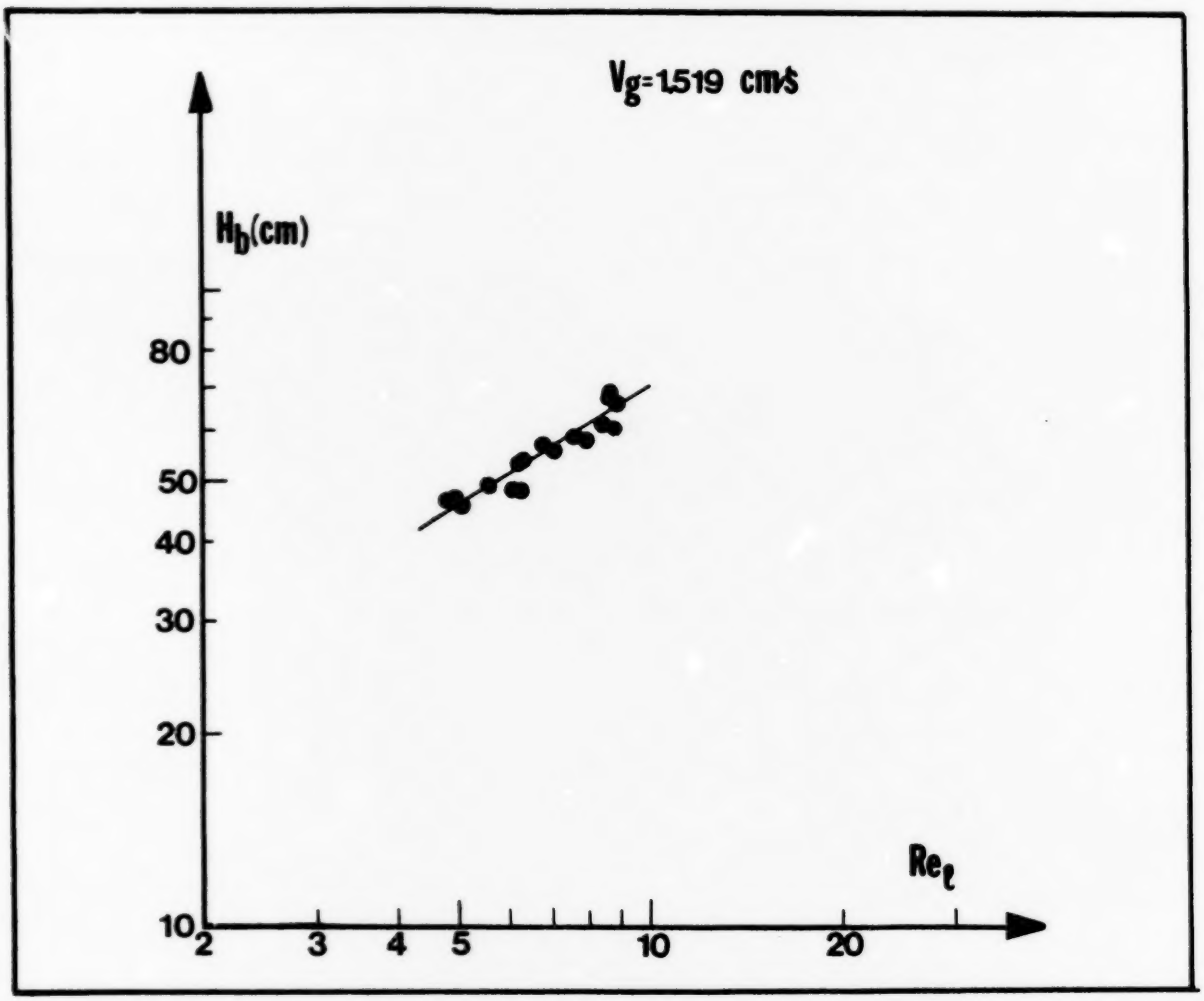

FIG. 26 VARIATION OF THE TOTAL HEIGHT OF THE BED H_b WITH Re_ℓ IN A THREE-PHASE FLUIDIZED BED.
Liquid: water, Gas: air, Solid: Glass beads of 335 µm, Vg = 1.519 cm/s

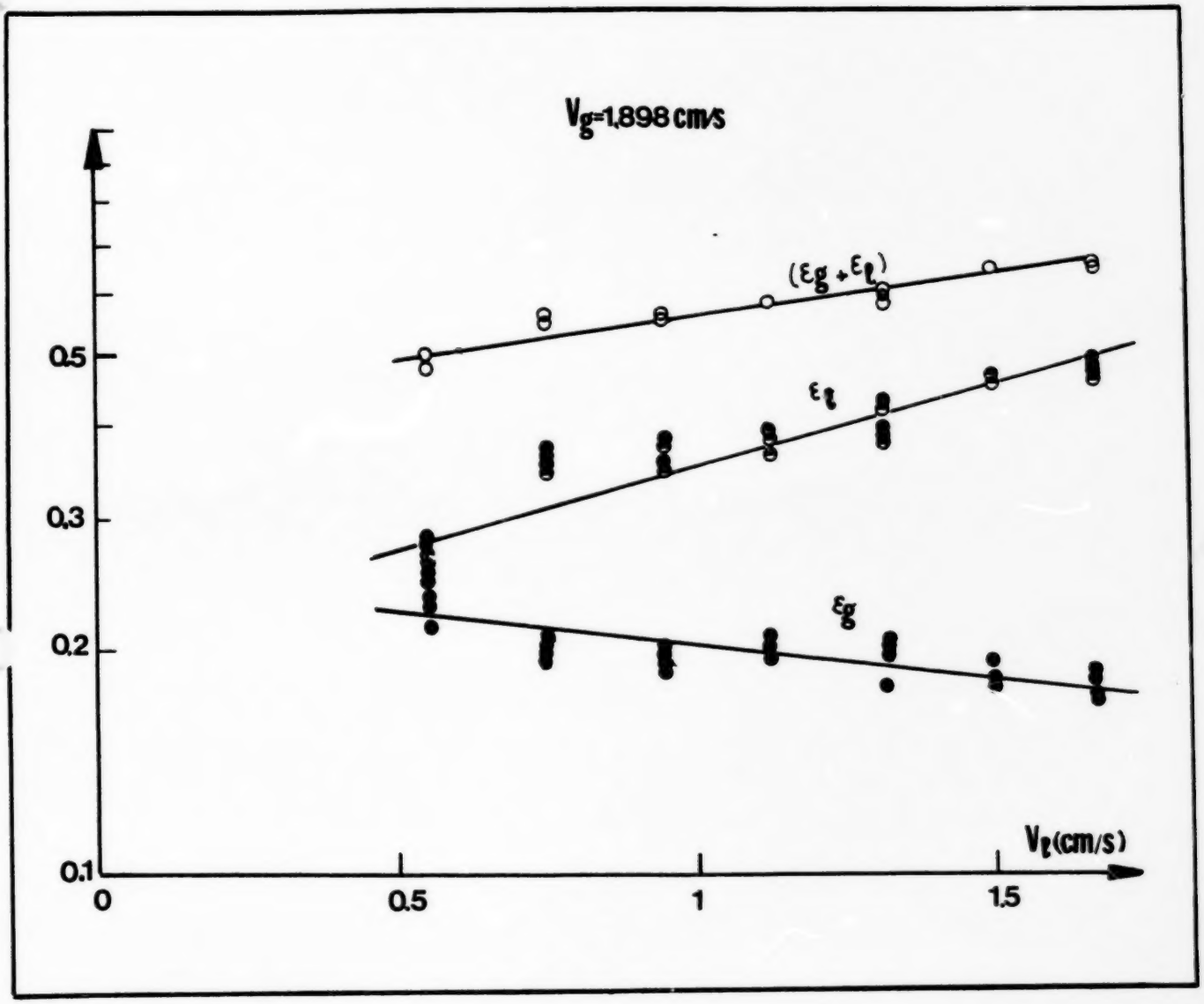

FIG. 27 VARIATION OF ε_ℓ, εg AND $(\varepsilon_\ell + \varepsilon g)$ FRACTIONS WITH THE VELOCITY OF THE LIQUID IN A THREE-PHASE FLUIDIZED BED.
Liquid: water, Gas: air, Solid: Glass beads of 335 µm, Vg = 1.898 cm/s

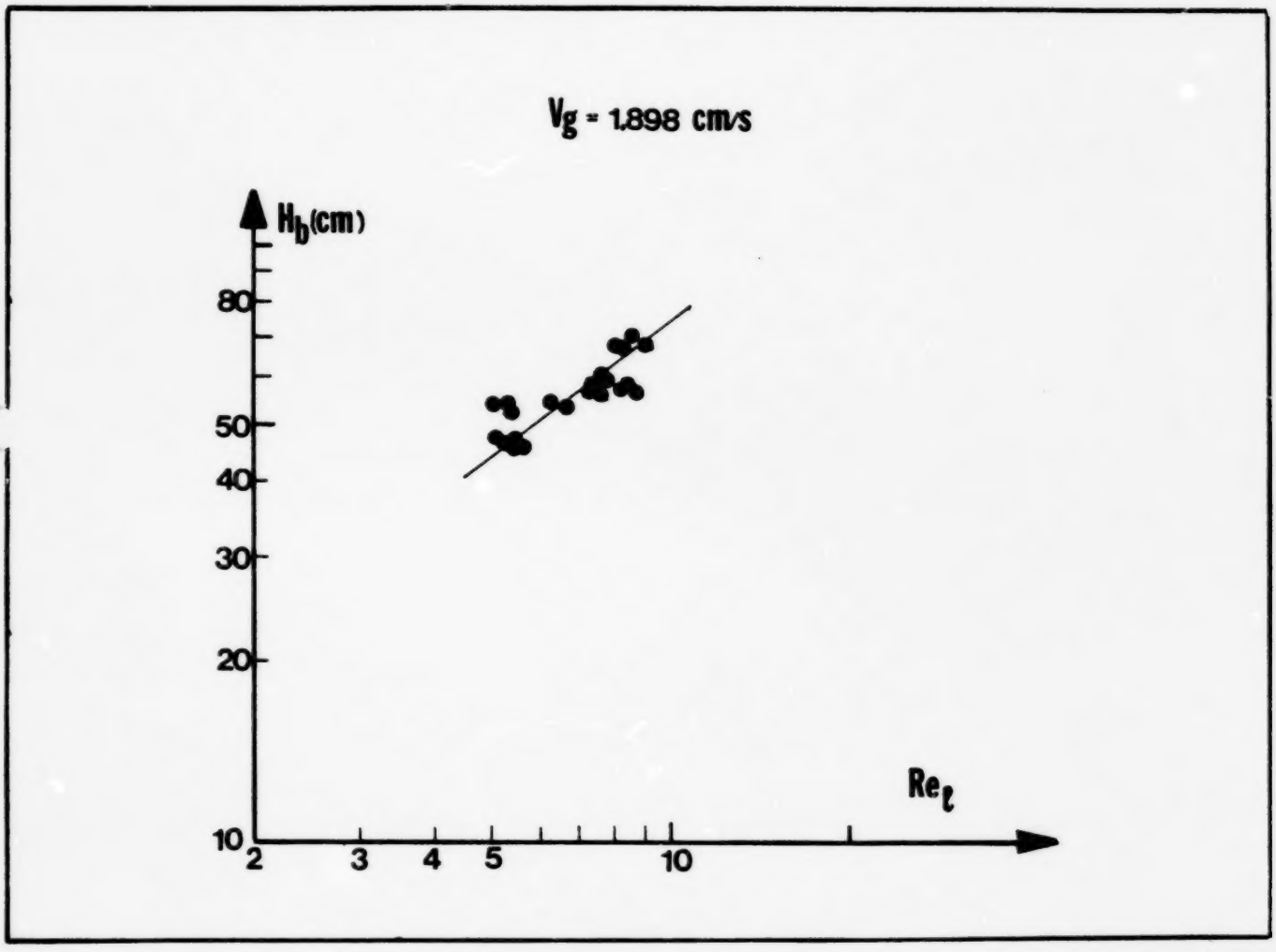

FIG. 28 VARIATION OF THE TOTAL HEIGHT OF THE BED H_b WITH Re_ℓ IN A THREE-PHASE FLUIDIZED BED.
Liquid: water, Gas: air, Solid: Glass beads of 335 µm, Vg = 1.898 cm/s.

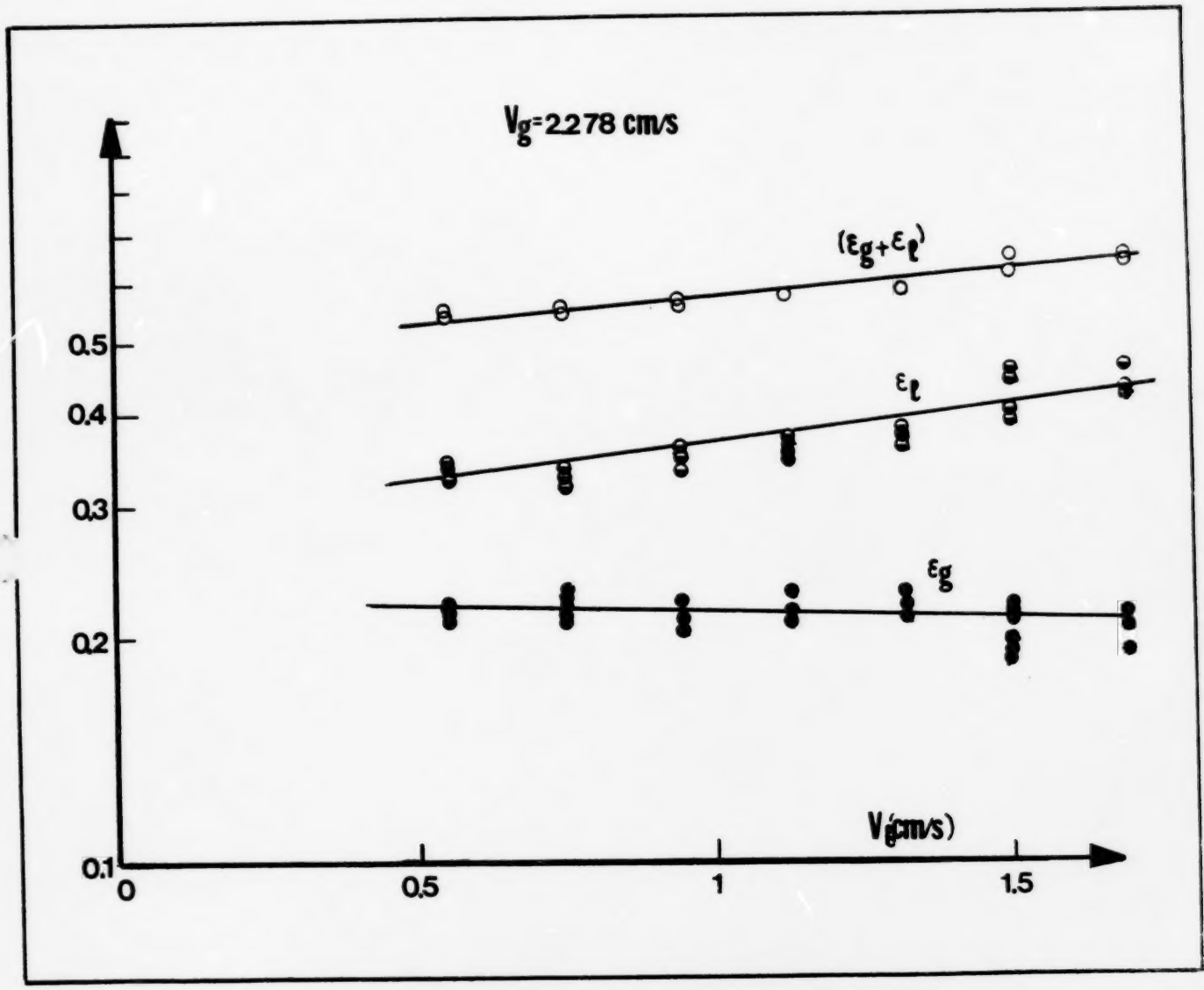

FIG. 29 VARIATION OF ε_ℓ, εg AND $(\varepsilon g + \varepsilon_\ell)$ FRACTIONS WITH THE VELOCITY OF THE LIQUID IN A THREE-PHASE FLUIDIZED BED.

Liquid: water, Gas: air, Solid: Glass beads of 335 µm
Vg = 2.278 cm/s

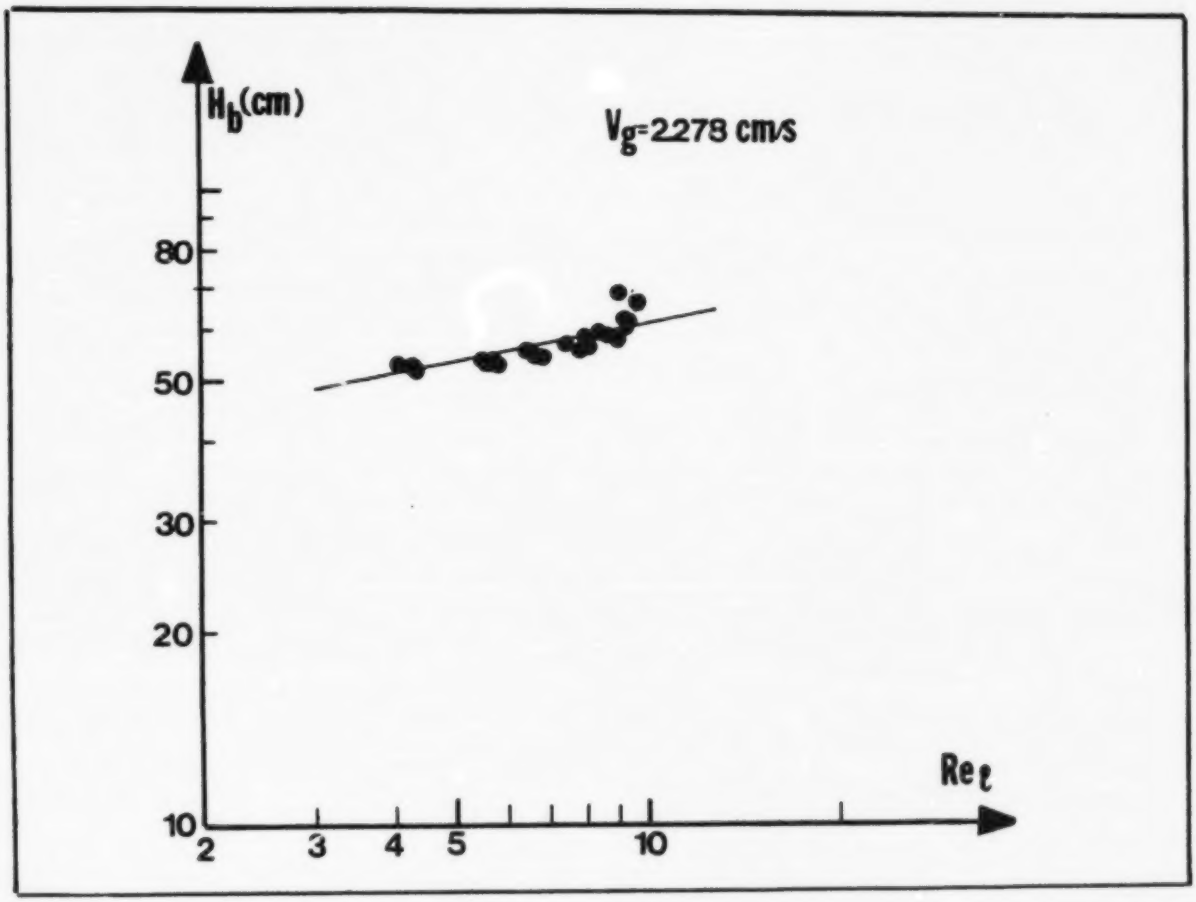

$$Re_\ell = \frac{u_\ell d_p \rho_\ell}{\mu_\ell}$$

FIG. 30 VARIATION OF THE TOTAL HEIGHT OF THE BED H_b WITH Re_ℓ IN A THREE-PHASE FLUIDIZED BED.
Liquid: water, Gas: air, Solid: Glass beads of 335 μ, Vg = 2.278 cm/s

*** DATE OF EXPERIMENT: 11 / 28 /198 0

*** DISK NUMBER: 51

*** FILE NAME: A1

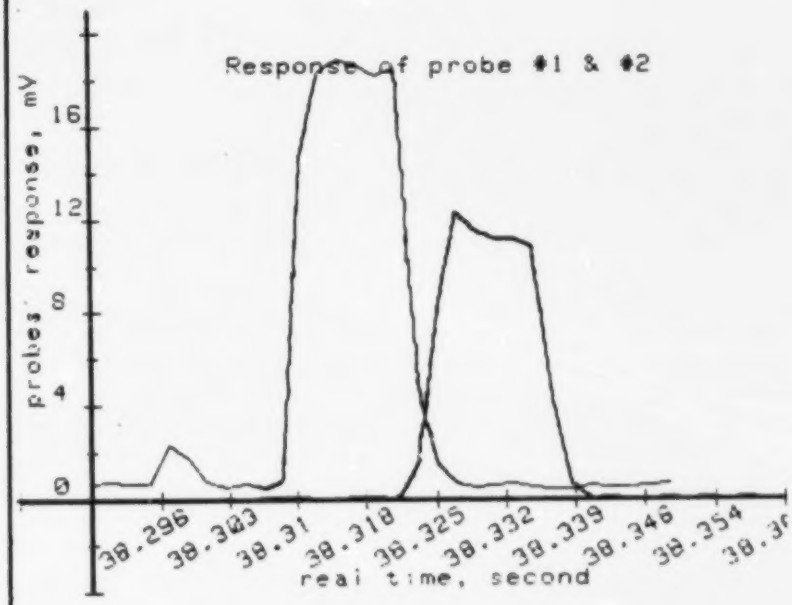

*** BUBBLE # 45

*** STARTING OF LOWER CHANNEL : 38.316 Sec
*** END OF LOWER CHANNEL : 38.336 Sec
*** DURATION OF BUBBLE : 10
*** MEAN= 38.324 Sec
*** VARIANCE= 1.4707E-5 Sec*Sec
*** STANADAR DEVIATION= .003835 Sec

*** STARTING OF UPPER CHANNEL : 38.33 Sec
*** END OF UPPER CHANNEL : 38.348 Sec
*** DURATION OF BUBBLE : 9
*** MEAN= 38.337 Sec
*** VARIANCE= 1.4465E-5 Sec*Sec
*** STANDARD DEVIATION= .0038034 Sec

*** BUBBLE VELOCITY : 58.77 cm/Sec

*** AVERAGE BUBBLE SIZE : 1.31 cm

Figure 31. Typical square wave signals recorded by the U-shaped fiber optic sensors. Probes 1 and 2. Cylindrical Column.

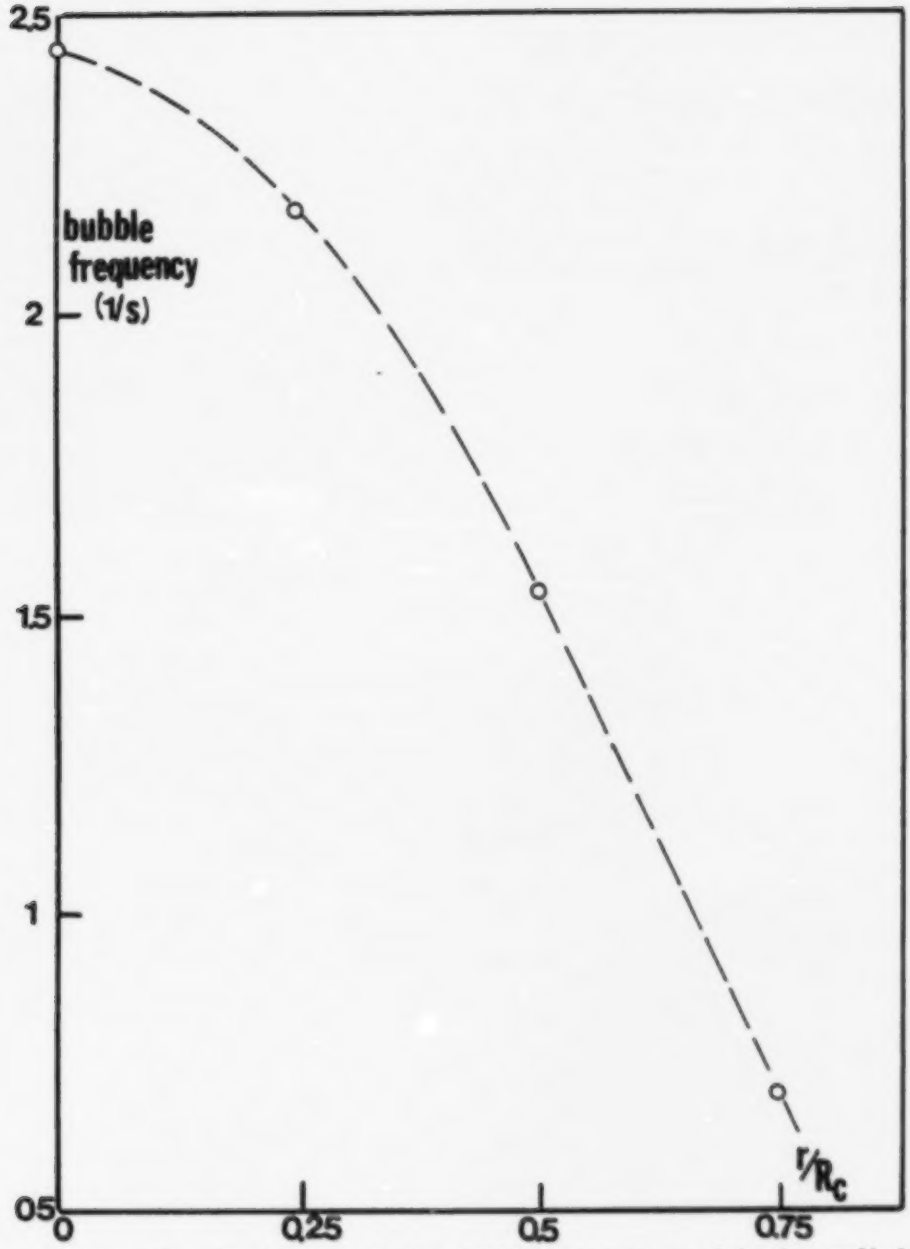

Figure 32. Variation of the bubble frequency with the radial position in the cylindrical column. Single injector located at r/R_c = 0, Liquid: water, Gas:air, Solid: glass beads of 335μm, V_g = 1.769 cm/s, V_ℓ = 0.778 cm/s.

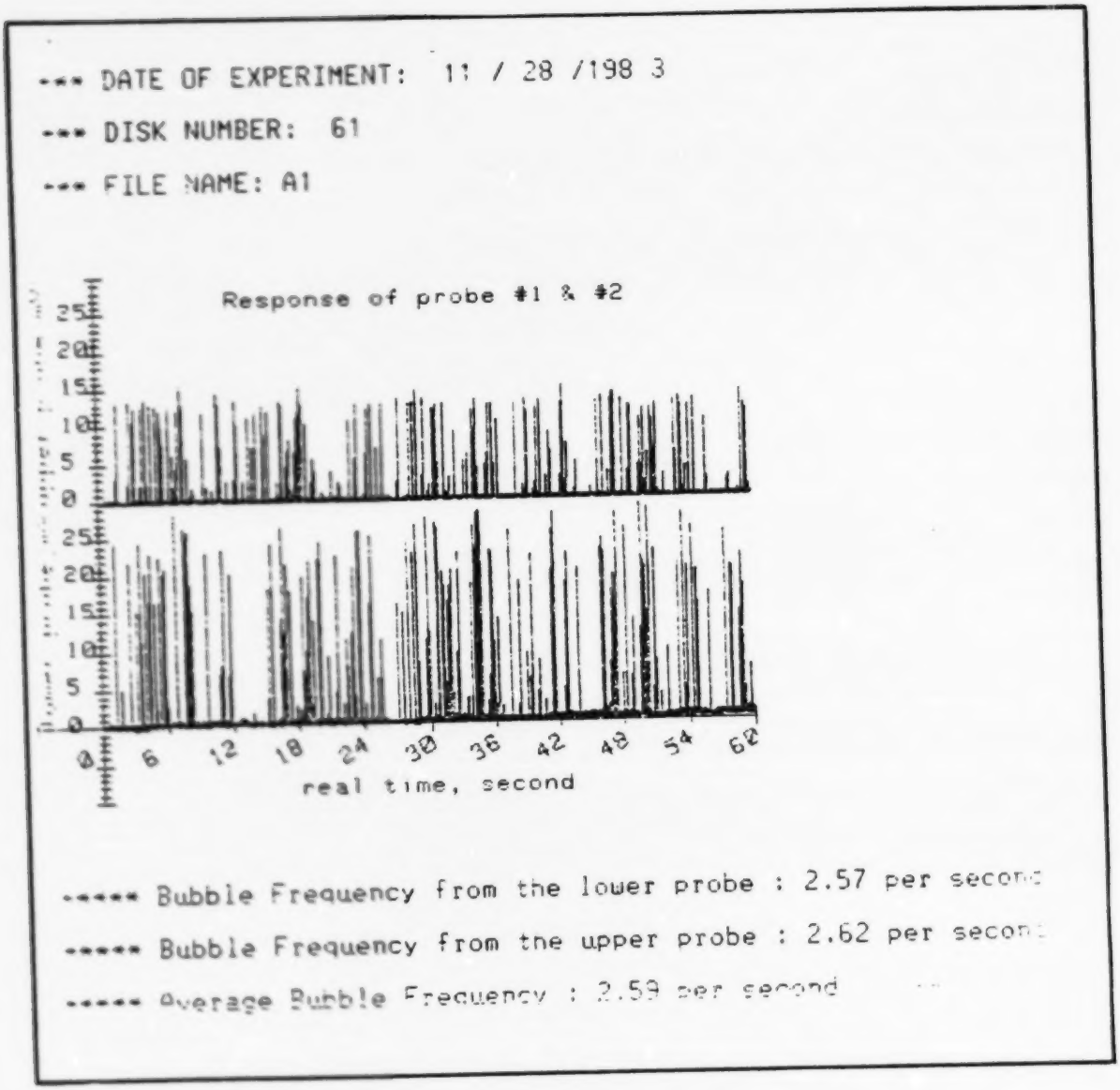
--- DATE OF EXPERIMENT: 11 / 28 /198 3
--- DISK NUMBER: 61
--- FILE NAME: A1
Response of probe #1 & #2
real time, second
----- Bubble Frequency from the lower probe : 2.57 per second
----- Bubble Frequency from the upper probe : 2.62 per second
----- Average Bubble Frequency : 2.59 per second

Figure 33. Bubbles in the cylindrical three phase fluidized bed column as viewed by Probes 1 and 2 located at $r/R_c = 0$, Liquid: water, Gas: air, Solid: glass beads of 335μm, V_g = 1.769 cm/s, V_ℓ = 0.778 cm/s, Gas injector: One positioned at r/R_c=0.

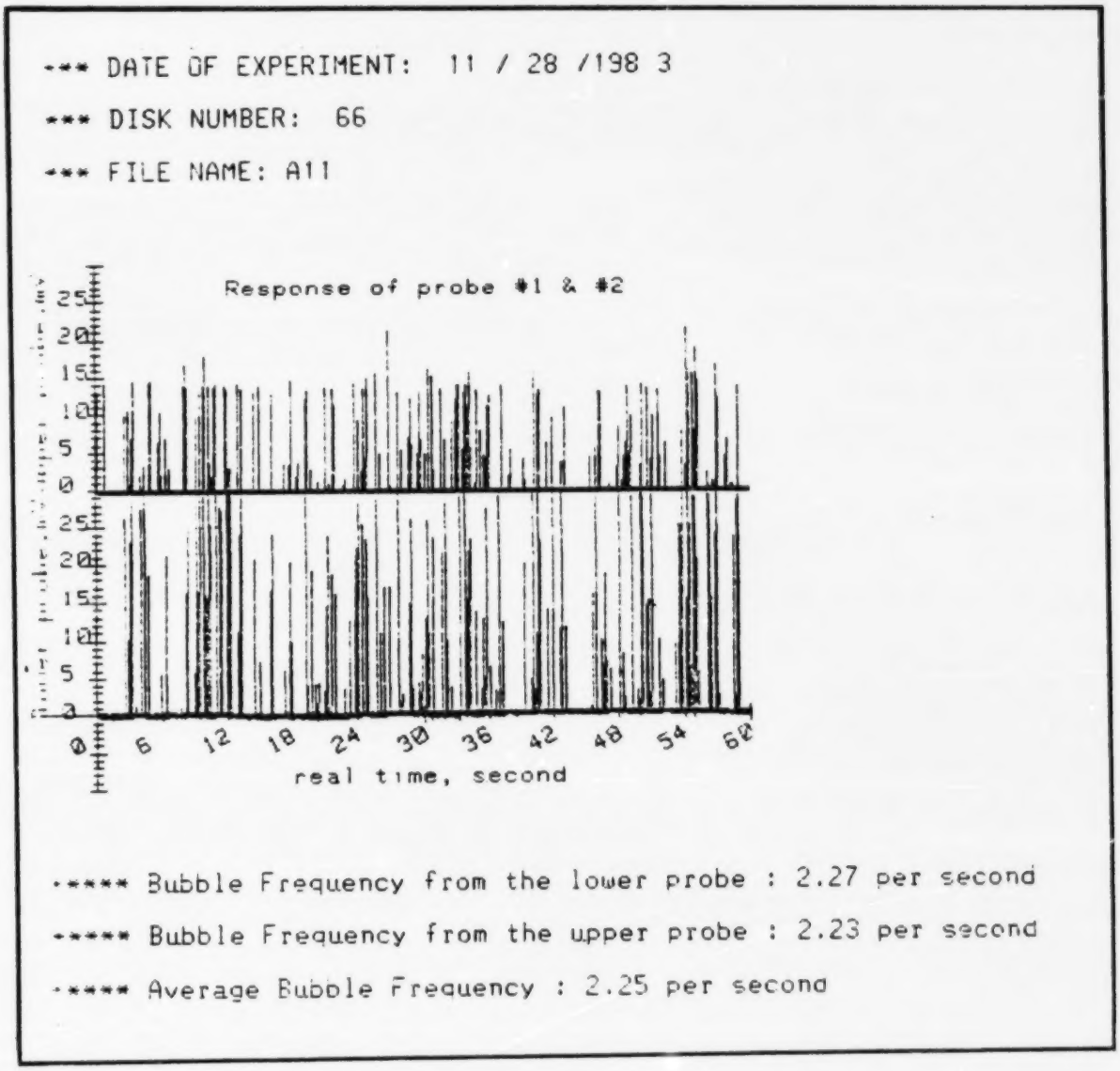
*** DATE OF EXPERIMENT: 11 / 28 /198 3
*** DISK NUMBER: 66
*** FILE NAME: A11
Response of probe #1 & #2
real time, second
***** Bubble Frequency from the lower probe : 2.27 per second
***** Bubble Frequency from the upper probe : 2.23 per second
***** Average Bubble Frequency : 2.25 per second

Figure 34. Bubbles in the cylindrical three phase fluidized bed column as viewed by Probes 1 and 2 located at r/R_c = 0.25. Liquid: water, Gas: air, Solid: glass beads of 335μm, $\bar{v}_g$ = 1.769 cm/s, V_ℓ 0.778 cm/s, Gas Injector: One positioned at r/R_c = 0.

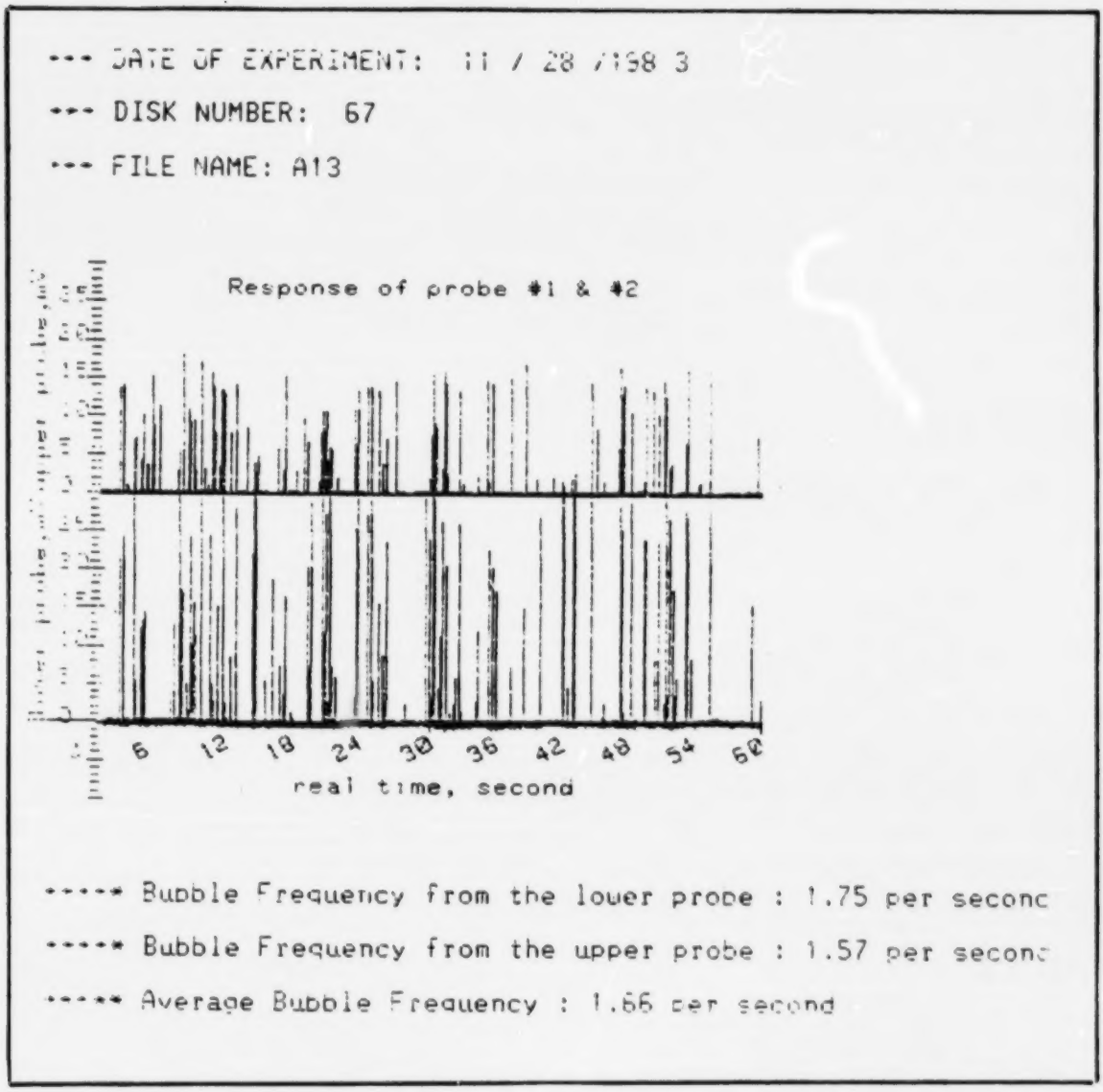

Figure 35. Bubbles in the cylindrical three phase fluidized bed column as viewed by Probes 1 and 2 located at r/R_c = 0.50. Liquid: water, Gas: air, Solid: glass beads of 335μm, V_g = 1.769 cm/s, V_ℓ = 0.778 cm/s, Gas Injector: One positioned at r/R_c = 0.

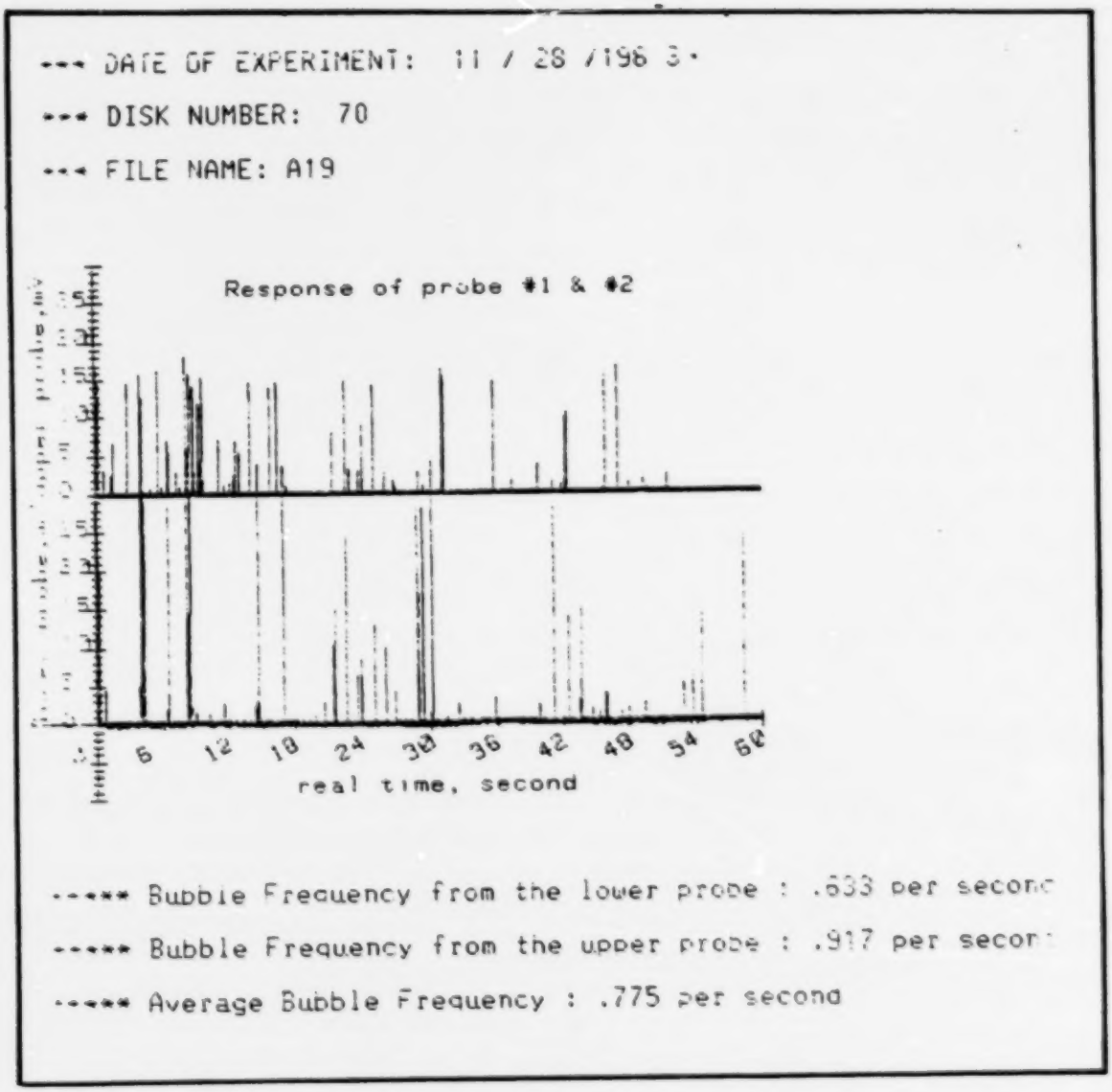

Figure 36. Bubbles in the cylindrical three phase fluidized bed column as viewed by probes 1 and 2 located at r/R_c = 0.75. Liquid: water, Gas: air, Solid: glass beads of 335μm, Vg = 1.769 cm/s, V_ℓ = 0.778 cm/s, Gas Injector: one positioned at r/R_c = 0.

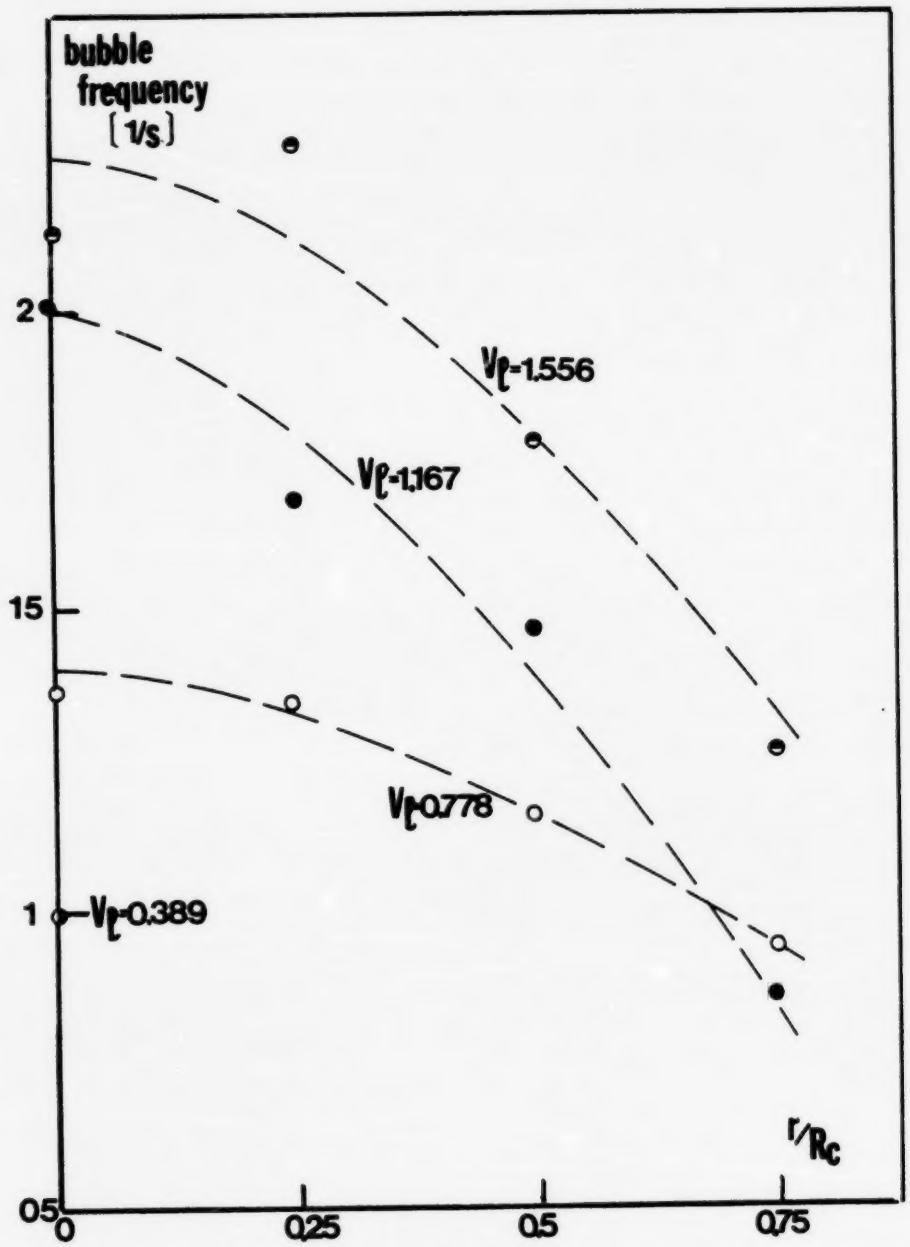

Figure 37. Variation of the bubble frequency with the radial position in the cylindrical column. Four injectors located as it is described in Figure 11. Liquid: water, Gas: air, Solid: glass beads of 335μm, Vg = 1.630 m/s.

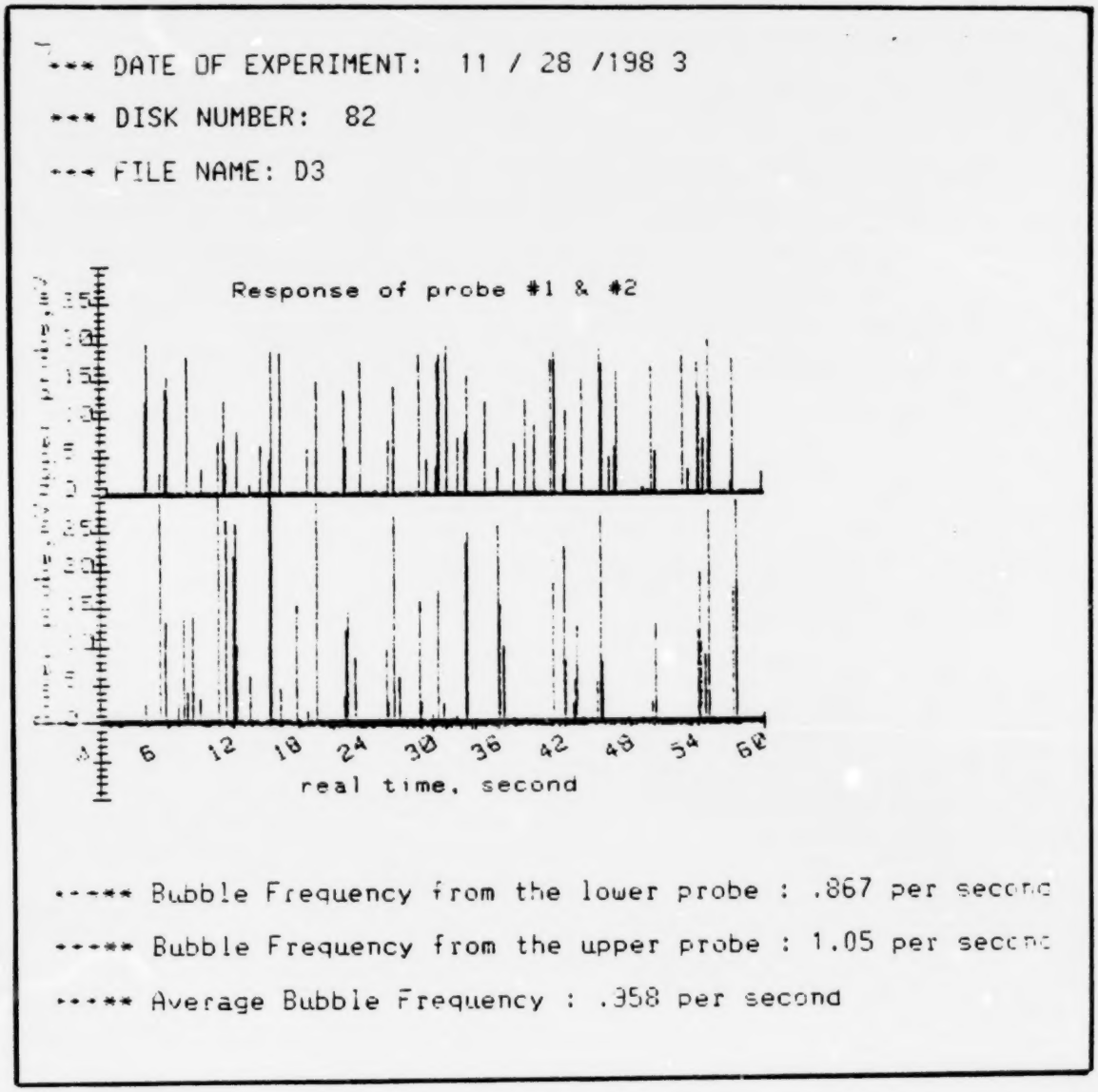

Figure 38. Bubbles in the cylindrical three phase fluidized bed column as viewed by Probes 1 and 2 located at $r/R_c = 0$. Liquid: water, Gas: air, Solid: glass beads of 335 μm, V_g = 1.630 cm/s, V_ℓ = 0.389 cm/s, Gas Injectors: four positioned as it is described in Figure 11.

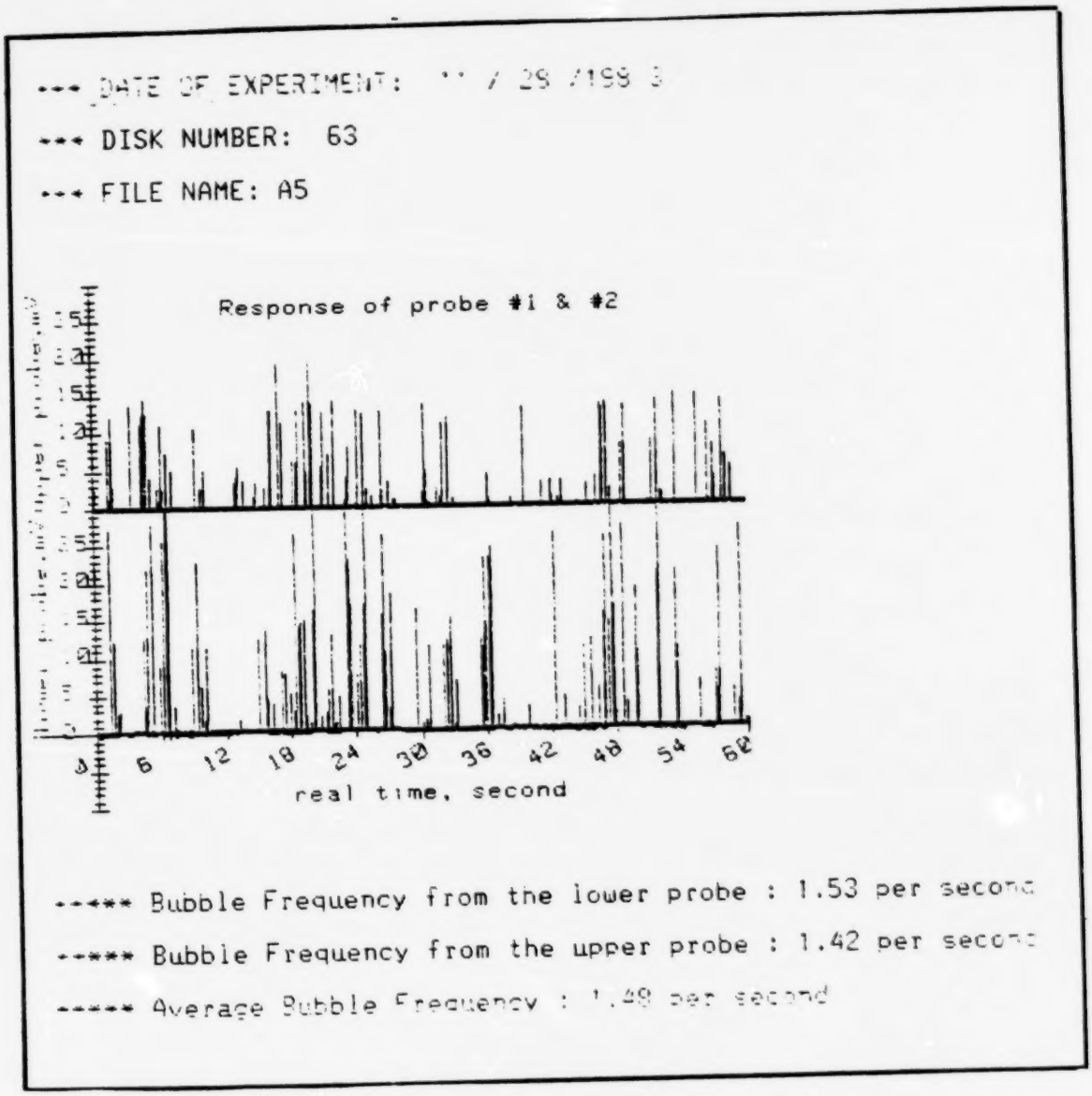

Figure 39. Bubbles in the cylindrical three phase fluidized bed column as viewed by probes 1 and 2 located at $r/R_c = 0$. Liquid: water, Gas: air, Solid: glass beads of 335μm, V_g = 1.630 cm/s, V_ℓ = 0.778 cm/s, Gas Injectors: four positioned as it is described in Figure 11.

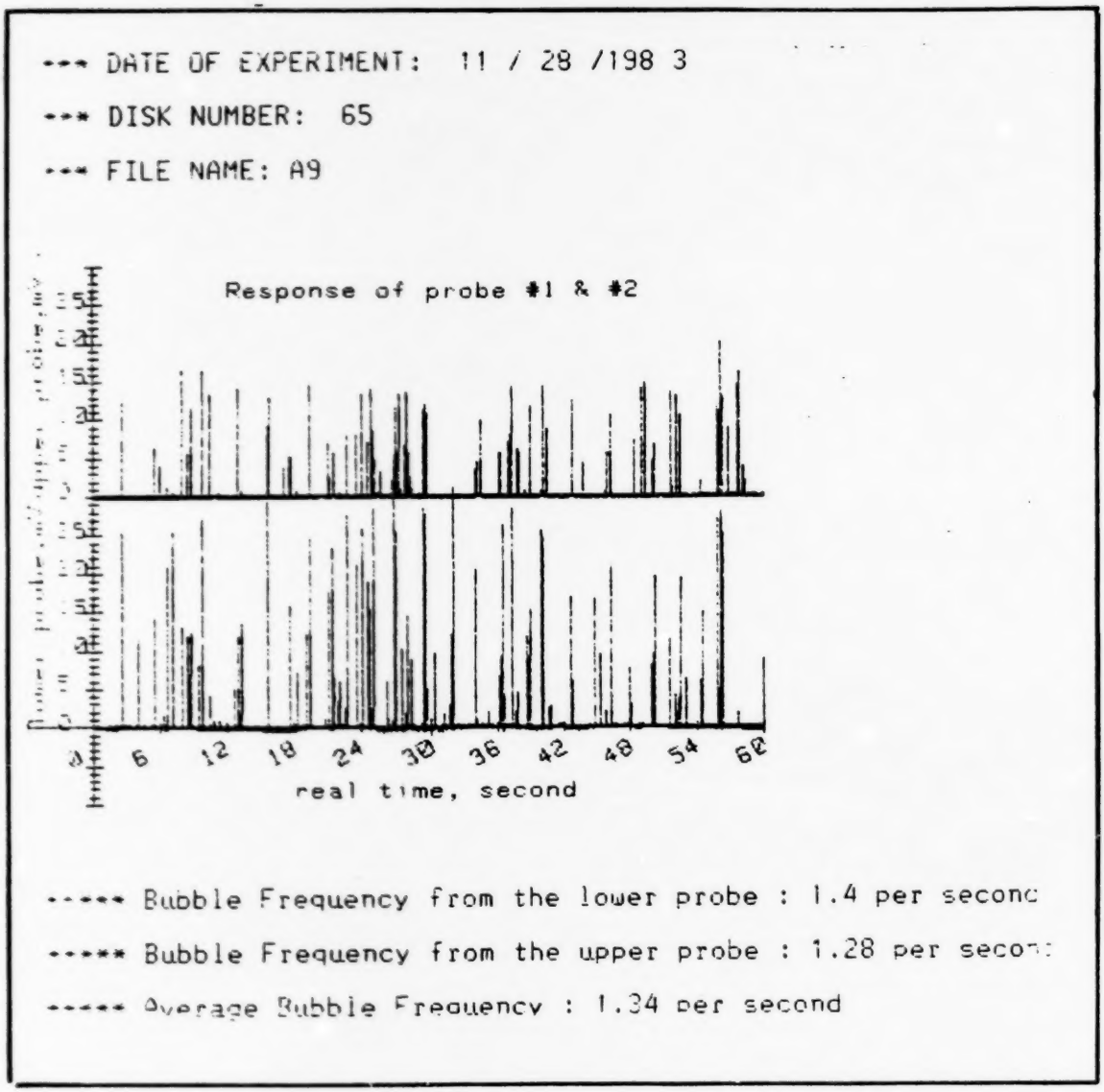

Figure 40. Bubbles in the cylindrical three phase fluidized bed column as viewed by probes 1 and 2 located at r/R_c = 0.25. Liquid: water, Gas: air, Solid: glass beads of 335μm, V_g = 1.630 cm/s, V_ℓ= 0.778 cm/s, Gas Injectors: four positioned as it is described in Figure 11.

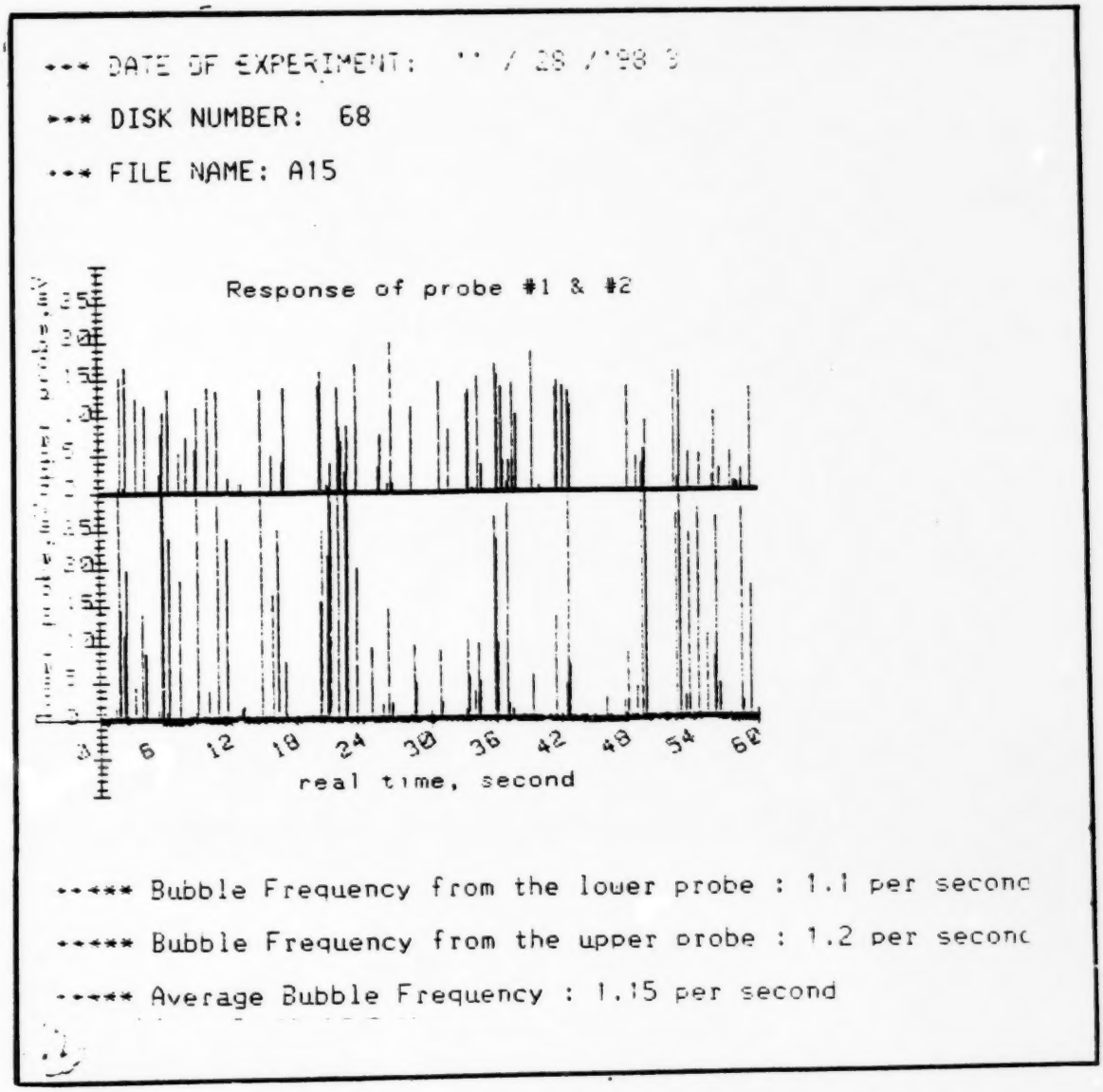
*** DATE OF EXPERIMENT: ** / 08 /'98 3
*** DISK NUMBER: 68
*** FILE NAME: A15
Response of probe #1 & #2
real time, second
***** Bubble Frequency from the lower probe : 1.1 per second
***** Bubble Frequency from the upper probe : 1.2 per second
***** Average Bubble Frequency : 1.15 per second

Figure 41. Bubbles in the cylindrical three phase fluidized bed column as viewed by probes 1 and 2 located at r/R_c = 0.5. Liquid: water, Gas: air, Solid: glass beads of 335μm, V_g = 1.630 cm/s, V_ℓ = 0.778 cm/s, Gas Injector: four positioned as it is described in Figure 11.

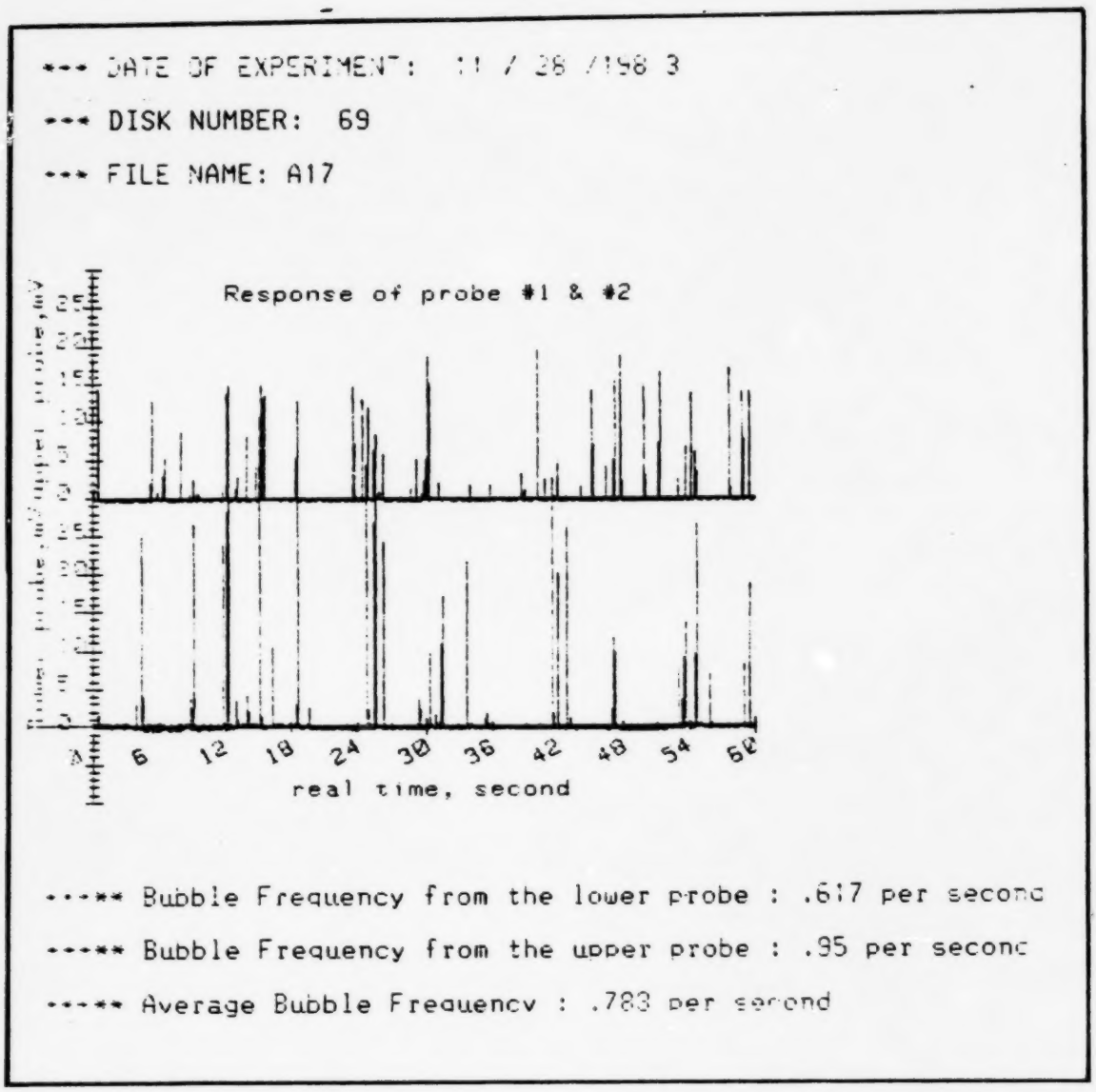
*** DATE OF EXPERIMENT: 11 / 28 /198 3
*** DISK NUMBER: 69
*** FILE NAME: A17
Response of probe #1 & #2
real time, second
***** Bubble Frequency from the lower probe : .617 per second
***** Bubble Frequency from the upper probe : .95 per second
***** Average Bubble Frequency : .783 per second

Figure 42. Bubbles in the cylindrical three phase fluidized bed column as viewed by probes 1 and 2 located at $r/R_c = 0.75$. Liquid: water, Gas: air, Solid: glass beads of 335μm, $V_g = 1.630$ cm/s, $V_\ell = 0.778$ cm/s, Gas Injectors: four positioned as it is described in Figure 11.

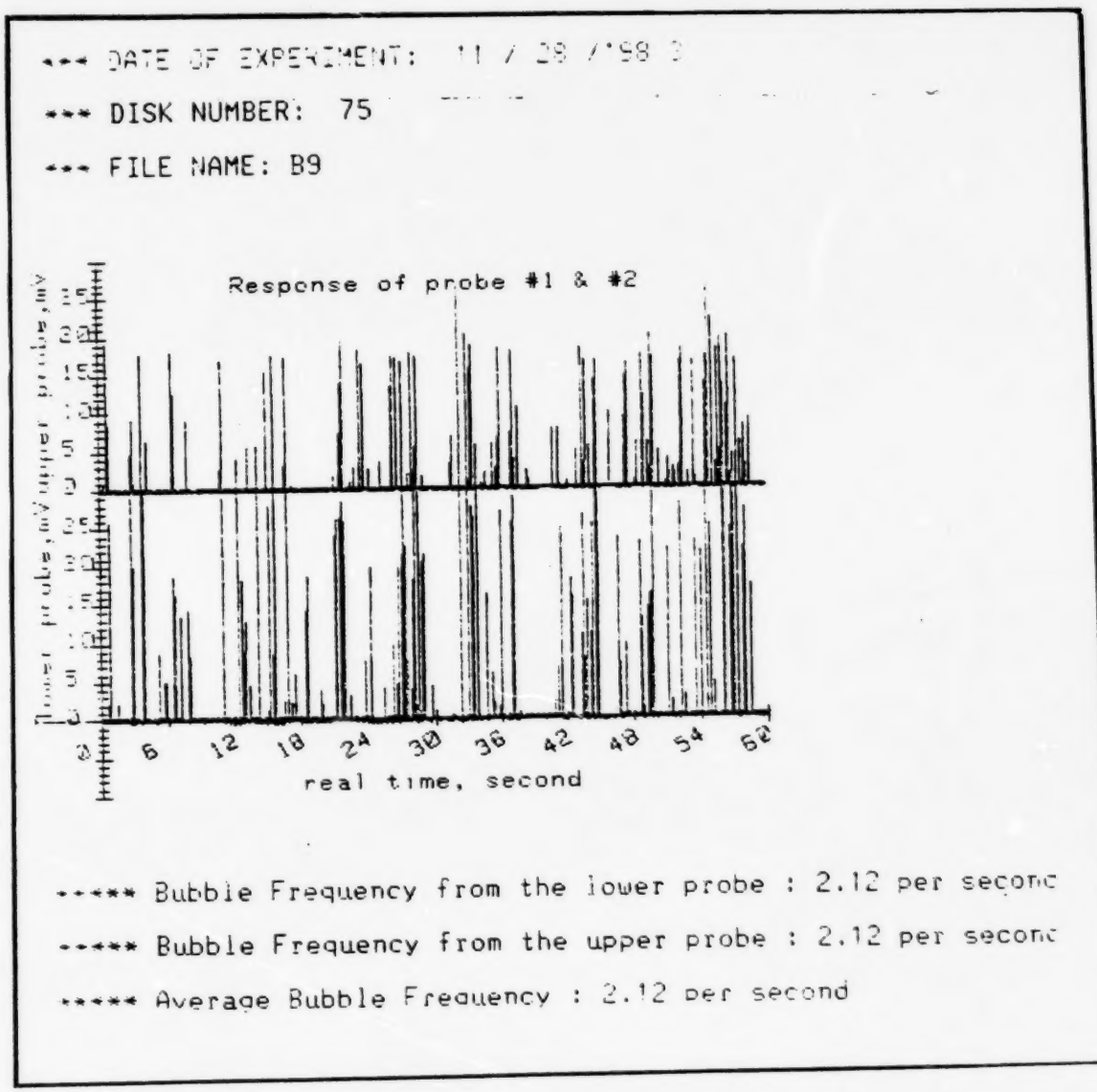
*** DATE OF EXPERIMENT: 11 / 28 /'98
*** DISK NUMBER: 75
*** FILE NAME: B9
Response of probe #1 & #2
real time, second
***** Bubble Frequency from the lower probe : 2.12 per second
***** Bubble Frequency from the upper probe : 2.12 per second
***** Average Bubble Frequency : 2.12 per second

Figure 43. Bubbles in the cylindrical three phase fluidized bed column as viewed by probes 1 and 2 located at $r/R_c = 0$. Liquid: water, Gas: air, Solid: glass beads of 335μm, $V_g = 1.630$ cm/s, $V_\ell = 1.167$ cm/s, Gas Injectors: four positioned as it is described in Figure 11.

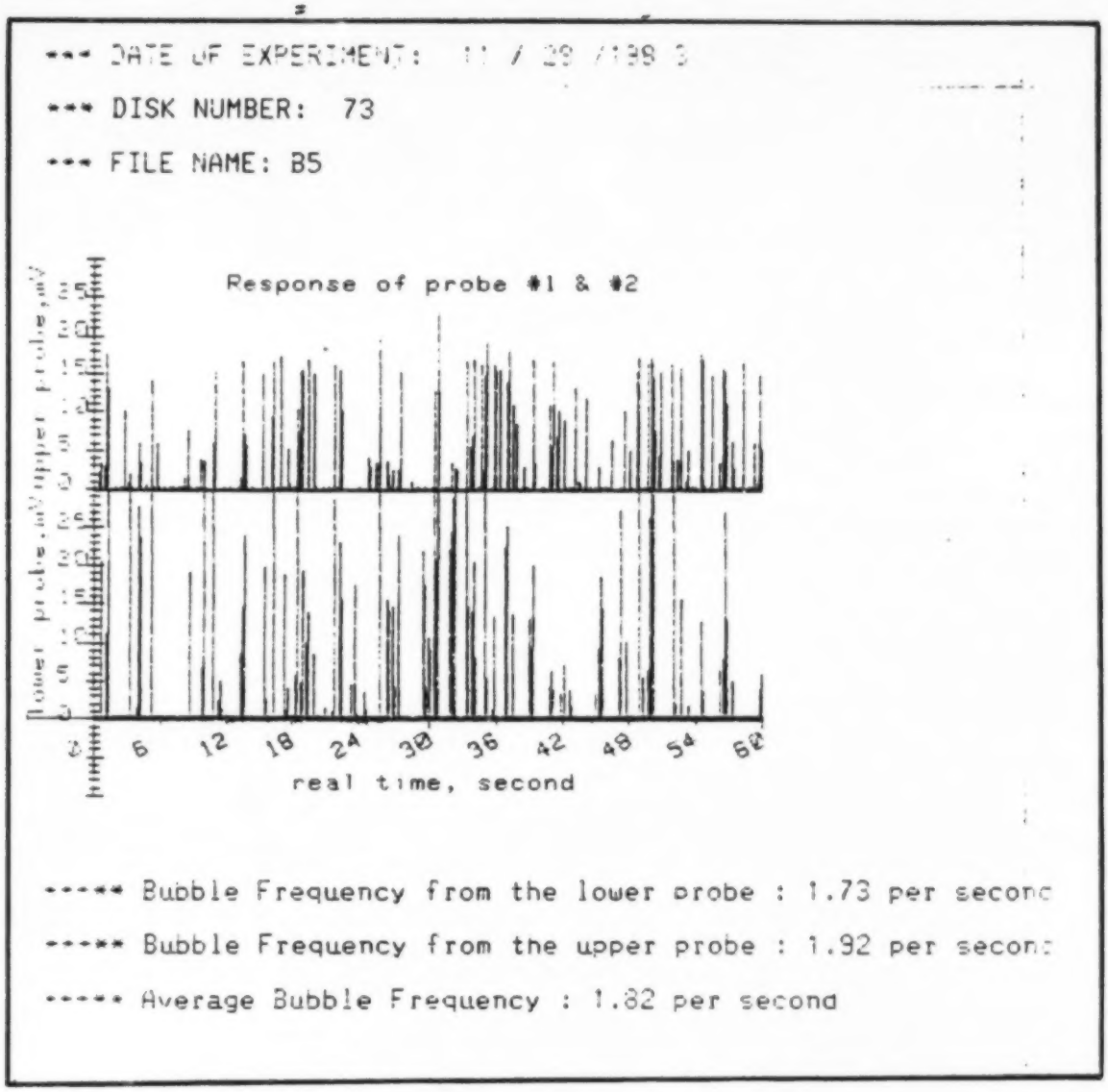
*** DATE OF EXPERIMENT: 11 / 29 /1988
*** DISK NUMBER: 73
*** FILE NAME: B5
Response of probe #1 & #2
real time, second
***** Bubble Frequency from the lower probe : 1.73 per second
***** Bubble Frequency from the upper probe : 1.92 per second
***** Average Bubble Frequency : 1.82 per second

Figure 44. Bubbles in the cylindrical three phase fluidized bed column as viewed by probes 1 and 2 located at $r/R_c = 0.25$. Liquid: water, Gas: air, Solid: glass beads of 335μm, $V_g = 1.630$ cm/s, $V_\ell = 1.167$ cm/s, Gas Injectors: four positioned as it is described in Figure 11.

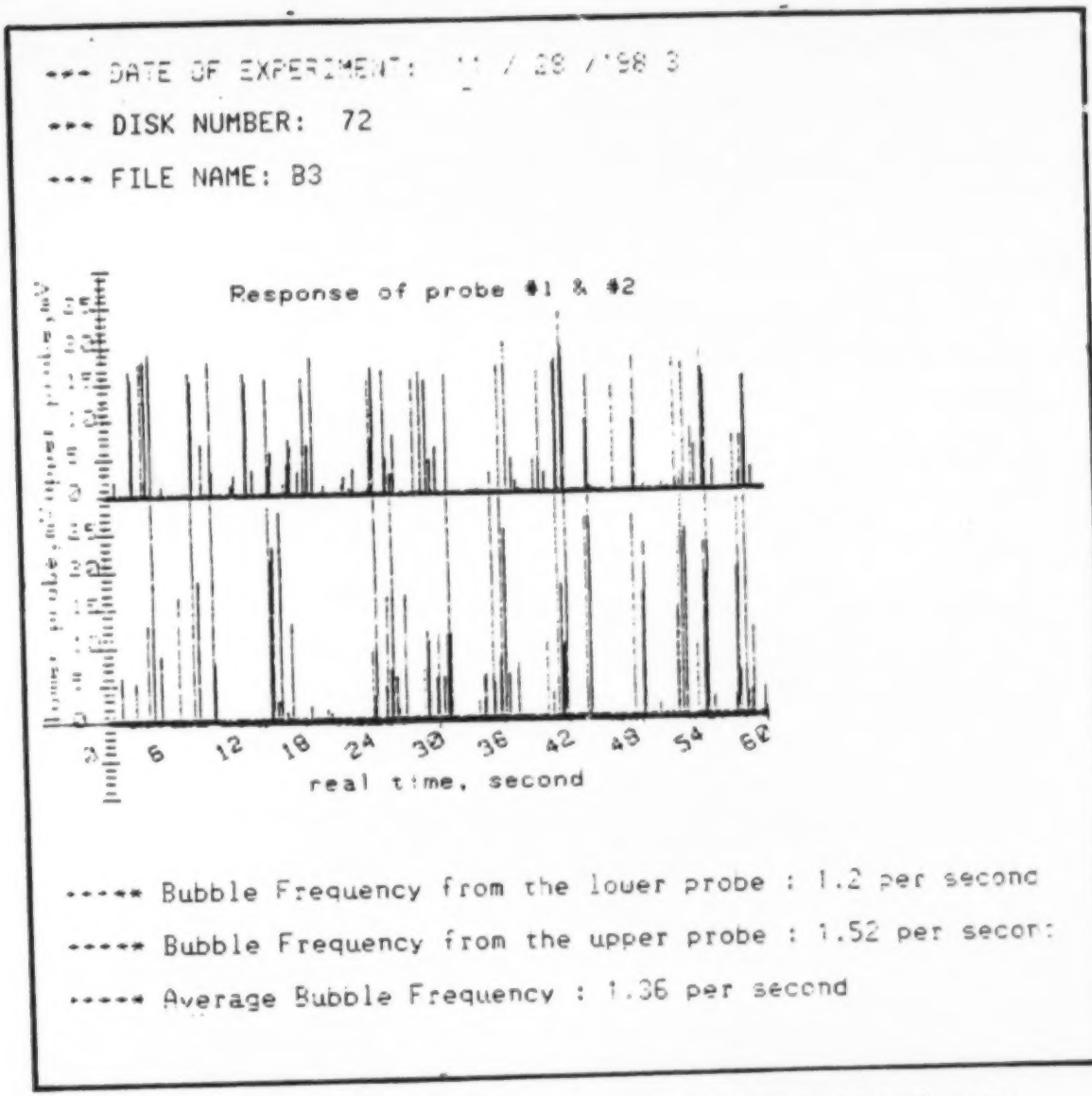

Figure 45. Bubbles in the cylindrical three phase fluidized bed column as viewed by probes 1 and 2 located at r/R_c = 0.5. Liquid: water, Gas: air, Solid: glass beads of 335μm, V_g = 1.630 cm/s, V_ℓ = 1.167 cm/s, Gas Injectors: four positioned as it is described in Figure 11.

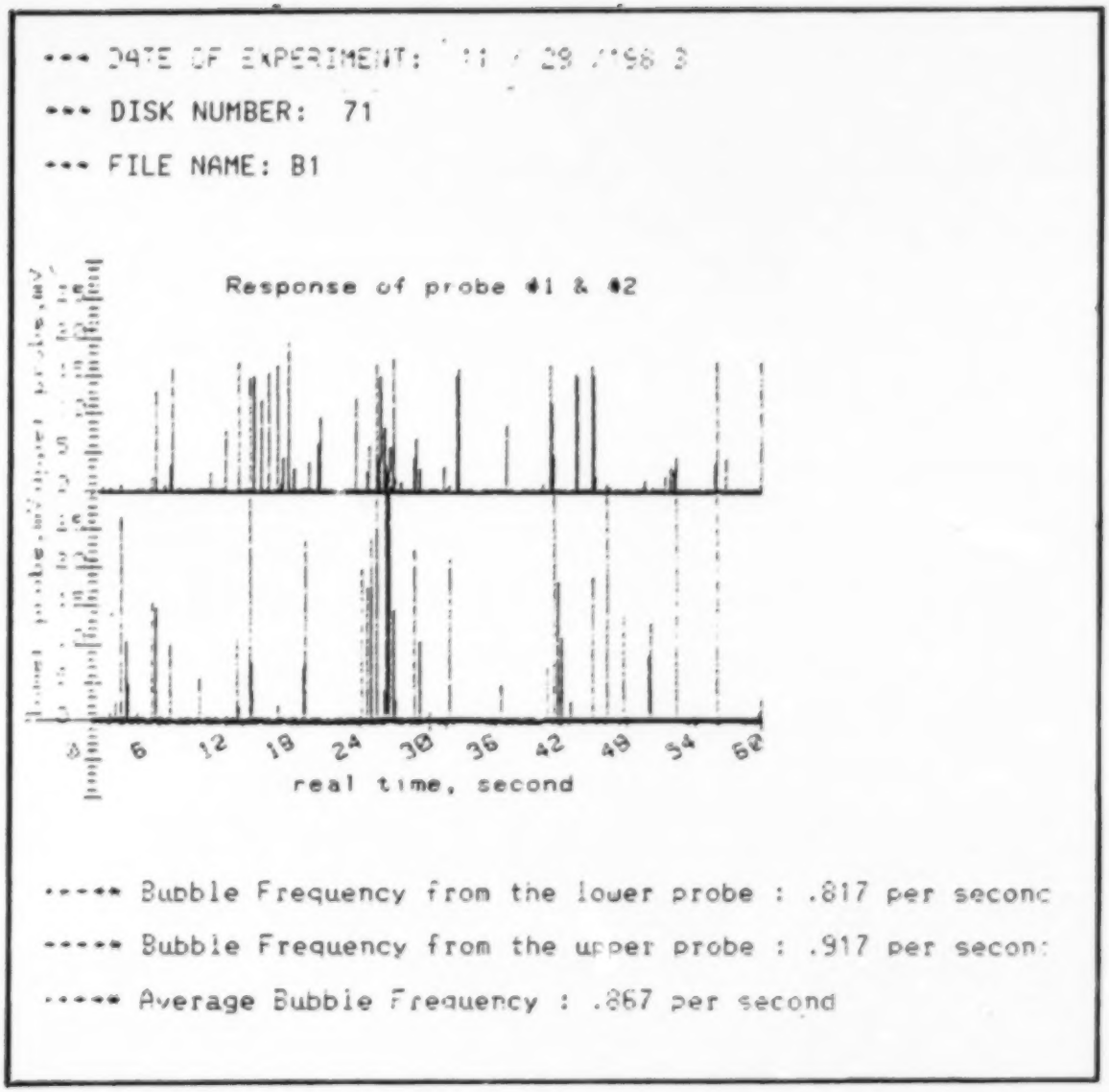

Figure 46. Bubbles in the cylindrical three phase fluidized bed column as viewed by probes 1 and 2 located at r/R_c = 0.75. Liquid: water, Gas: air, Solid: glass beads of 335μm, Vg = 1.630 cm/s, V_ℓ = 1.167 cm/s, Gas Injectors: four positioned as it is described in Figure 11.

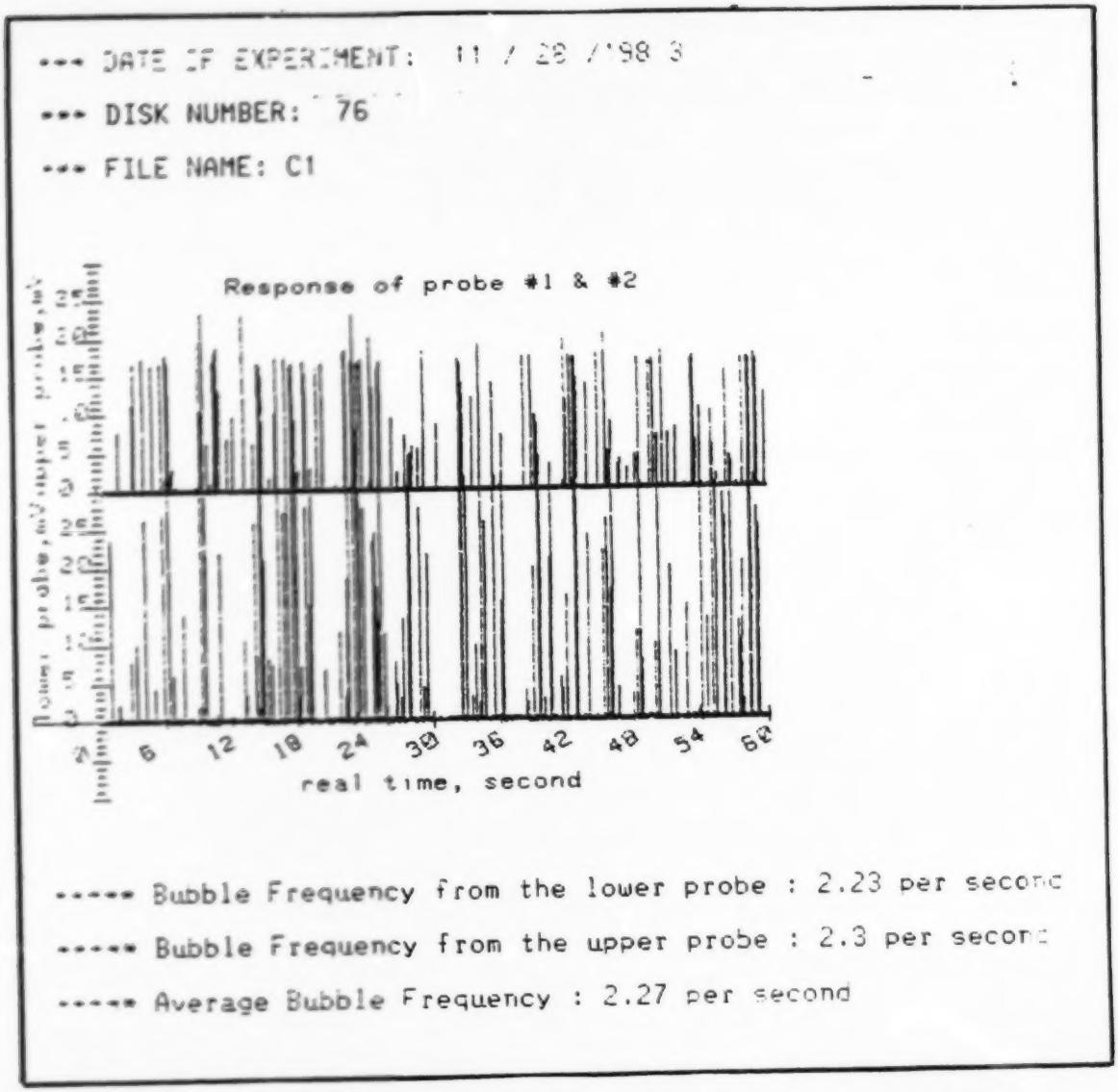
*** DATE OF EXPERIMENT: 11 / 28 /'98 3
*** DISK NUMBER: 76
*** FILE NAME: C1
Response of probe #1 & #2
real time, second
***** Bubble Frequency from the lower probe : 2.23 per second
***** Bubble Frequency from the upper probe : 2.3 per second
***** Average Bubble Frequency : 2.27 per second

Figure 47. Bubbles in the cylindrical three phase fluidized bed column as viewed by probes 1 and 2 located at $r/R_c = 0$. Liquid: water, Gas: air, Solid: glass beads of 335μm, $V_g = 1.630$ cm/s, $V_\ell = 1.556$ cm/s, Gas Injectors: four positioned as it is described in Figure 11.

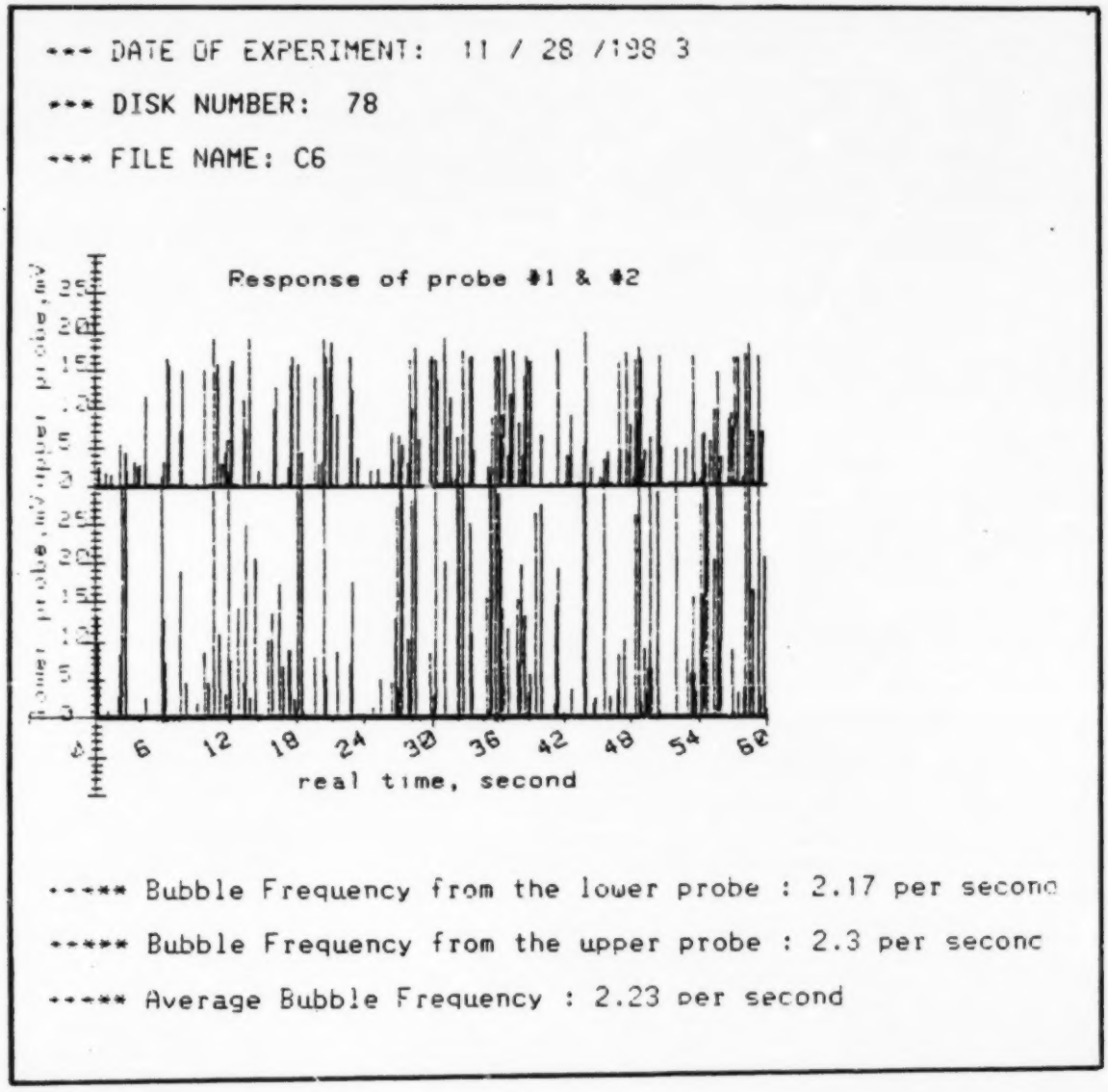
*** DATE OF EXPERIMENT: 11 / 28 /198 3
*** DISK NUMBER: 78
*** FILE NAME: C6
Response of probe #1 & #2
real time, second
***** Bubble Frequency from the lower probe : 2.17 per second
***** Bubble Frequency from the upper probe : 2.3 per second
***** Average Bubble Frequency : 2.23 per second

Figure 48. Bubbles in the cylindrical three phase fluidized bed column as viewed by probes 1 and 2 located at r/R_c = 0.25. Liquid: water, Gas: air, Solid: glass beads of 335μm, Vg = 1.630 cm/s, V_ℓ = 1.556 cm/s, Gas Injectors: four positioned as it is described in Figure 11.

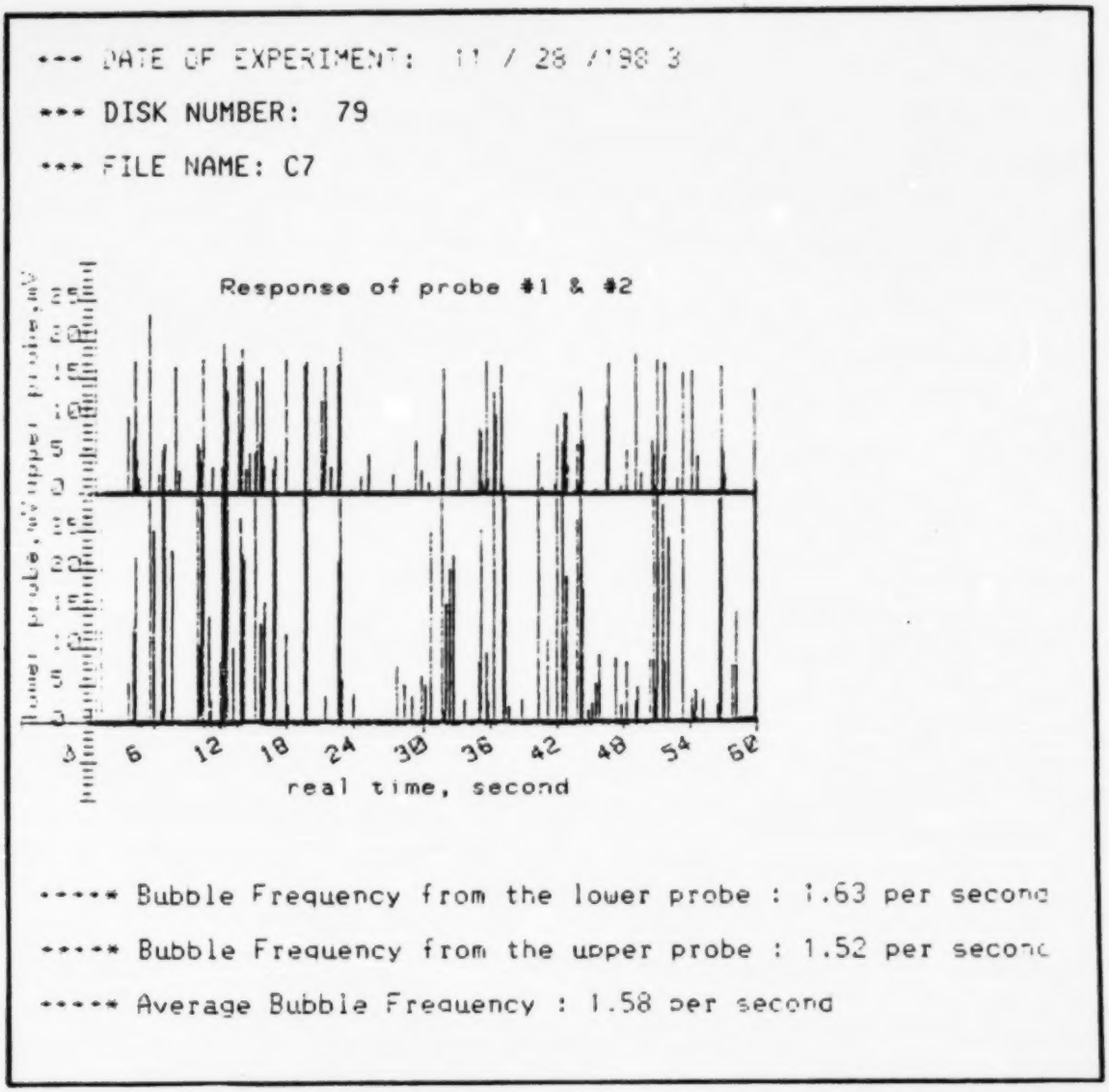
*** DATE OF EXPERIMENT: 11 / 28 /'88 3
*** DISK NUMBER: 79
*** FILE NAME: C7
Response of probe #1 & #2
real time, second
***** Bubble Frequency from the lower probe : 1.63 per second
***** Bubble Frequency from the upper probe : 1.52 per second
***** Average Bubble Frequency : 1.58 per second

Figure 49. Bubbles in the cylindrical three phase fluidized bed column as viewed by probes 1 and 2 located at r/R_c = 0.5. Liquid: water, Gas: air, Solid: glass beads of 335μm, V_g = 1.630 cm/s, V_ℓ = 1.556 cm/s, Gas Injectors: four positioned as it is described in Figure 11.

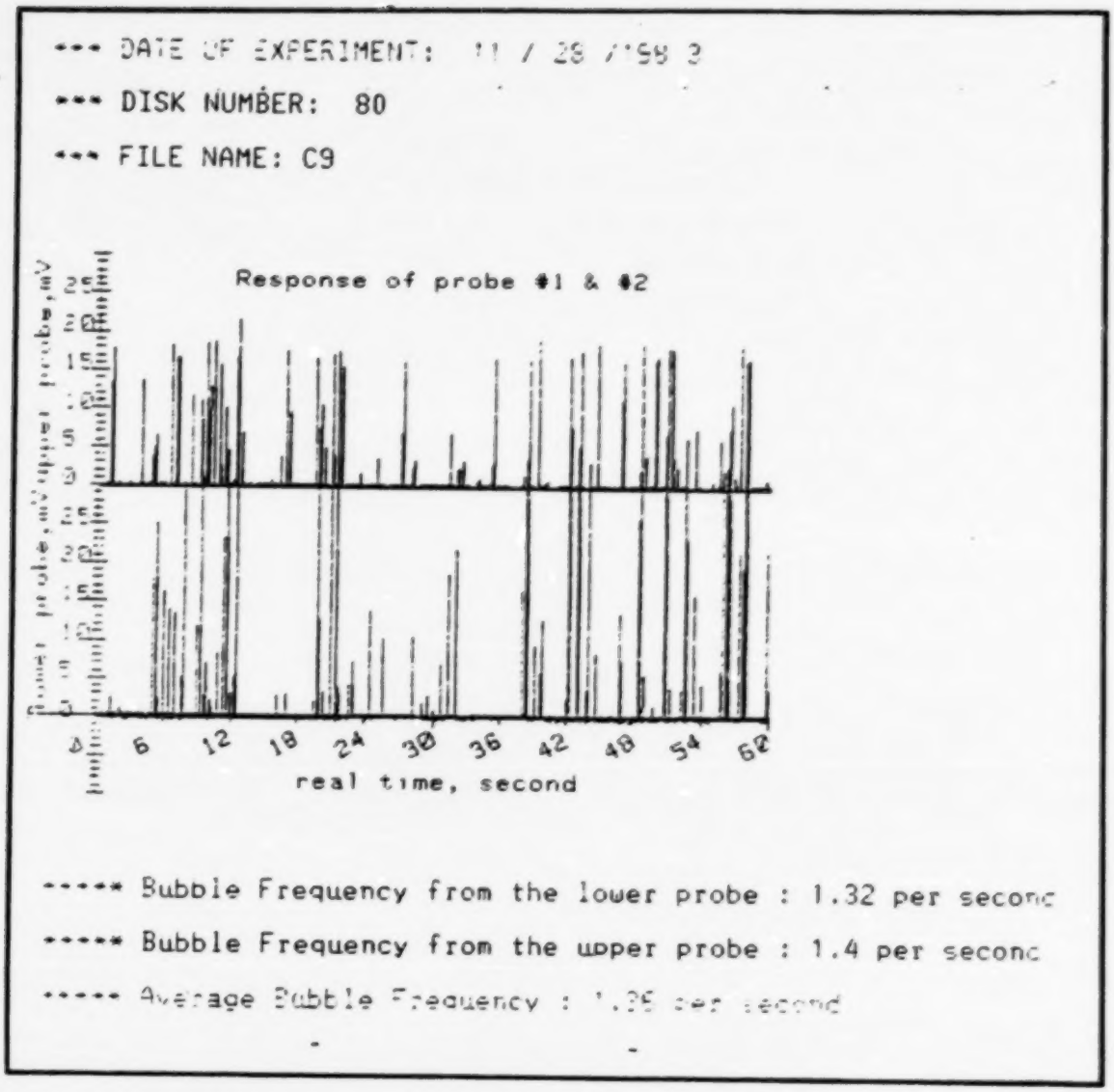
*** DATE OF EXPERIMENT: 11 / 28 /'88 3
*** DISK NUMBER: 80
*** FILE NAME: C9
Response of probe #1 & #2
real time, second
***** Bubble Frequency from the lower probe : 1.32 per second
***** Bubble Frequency from the upper probe : 1.4 per second
***** Average Bubble Frequency : 1.36 per second

Figure 50. Bubbles in the cylindrical three phase fluidized bed column as viewed by probes 1 and 2 located at $r/R_c = 0.75$. Liquid: water, Gas: air, Solid: glass beads of 335μm, $V_g = 1.630$ cm/s, $V_\ell = 1.556$ cm/s, Gas Injectors: four positioned as it is described in Figure 11.

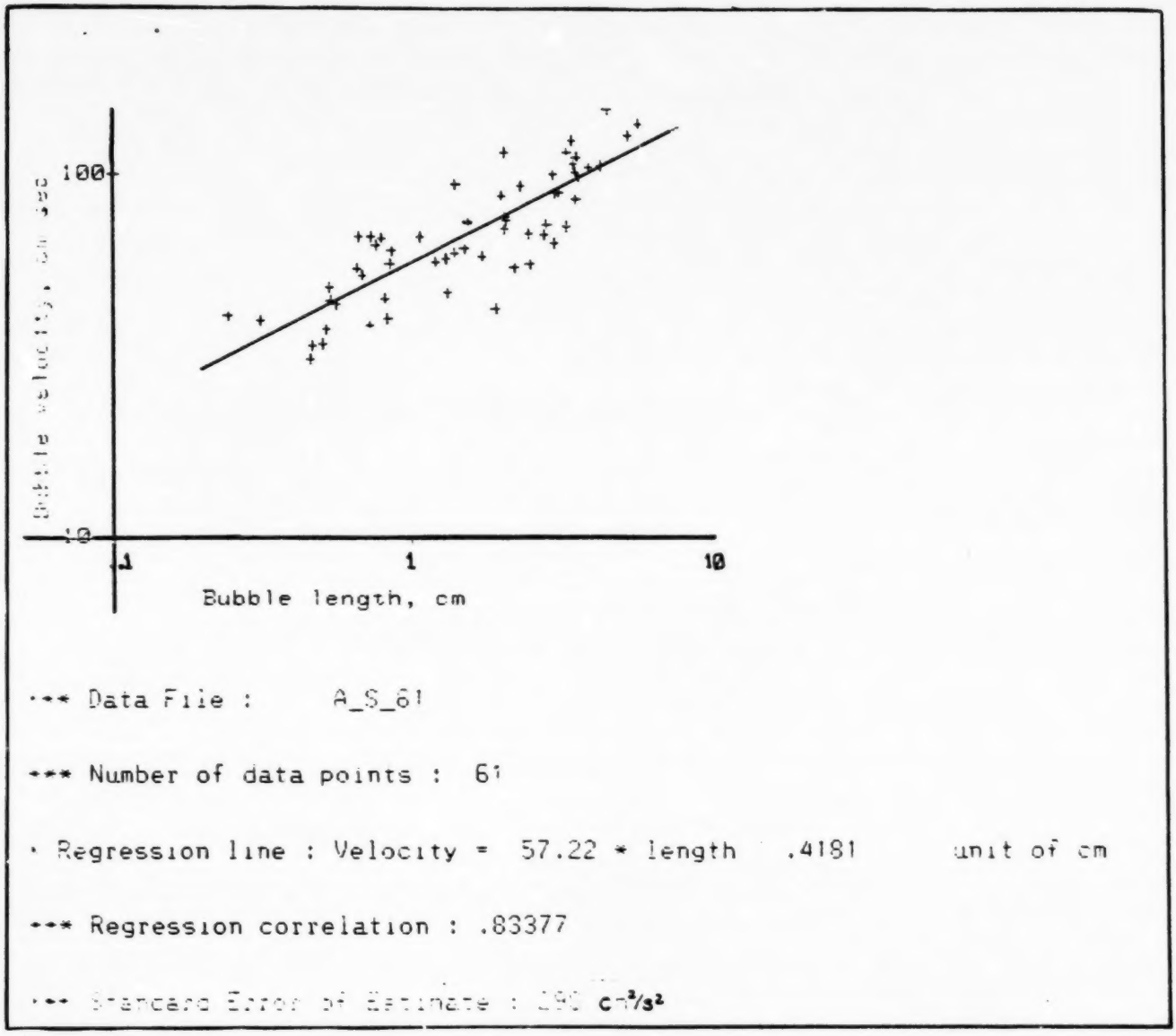
100
10
.1
1
10
Bubble length, cm
*** Data File : A_S_61
*** Number of data points : 61
* Regression line : Velocity = 57.22 * length .4181 unit of cm
*** Regression correlation : .83377
*** Standard Error of Estimate : 290 cm²/s²

Figure 51. Relationship of the bubble velocity to the measured axial bubble length estimated with the U-shaped optical fiber probes. Cylindrical column. Gas Injector: one positioned at $r/R_C = 0$. Liquid: water, Gas: air, Solid: glass beads of 335μm, Vg = 1.769 cm/s, V_ℓ = 0.778 cm/s.

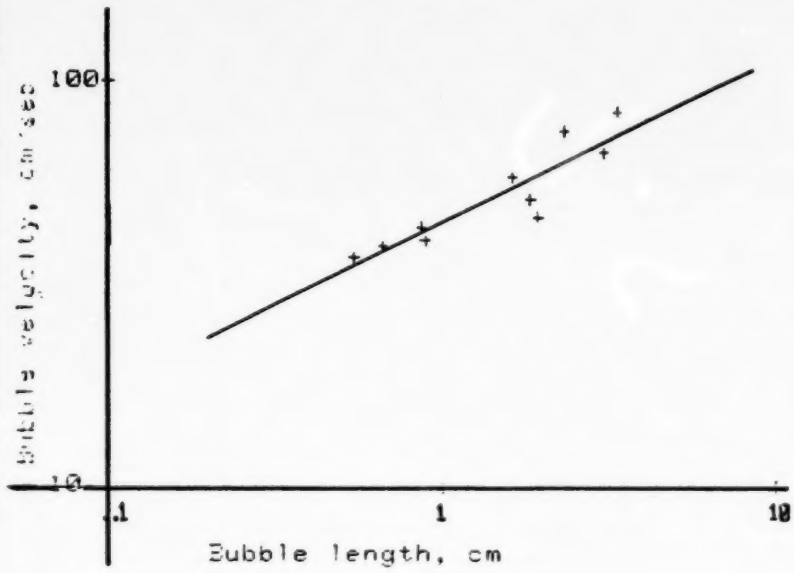

*** Data File : D1_D4_10

*** Number of data points : 10

* Regression line : Velocity = 44.77 * length .4084 unit of cm

*** Regression correlation : .90708

*** Standard Error of Estimate : 60.8 cm^2/s^2

Figure 52. Relationship of the bubble velocity to the measured axial bubble length estimated with the U-shaped optical fiber probes. Cylindrical column. Gas Injectors: four. Liquid: water, Gas: air, Solid: glass beads of 335μm, Vg = 1.630 cm/s, V_ℓ = 0.389 cm/s.

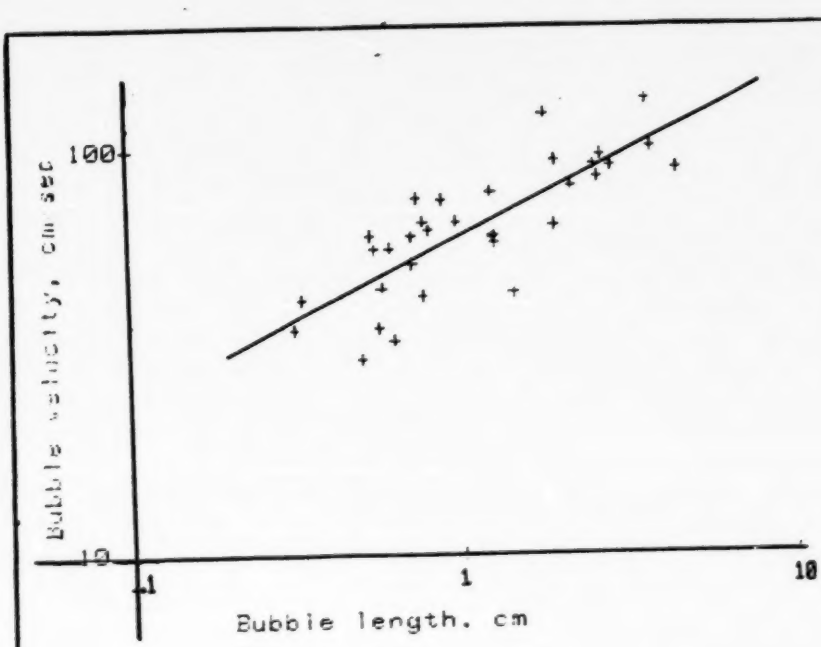

*** Data File : A_M_33

*** Number of data points : 33

* Regression line : Velocity = 60.21 * length .4131 unit of cm

*** Regression correlation : .80249

*** Standard Error of Estimate : 225 cm^2/s^2

Figure 53. Relationship of the bubble velocity to the measured axial bubble length estimated with U-shaped optical fiber probes. Cylindrical column. Gas Injectors: Four, liquid: water, Gas: air, Solid: glass beads of 335µm, Vg = 1.630 cm/s, V_ℓ = 0.778 cm/s.

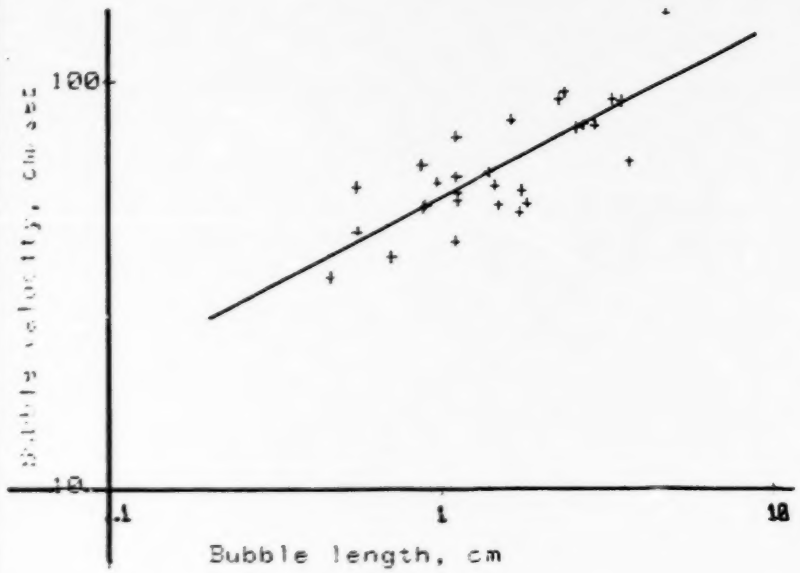

*** Data File : B_M_29

*** Number of data points : 29

* Regression line : Velocity = 52.07 * length + .4249 unit of cm

*** Regression correlation : .79179

*** Standard Error of Estimate : 223 cm^2/s^2

Figure 54. Relationship of the bubble velocity to the measured axial bubble length estimated with U-shaped optical fiber probes. Cylindrical Column. Gas Injectors: Four. Liquid: water, Gas: air, Solid: glass beads of 335μm, Vg = 1.630 cm/s, V_ℓ = 1.167 cm/s.

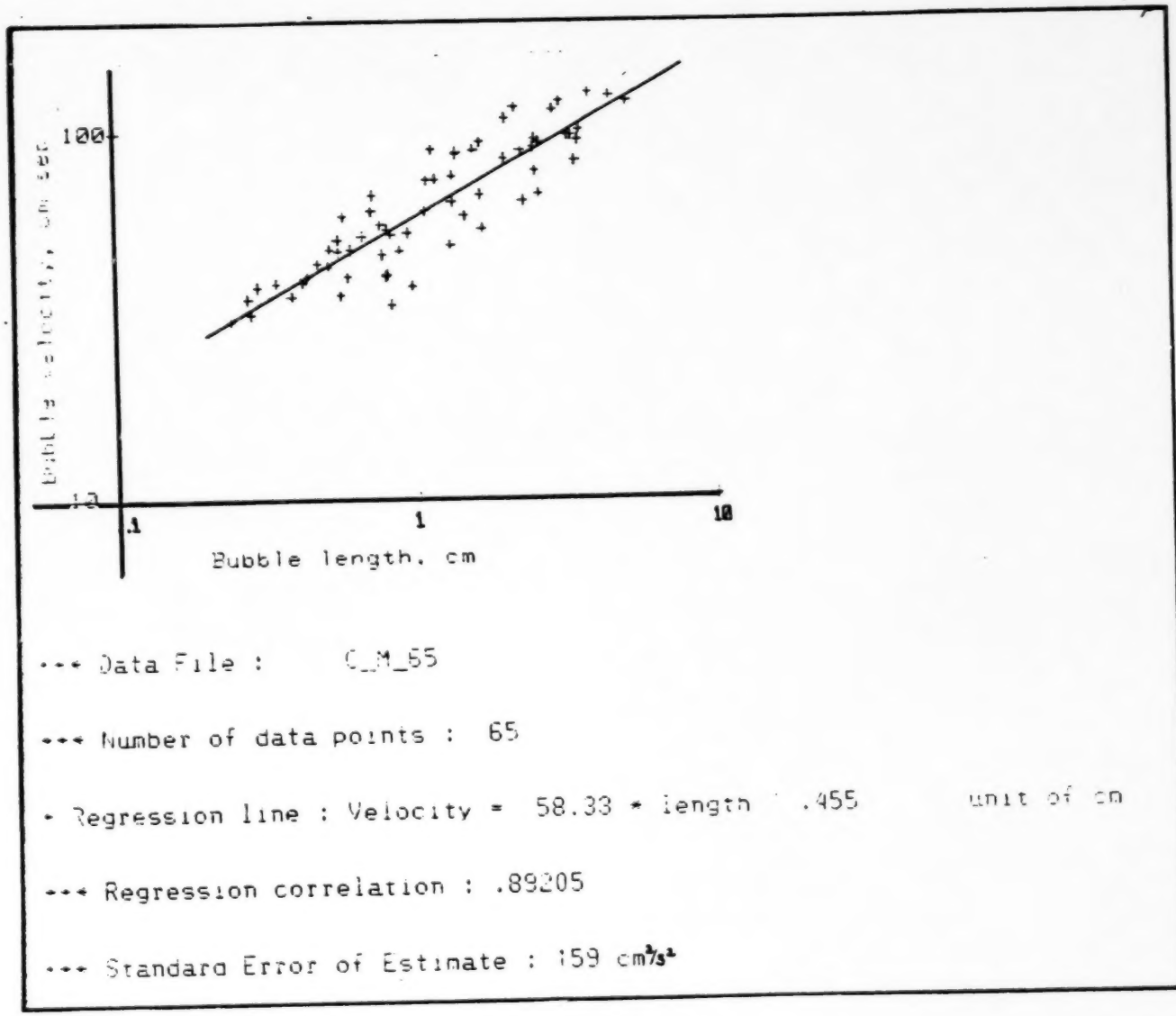
100
.1
1
10
Bubble length, cm
--- Data File : C_M_55
--- Number of data points : 65
- Regression line : Velocity = 58.33 * length .455 unit of cm
--- Regression correlation : .89205
--- Standard Error of Estimate : 159 cm²/s²

Figure 55. Relationship of the bubble velocity to the measured axial bubble length estimated with the U-shaped optical fiber probes. Cylindrical column. Gas Injectors: four. Liquid: water, Gas: air, Solid: glass beads of 335μm, Vg = 1.630 cm/s, V_ℓ = 1.556 cm/s.

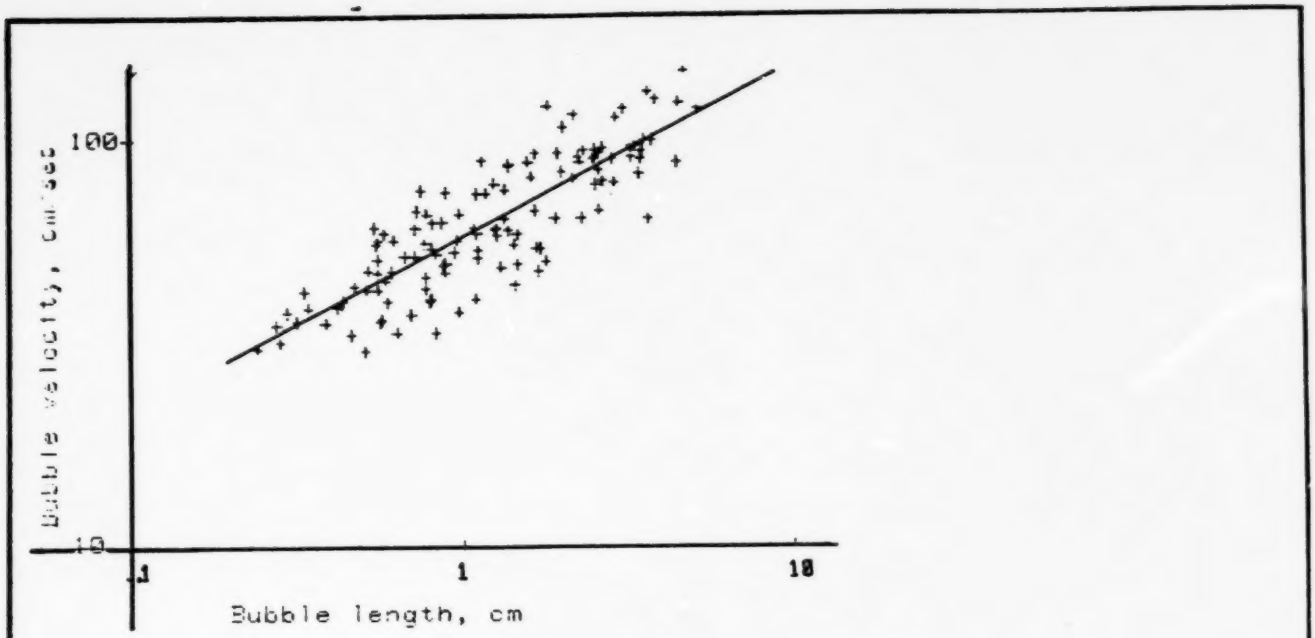

*** Data File : ABCM_127

*** Number of data points : 127

* Regression line : Velocity = 57.35 * length .429! unit of cm

*** Regression correlation : .84095

*** Standard Error of Estimate : 199 cm^2/s^2

Figure 56. Relationship of the bubble velocity to the measured axial bubble length estimated with the U-shaped optical fiber probes. Cylindrical column. Gas injectors: four. Liquid: water, Gas: air, Solid: glass beads of 335μm. The data of Figures 53, 54 and 55 are plotted together.

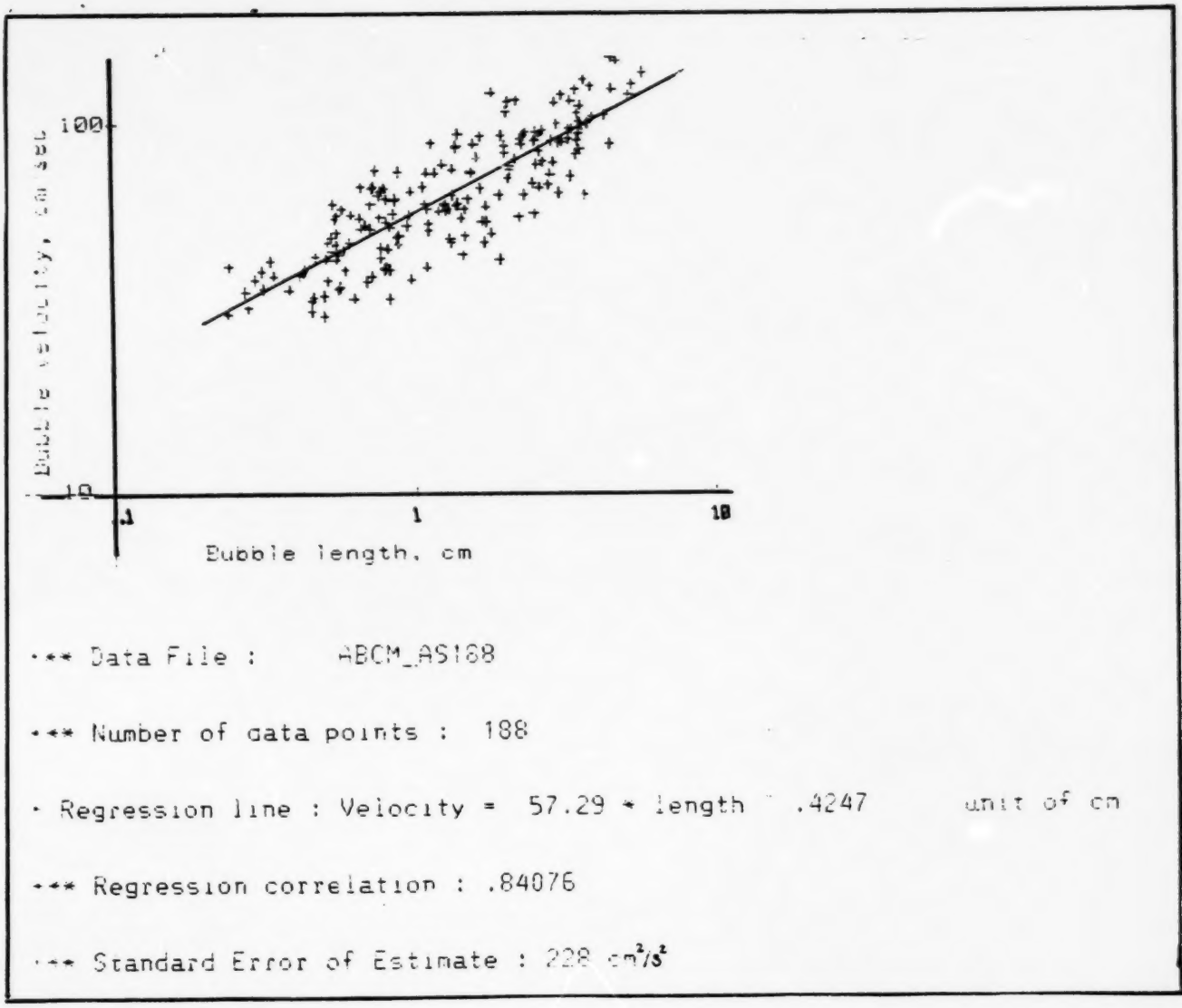
100
10
.1
1
10
Bubble length, cm
*** Data File : ABCM_AS188
*** Number of data points : 188
* Regression line : Velocity = 57.29 * length ^ .4247 unit of cm
*** Regression correlation : .84076
*** Standard Error of Estimate : 228 cm²/s²

Figure 57. Relationship of the bubble velocity to the measured axial bubble length estimated with the U-shaped optical fiber probes. Cylindrical column. Gas injectors: four. Liquid: water, Gas: air, Solid: glass beads of 335μm. The data of Figures 51, 53, 54 and 55 are plotted together.